Improving uranium recovery by utilising compressor waste heat

R Siecker

orcid.org/0000-0003-2166- 6920

Dissertation accepted in fulfilment of the requirements for the degree *Master of Engineering in Mechanical Engineering* at the North-West University

Supervisor: Dr JC Vosloo

Graduation: August 2023

Student number: 28430492

ACKNOWLEDGEMENTS

The following parties assisted and always supported me enormously during the study:

- Firstly, I would like to thank the Lord for providing me with the strength and dedication to complete this dissertation, for without Him, this study would not be possible.
- I would like to thank my brother, Juan Siecker, for assisting me throughout the study and always availing himself when I was struggling with my dissertation. Thank you for all the motivation and willingness.
- I would like to thank my study leader, Jan Vosloo, for assisting me with the dissertation and always aiming to improve the document by working weekends to provide feedback. It has been a privilege to receive your guidance.
- I would like to thank my parents, Doctor Adriaan Siecker and Mrs Christa Siecker, as well as my sister, Marianka Knox, for their continuous support throughout the study.
- I would also like to thank ETA Operations (Pty) for allowing me this opportunity and assisting me with achieving my goals throughout the study while improving my engineering expertise.

ABSTRACT

Title: Improving uranium recovery by utilising waste heat

Author: R Siecker

Supervisor: Dr JC Vosloo

Keywords: Waste heat, uranium recovery, uranium leaching

Leaching is the key process used for uranium extraction in a slurry mixture. Heat is often introduced in the leaching process to increase the uranium extraction yield. However, acquiring heat is expensive due to electricity tariff increases and is thus seldom feasible. Therefore, this study investigated alternative heating strategies for the leaching process. Different heat sources such as photovoltaic systems, heat pumps, boilers and compressor waste heat were considered. Waste heat was selected since the waste heat on mine compressed air systems is often available to be utilised and was proven to be the most cost-effective option.

A method was created to assess the impact of waste heat on the extraction of uranium. The approach involved examining and simulating a standard heat recovery system. The simulation was verified using gathered data. Additionally, a potential heat source was assessed and simulated, with the possibility of incorporating it into heat recovery. An empirical model of the uranium plant was constructed and validated with relevant literature, enabling an analysis of the impact of the recovered heat. Finally, the validated models were integrated into a single system to evaluate the influence of a heat recovery system.

The South African uranium processing mine implemented the suggested method, with each model being utilised to simulate current operations. The resulting accuracy level of the models was around 95%. The integrated model was used to simulate a heat recovery system that could potentially use the heat recovered from the mine compressors and quantify the impact by evaluating the transferred heat to the uranium plant. An economic feasibility analysis showed an annual benefit of R8.0m, with a total revenue of R48.2m over a life of mine of six years, resulting in a payback period of 2.6 years.

TABLE OF CONTENTS

ACKNOWLEDGEMENTS ..... **II**

ABSTRACT ..... **III**

TABLE OF CONTENTS ..... **IV**

LIST OF FIGURES ..... **VI**

LIST OF TABLES ..... **IX**

ABBREVIATIONS ..... **X**

NOMENCLATURE ..... **XI**

CHAPTER 1 – INTRODUCTION **1**

1.1 Background 1

1.2 Uranium mining in South Africa 1

1.3 Uranium recovery process 3

1.4 Literature study 11

1.5 Need for the study and objectives 20

1.6 Dissertation overview 21

CHAPTER 2 – METHODOLOGY **23**

2.1 Preamble 23

2.2 Heat recovery system 25

2.3 Heat source system 30

2.4 Empirical model 34

2.5 Model integration 38

2.6 Feasibility study 41

2.7 Conclusion 42

CHAPTER 3 – RESULTS **44**

3.1 Preamble 44

3.2 Case study background 44

3.3 Current heat recovery system results 45

3.4 Heat source system results 52

3.5 Empirical model results 58
3.6 Model integration 66
3.7 Feasibility study of the heat recovery system 75
3.8 Validation and conclusion 79
CHAPTER 4 – CONCLUSION 81
4.1 Summary 81
4.2 Future recommendations 82
REFERENCE LIST 84
APPENDIX A: SPIRAL HEAT EXCHANGER 94
APPENDIX B: HEAT RECOVERY SYSTEM 97
APPENDIX C: HEAT SOURCE SYSTEM 98
APPENDIX D: HEAT RECOVERY ANALYSIS 100

LIST OF FIGURES

Figure 1: Gold production in South Africa [17] 2
Figure 2: South African average gold grade vs years [18] 2
Figure 3: South African uranium production [22] 3
Figure 4: Effect of temperature on uranium dissolution [30] 5
Figure 5: Flow diagram of uranium extraction process 7
Figure 6: Effect of time on the leaching process [6] 8
Figure 7: Effect of sulphuric acid concentration on the leaching process [35] 9
Figure 8: Temperature effect on uranium extraction over a 24-hour period [29] 10
Figure 9: Effect of temperature on uranium dissolution [5] 12
Figure 10: Comparison between technologies based on average levelised cost of energy [44] 15
Figure 11: M-Tech heat pump study break-even point [51] 16
Figure 12: Compressor aftercooler [54] 17
Figure 13: Spiral heat exchanger [57] 18
Figure 14: Simplified steps of the methodology 24
Figure 15: Heat recovery methodology breakdown 25
Figure 16: Data collection methods [68] 26
Figure 17: Baseline heat recovery model development 28
Figure 18: Verification of heat recovery model 29
Figure 19: Heat source methodology breakdown 30
Figure 20: Heat source model process flow 32
Figure 21: Heat source model development 33
Figure 22: Verification process of heat source model 34
Figure 23: Empirical methodology breakdown 35
Figure 24: Empirical model process flow 36
Figure 25: Verification procedure of empirical model 37
Figure 26: Solution model methodology breakdown 38
Figure 27: Solution model process flow 39
Figure 28: Feasibility analysis flow diagram [9] 41
Figure 29: Detailed layout of Mine A heat recovery system 46
Figure 30: Mine A heat recovery simulation model 49

Figure 31: Stage 1 aftercooler temperature comparison 51
Figure 32: Stage 2 aftercooler temperature comparison 51
Figure 33: Change house heat exchanger temperature comparison..... 51
Figure 34: Mine B compressor water-cooling circuit 53
Figure 35: Mine B compressor simulation system..... 55
Figure 36: Compressor 3 aftercooler winter temperatures comparison 57
Figure 37: Compressor 3 aftercooler summer temperatures comparison 57
Figure 38: Outlet slurry temperature for different tonnages treated at different slurry inlet temperatures 61
Figure 39: Uranium recovery for different tonnages treated at different inlet temperatures 62
Figure 40: Uranium recovery for different inlet temperatures at different tonnages treated 63
Figure 41: Overall dissolution vs slurry temperatures at Plant X 64
Figure 42: Verification of dissolution graph 65
Figure 43: Solution model heat recovery layout 67
Figure 44: Mine B heat recovery proposed layout..... 68
Figure 45: Heat exchanger potential at different water flow rates during winter conditions 69
Figure 46: Heat exchanger potential at different water flow rates during summer conditions ... 69
Figure 47: Slurry outlet temperature from the different heat recovery combinations at winter and summer conditions 74
Figure 48: Monthly benefit for Year 1 of solution model 76
Figure 49: Monthly benefit for Year 2 of solution model 77
Figure 50: Heat recovery break-even point for six years 78
Figure 51: Normal operations revenue versus its heat recovered benefit 79
Figure 52: Spiral heat exchanger self-cleaning channel [57]..... 94
Figure 53: Spiral heat exchanger as in the industry 95
Figure 54: Flow process of spiral heat exchanger [57]..... 95
Figure 55: Design specification of the spiral heat exchanger [57] 96
Figure 56: SCADA view of the two-stage aftercooler used at Mine A..... 97
Figure 57: Simulation used to calculate the airflow needed in the aftercooler 97
Figure 58: Compressor 1 aftercooler winter temperatures comparison 98
Figure 59: Compressor 2 aftercooler winter temperatures comparison 98
Figure 60: Compressor 1 aftercooler summer temperatures comparison 99
Figure 61: Compressor 2 aftercooler summer temperatures comparison 99

Figure 62: Monthly cost versus benefit for Year 3 of heat recovery model 100
Figure 63: Monthly cost versus benefit for Year 4 of heat recovery model 100
Figure 64: Monthly cost versus benefit for Year 5 of heat recovery model 101
Figure 65: Monthly cost versus benefit for Year 6 of heat recovery model 101

LIST OF TABLES

Table 1: Equipment for data collection [71] 26
Table 2: Components in system [73] 27
Table 3: Components in heat source system [73] 31
Table 4: Basic information needed to identify heat recovery application [74] 35
Table 5: Different factors that may influence chemical processing [5, 6, 30] 35
Table 6: Mine A compressor operating conditions 45
Table 7: Aftercooler heat recovered data on Mine A 47
Table 8: Change house heat exchanged data on Mine A 48
Table 9: Aftercooler heat recovered results on Mine A 50
Table 10: Change house heat exchanged results on Mine A 50
Table 11: Mine B compressor operating conditions 52
Table 12: Winter heat source data obtained of Mine B 54
Table 13: Summer heat source data obtained of Mine B 54
Table 14: Simulation results of Mine B compressor system during winter conditions 56
Table 15: Simulation results of Mine B compressor system during summer conditions 56
Table 16: Plant X audit data of the leaching process 58
Table 17: Life of mine plan of Plant X 60
Table 18: Heat recovery scenarios for Solution model 70
Table 19: Results for Scenario 1 at winter conditions 70
Table 20: Results for Scenario 2 at winter conditions 71
Table 21: Results for scenario 3 at winter conditions 71
Table 22: Results for Scenario 1 during summer conditions 72
Table 23: Results for Scenario 2 during summer conditions 72
Table 24: Results for Scenario 3 during summer conditions 73
Table 25: Heat recovery results from only the aftercooler during winter 73
Table 26: Heat recovery results from only the aftercooler during summer 74
Table 27: Cost analysis of heat recovery [78] 75
Table 28: Yearly costs and benefits 75

ABBREVIATIONS

Abbreviation	Description
capex	capital expenditure
CFD	Computational Fluid Dynamics
HX	heat exchanger
MATLAB	Matrix Laboratory
opex	operational expenditure
PTB	Process Toolbox
SCADA	supervisory control and data acquisition

NOMENCLATURE

Unit of measure	Description	Parameter
°C	degrees Celsius	temperature
Cfm	cubic feet per minute	airflow volume
Btu	british thermal unit	thermal energy
EJ	exajoule	energy
g/L	gram per litre	acid concentration
GWh	gigawatt-hour	electrical energy
kg	kilogram	mass
kg/s	kilogram per second	airflow
kPa	kilopascal	pressure
kW	kilowatt	power
kW/°C	kilowatt per degrees Celsius	heat transfer coefficient
kWh	kilowatt-hour	electrical energy
L	litre	volume
L/s	litre/second	velocity or flow rate
m	metre	length or distance
m^3/s	cubic metre per second	velocity
mm	millimetre	length
MW	megawatt	electrical energy
s	second	duration
Wh	watt-hour	electrical energy

CHAPTER 1 – INTRODUCTION

1.1 Background

South African mining contributes to a variety of mineral extraction – one of which is uranium production [1]. Uranium leaching is used to extract the uranium from the slurry from gold plants [2-6]. Higher slurry temperatures accelerate the uranium leaching process. Preheating the slurry can be an energy-intensive process. If the uranium can be leached at higher temperatures, the time taken to extract the uranium decreases, leading to more efficient processes that deliver higher yields and cost savings [5, 7].

Different types of heat source can be used to preheat uranium-carrying slurry. In the past, boilers were used for similar industry heating but the running costs were too high [8]. Other energy sources such as compressor waste heat, photovoltaic systems and heat pumps can also be used; however, they require additional infrastructure and extensive capital layouts to make these systems compatible for heat exchange with the uranium-carrying slurry [9-11].

Mining equipment such as compressors, pumps, fans, and motors produce heat during operation [3]. Plants that are located near these type of mining equipment use large energy systems and produce great amounts of waste heat, which could be investigated [12]. This heat could be recovered as the current industry practice rejects the waste heat into the atmosphere [13]. Heat recovery systems could be integrated into various applications, such as mine compressors, to recover the generated heat [4]. This heat could be used to preheat uranium-carrying slurry, which should improve uranium recovery and decrease operational costs.

1.2 Uranium mining in South Africa

Gold contributes enormously to the global mining sector since it has great value. Previously, gold was a partly defining factor of the country's currency; however, it has grown to influence the currency greatly, especially countries that export gold actively [14]. South Africa had dominated the world gold producers until 2009, but it became the fifth-largest producer thereafter [15].

Inputs such as mineral and people utilisation as well as capital expenditure (capex) and operational expenditure (opex) assigned to the mining operations should be monitored closely [16]. The mining sector faces social, operational, technical, and economical challenges, which greatly influence competitiveness in the gold mining sector. The negative influence thereof can be observed in the declining production trend over the past 10 years as depicted in Figure 1 [17].

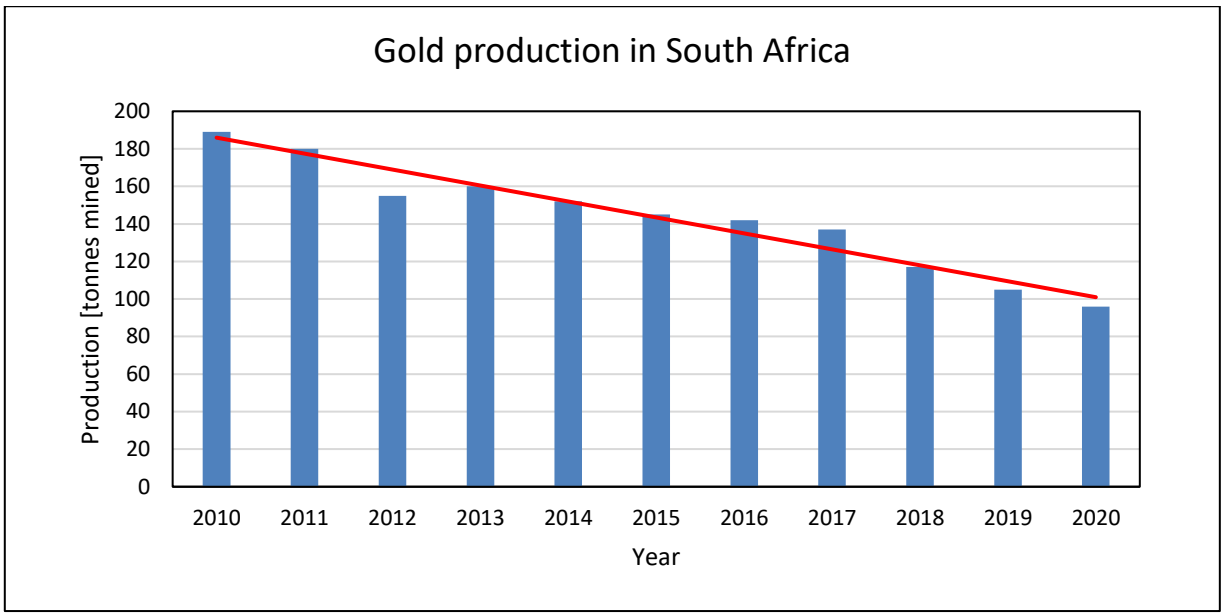

Figure 1: Gold production in South Africa [17]

Although the ore deposits mined in the past were rich, they have been declining steadily since then. For example, in the 1970s, gold mines produced a resource grade of approximately 12 g/tonne compared with the more recent resource grade of approximately 5 g/tonne [18].

Figure 2 presents the recovery resource grade from 2002 to 2013. In 2005, the recovery resource grade peaked but has been reducing steadily since then. It implies that greater tonnage of ore needs to be retrieved from deeper mine locations to remain profitable [18]. These lower ore grades require more consumables, such as water, reagents, and energy, which leads to another challenge South Africa is facing, namely the continuous increase in electricity cost [19].

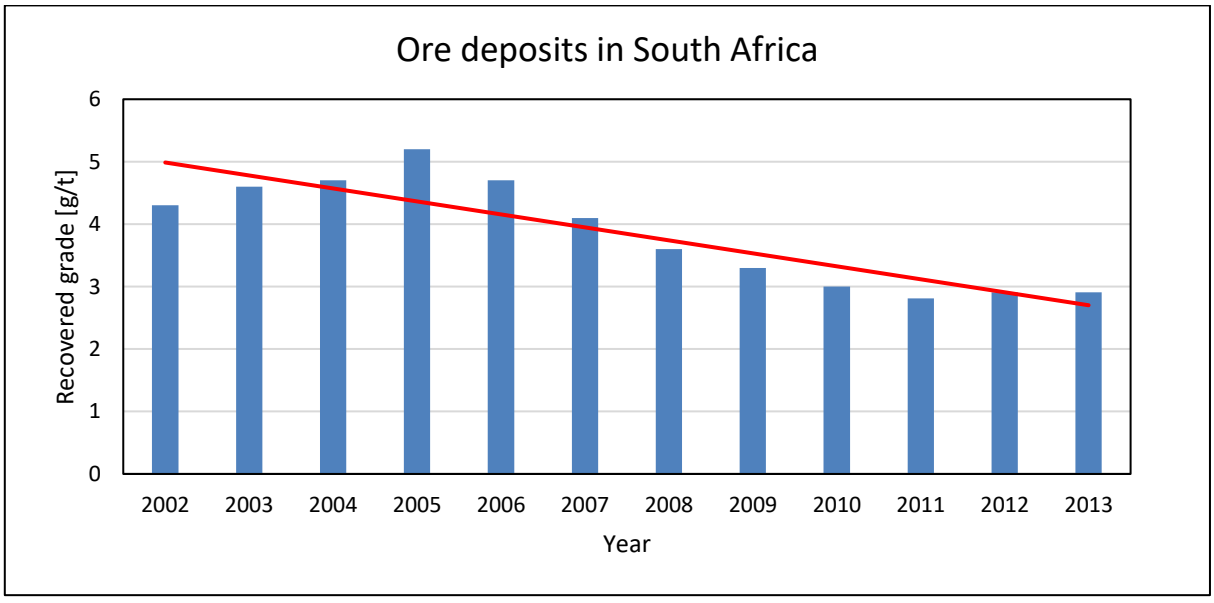

Figure 2: South African average gold grade vs years [18]

Other secondary elements, such as uranium, are also produced during gold production [17]. The early indication of uranium in ore was identified during the late nineteenth century. Minute diamonds recovered from old ore at Witwatersrand in South Africa displayed green fluorescence caused by radioactivity. Uraninite, which is a uranium material, was identified in high mineral concentrates, but it raised very little interest due to its lack of commercial value. However, with the development of the atomic bomb in the 1900s, the focus was redirected [20]. The production of uranium in South Africa started in 1952 and reached a peak during the early 1980s with a total of 6 000 tonnes of uranium per annum. Production has since declined to approximately 250 tonnes of uranium per year in 2020 and has since decreased [21, 22]

Figure 3 depicts the declining trend of uranium production as a by-product of gold mining.

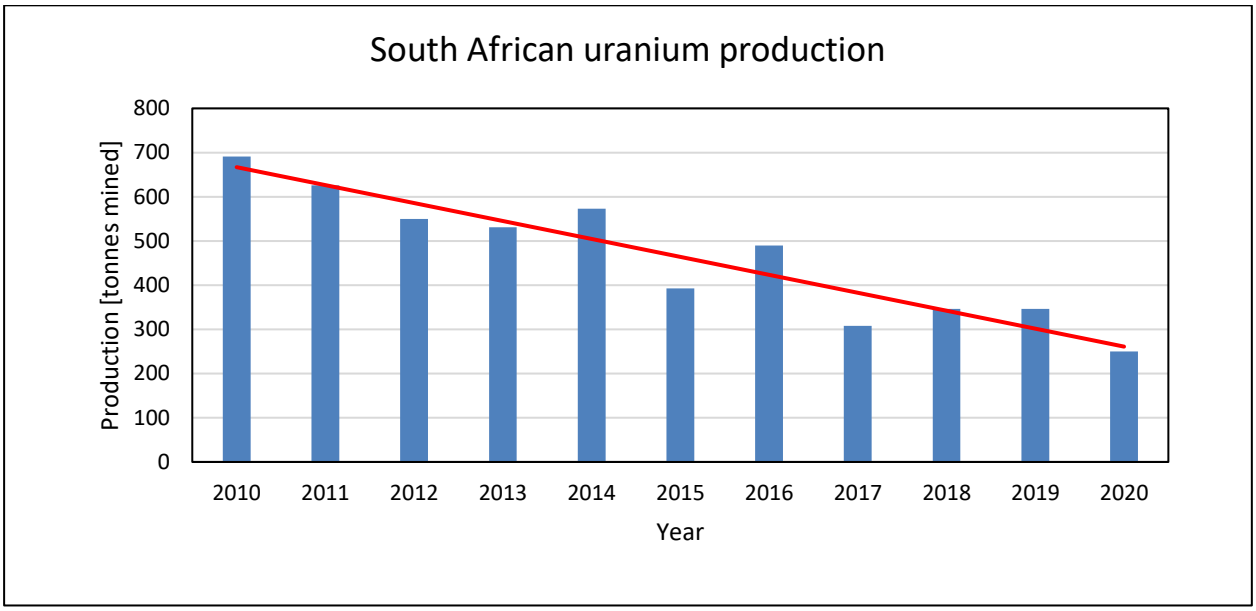

Figure 3: South African uranium production [22]

Since gold mines focus on extracting gold in an efficient manner to reduce operational costs, not much focus has been placed on the uranium retrieved from mined ore. As the operational cost increases and ore grade decreases, focus needs to be directed to the efficiency of the process [14]. Therefore, opportunities exist to treat the uranium for financial benefit. This study focuses on the different factors affecting uranium recovery along with the different methods for improving the uranium recovery process.

1.3 Uranium recovery process

Recovering uranium from ore is a unique process. In the early 1950s, underground mines were responsible for most of the uranium ore. It has since developed from a bare operational industry to a major hydrometallurgical industry. As the industry grew, hydrometallurgical processes such as leaching, solid-liquid separation, ion exchange and solvent extraction became the leaders in these operations [23].

Currently, open-pit mines produce more ore than underground mines. Due to underground mines having a higher quality ore grade, they produce more uranium than open-pit mines even with less tonnage [23]. Even if the uranium recovered from gold production is low compared with other international cases, recovery is still recommended as it improves the overall economic condition. Another benefit is that extra gold can be retrieved from the ore after the acid-leaching process [6].

An ideal mining and processing system can be complex since there are different factors to consider, such as ground conditions, ore depth and ore grade [23]. Lunt et al. [24] reviewed the key factors that affect the flowsheet of uranium, namely uranium mineralogy, capex and opex, and process flow options for the acid-leaching process. The general steps in uranium processing can be summarised as:

- Crushing and grinding.
- Leaching.
- Solid-liquid separation.
- Ion exchange/solvent extraction.
- Yellow cake drying.

A brief description of each step during the process follows, including the impact thereof relevant to the study.

1.3.1 Crushing and grinding

The ore mined during gold production must be crushed into finer pieces until it reaches a fine sand consistency for the extraction process. This process is known as crushing and grinding. A grinding technique commonly used is wet grinding, which physically breaks the uranium ore down to produce *yellow cake* in preparation for the hydrometallurgical processes. This chemical process ensures that a product with a uranium content of at least 65% is supplied to the leaching circuit [23].

1.3.2 Leaching

There are two main types of leaching processes, namely acid leaching and alkaline leaching. Acid leaching was used during this dissertation [25]. Acid leaching is preferred over alkaline leaching since acid dissolve more effectively with coarser grinds and yield more rapid dissolution kinetics [26]. Other reasons for using acid leaching include that it results in shorter leaching times, yields higher extraction efficiencies, and enables the recovery processes after leaching [27].

The most general acid-leaching process used in the industry is sulphuric acid leaching. Sulphuric acid is a widely favoured leachant as it is not expensive and produces an anionic uranyl complex.

This uranyl complex eases the extraction process further by using an anionic exchanger to separate the uranium from other cationic gangue material [28].

According to a study conducted by Siedel [23], the acid used is controlled by the gangue constituents (carbonate minerals) and not the uranium content, but higher ore content results in the ability to control a greater acid concentration [24]. A typical range varying from 10 kg/tonne to 100 kg/tonne of sulphuric acid is used during leaching. The process can vary from a few hours to more than 24 hours depending on the ore grade and temperature of the product. The leaching time can be reduced greatly by heating the slurry [2-6, 23, 29] since a temperature of between 40°C and 60°C are preferred in a variety of mills.

The effect of temperature on the overall uranium recovery is shown in Figure 4. Uranium dissolution is seen to increase along with the increasing temperature of the mixture.

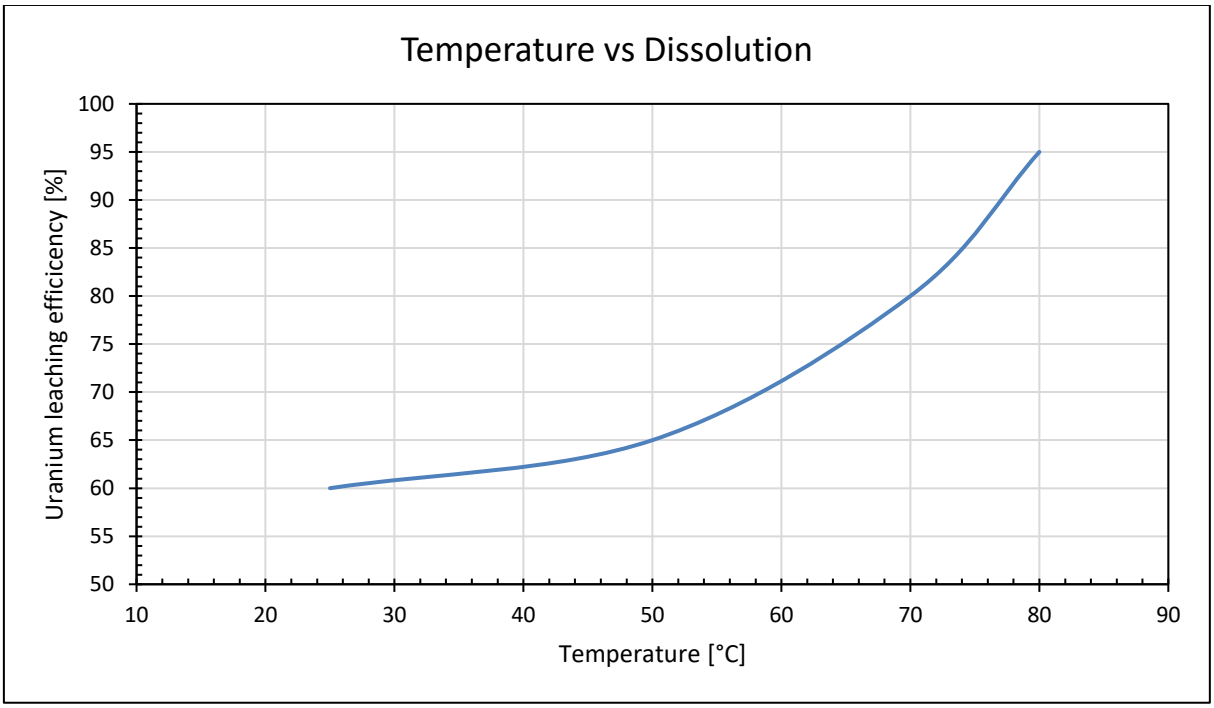

Figure 4: Effect of temperature on uranium dissolution [30]

As acid is added to the mixture, an oxidant such as manganese dioxide should be added since the uranium is in a quadrivalent form [23, 28]. This quadrivalent form is only slightly soluble in the leach solution, and the oxidant promotes the force needed for conversion to the hexavalent form, which enables solubility. Another aspect to assist the leaching process is to vary the acid concentration, which has a great effect on uranium recovery [2-6, 23, 29]. A typical leaching process normally yields a recovery of between 85% and 95% [23].

1.3.3 Solid-liquid separation

Following the leaching process, the solids and liquids of the mixture are separated. The solids are washed to recover adhering leaching solutions. Most mills use countercurrent thickener circuits for washing operations [23]. Chemical agents, known as flocculants, reduce the size of the thickeners by gathering particles in a cluster, which suspends faster and produces a cleaner organic solvent mixture, which is referred to as “OK liquor”. This thickener technique and flocculants used at uranium mills are favoured by hydrometallurgical industries [23].

1.3.4 Ion exchange/solvent extraction

After the solids and liquids have been separated, the process further uses an ion exchange or solvent extraction technique to separate the uranium from the leaching liquor. The uranium industry was the first hydrometallurgical industry to use these two operations. The process starts by adding an agent such as anime salt to extract uranium ions, making it insoluble in water due to the organic complex [23].

The aqueous phase is further separated from the organic phase through decantation and settling techniques. An inorganic salt solution is added to remove the uranium from the organic phase. A typical salt solution is sodium chloride or ammonium sulphate [23].

1.3.5 Yellow cake drying

Once the uranium has been separated, the yellow cake can be precipitated from the solution. When the yellow cake solution is dry and contains no moisture, the product is ready for shipment. It is usually transported to plants that refine the yellow cake to produce nuclear-grade uranium compounds.

The entire milling operating process is shown in Figure 5.

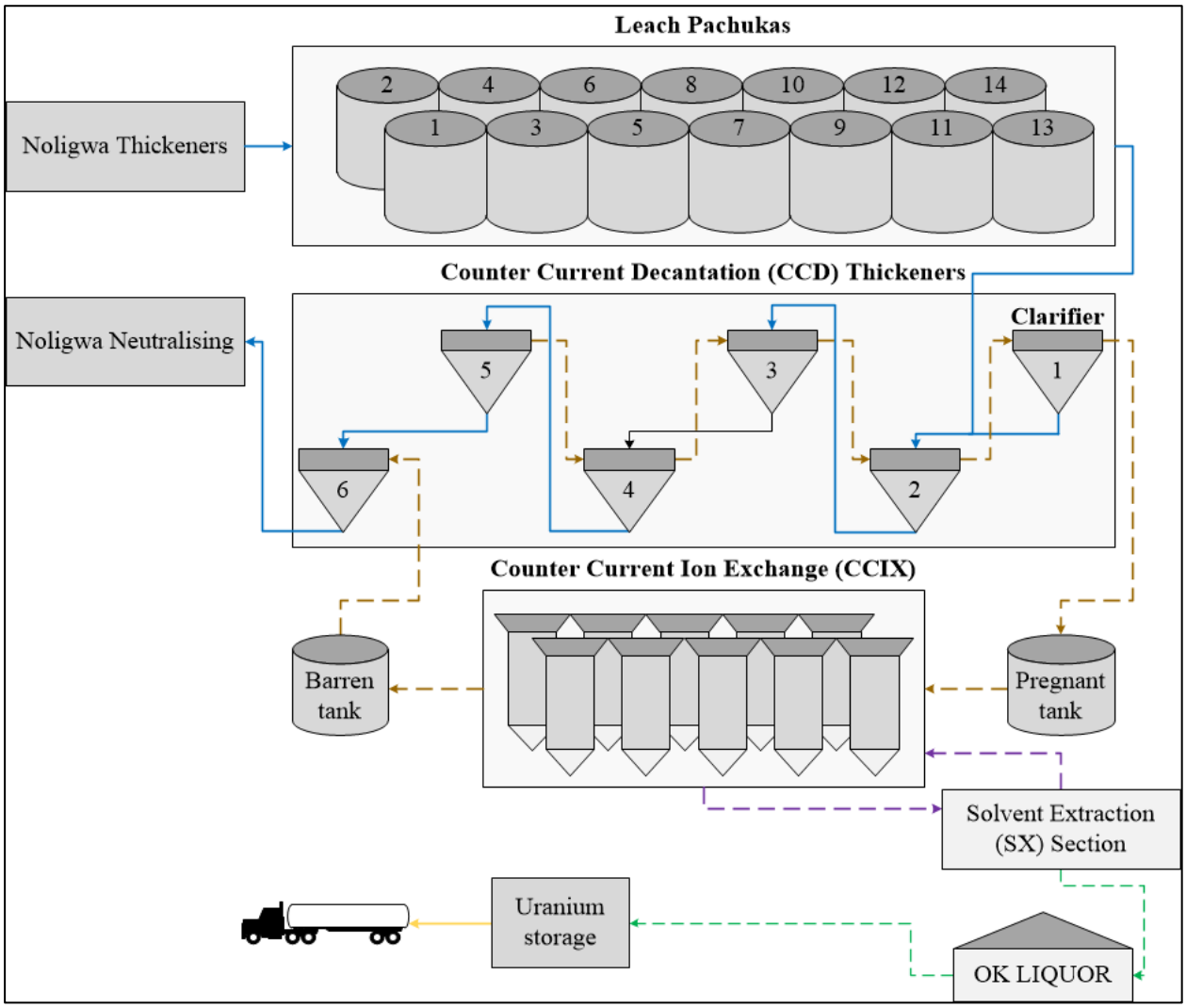

Figure 5: Flow diagram of uranium extraction process

1.3.6 Parameters affecting uranium leaching

Once the uranium recovery process is understood, more focus can be directed to analyse the different parameters that influence the extraction process. These factors are discussed briefly to ensure a full understanding is obtained of their importance.

Leaching time

The first factor affecting dissolution is the duration of the leaching process. Different studies have been conducted to determine the effect of leaching time on the duration of dissolution. Various studies have shown that most dissolution takes place during the early stages of the leaching process [2, 3, 5, 6, 27, 31, 32]. For illustrative purposes, the dissolution of uranium for a 24-hour period is shown in Figure 6.

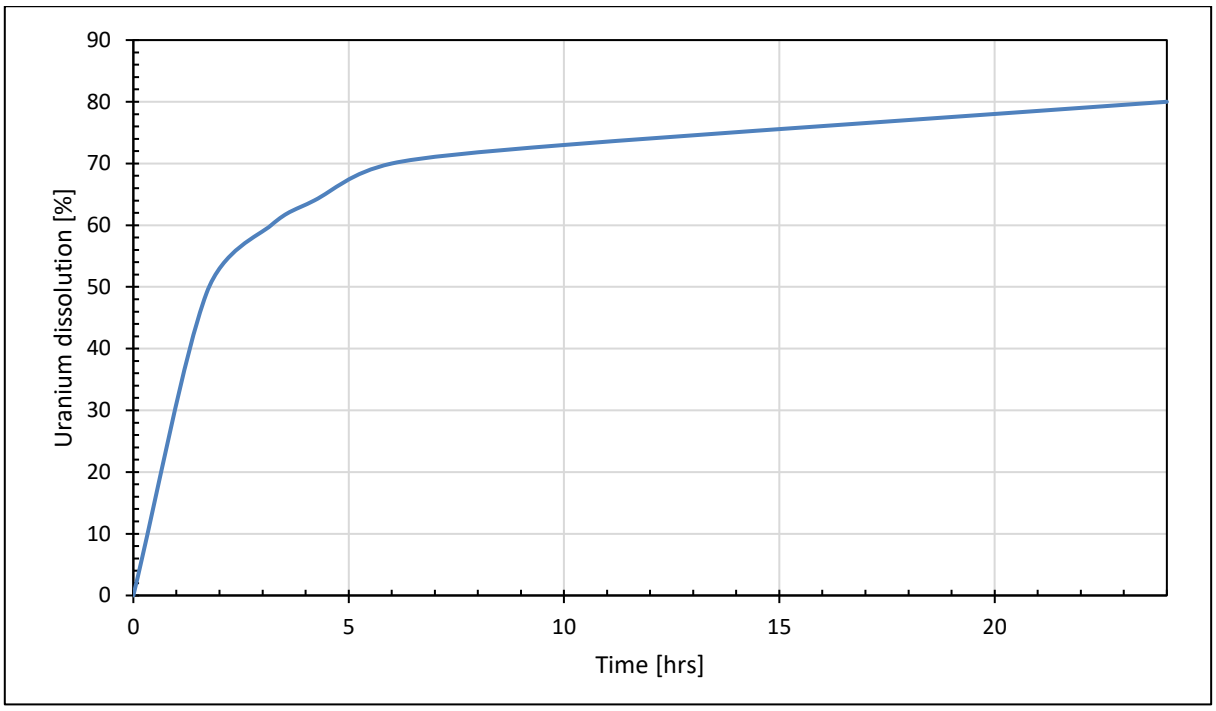

Figure 6: Effect of time on the leaching process [6]

Figure 6 displays the results obtained from the study done by Lottering et al. [6]. The leaching time was investigated with a slurry temperature of 50°C, a manganese dioxide concentration of 3 kg/tonne, and a sulphuric acid concentration of 12.8 kg/tonne. The leaching tests conducted yielded a maximum uranium dissolution of 80%. This yield was not exceeded in a 24-hour leaching period. These parameters and concentrations are typically used for South African uranium recovery [6]. However, different types of ore result in different extraction rates, which is discussed later in the section [33, 34].

The research done during studies conducted by various authors [2, 29, 31, 35] concluded on the same trend as depicted by Figure 6. Each study kept the acid concentration and temperature constant to investigate the effect of leaching time. These studies all concluded that the highest amount of uranium is extracted during the early stages of the leaching process. The next major aspect that affects the leaching process is the effect of acid concentration.

Sulphuric acid concentration

The second aspect that affects uranium dissolution is acid concentration. Sulphuric acid is one of the important aspects that influence the recovery rate of uranium from ore [2, 3, 5, 6, 27, 31, 32]. The effect of acid concentration on uranium leaching is shown in Figure 7.

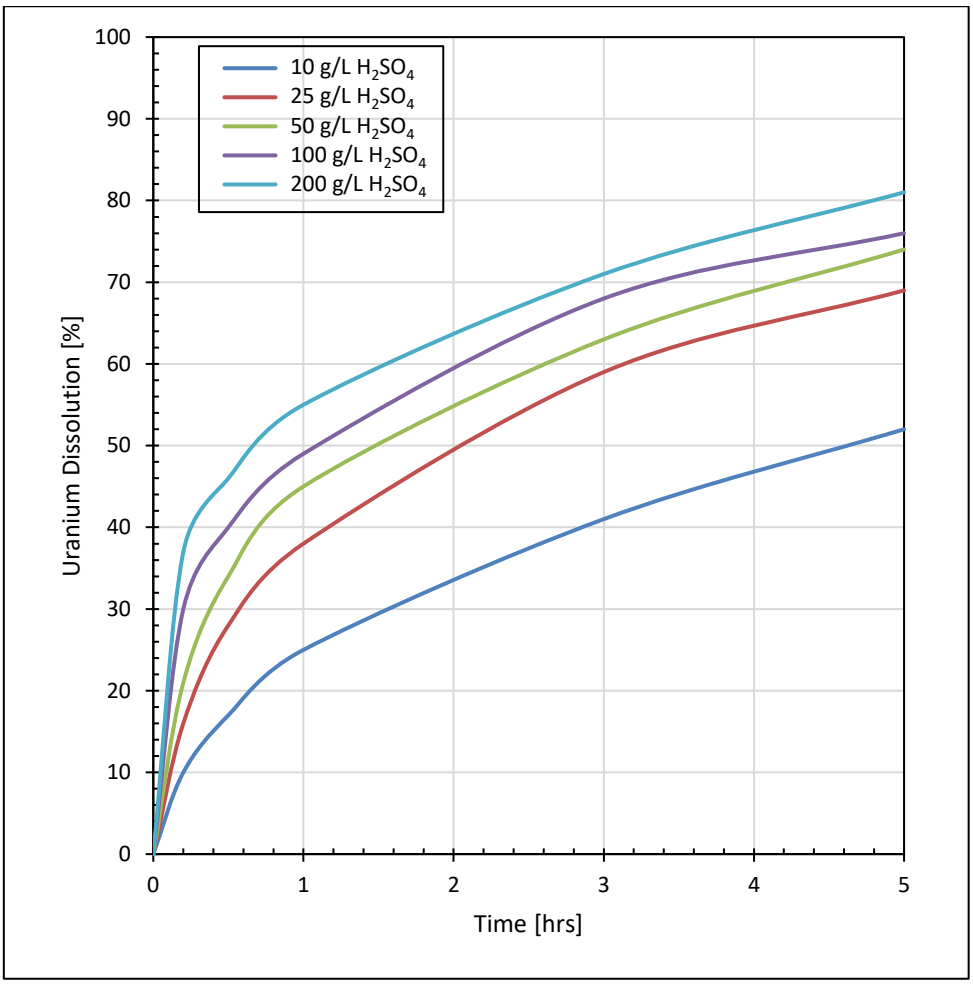

Figure 7: Effect of sulphuric acid concentration on the leaching process [35]

The depiction as seen in Figure 7 clearly shows how sulphuric acid concentration influences uranium extraction over a time of five hours. With a low sulphuric acid concentration, the uranium extraction at the end of the five-hour period is very low compared with the reactions where a more intense sulphuric acid concentration was used. This clearly demonstrates how sulphuric acid concentration affects the uranium dissolution of a mixture. For consistency, the same studies that were considered for the description of the leaching behaviour over time were used to test the effect of sulphuric acid concentration.

The results in Figure 7 were obtained from the study conducted by Gilligan and Nikoloski [35]. The temperature of the mixture used for this study was kept constant at 52°C. The study reviewed sulphuric acid concentration in a range between 10 g/L and 200 g/L. The researchers concluded that increasing the sulphuric acid concentration from 10 g/L to 50 g/L increases the uranium extraction by roughly 25%.

Research done by similar studies resulted in the same conclusion [2, 6, 29, 31]. Every study discussed above clearly indicated the effect of the sulphuric acid concentration. When sulphuric acid concentration increases, so does uranium extraction. Some studies recovered more uranium

for similar sulphuric acid concentrations, but this was due to the temperature difference of the mixture. There are studies that evaluated at very high sulphuric acid concentrations, but for South Africa, these acid amounts are seldom reached [6]. The last and very important aspect to discuss is the temperature of the mixture.

Temperature

A factor affecting uranium recovery greatly is the effect of slurry temperature. To effectively observe the influence of temperature, the different studies discussed kept the leaching time and sulphuric acid concentrations constant. Several studies concluded that increasing the temperature increased the leaching process [2, 3, 5, 6, 27, 31, 32]. For better visualisation, Figure 8 shows the effect of temperature over a 24-hour period.

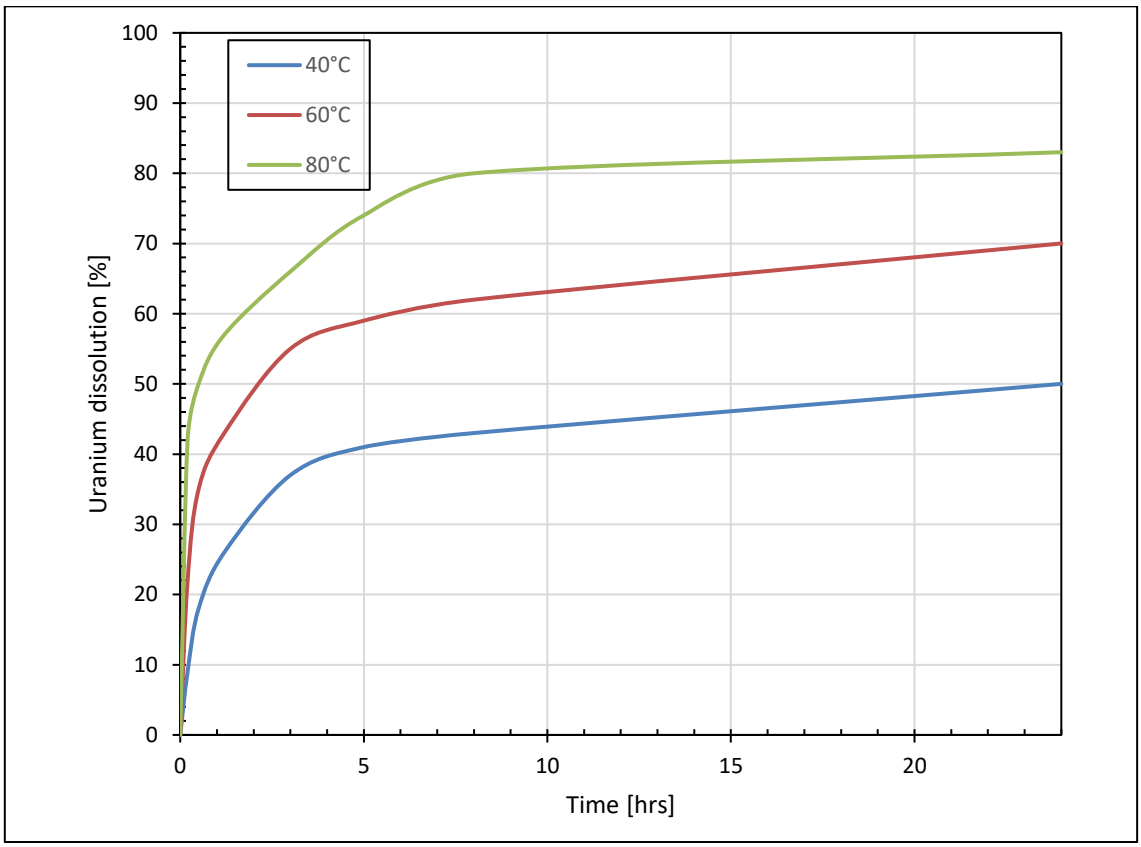

Figure 8: Temperature effect on uranium extraction over a 24-hour period [29]

Figure 8 clearly shows how slurry temperature influences uranium extraction over an entire day of leaching (24 hours). Lower temperatures result in lower uranium recovery – not only lower final extractions but also slower initial dissolution increases. This figure clearly shows that higher temperatures yield higher dissolution rates and final dissolution.

The study conducted by Costine et al. [29] revealed an increase in dissolution as temperature increased. Increasing the temperature of the mixture from 40°C to 80°C resulted in a 30% yield in uranium extraction. The other investigations done are discussed in the literature review.

1.3.7 Summary

Referring to the uranium recovery process as described above, there are several factors that influence the leaching process. Of the different factors, temperature has the most substantial effect on recovery rate [2-6, 23, 29, 35], but sulphuric acid concentration also influences the recovery rate greatly [2-6, 23, 29, 35]. The effect of temperature is discussed more intensively in the following section to highlight the importance of temperature on such a chemical process.

1.4 Literature study

1.4.1 Background

The previous section investigated the uranium recovery process and the conditions that affect the uranium extraction process the most. Different studies concluded that when the temperature of the slurry mixture increases, so does uranium extraction. It is known that brannerite ores typically require high temperatures, high acid concentrations, and longer leaching times to yield a sufficient amount of uranium [4]. Referring to Section 1.3.6, the effect of temperature is considered as the focus of this dissertation.

This section analyses the findings from other studies that investigated the effect of temperature. It further considers the heat sources used in the past that are still applicable. Along with these considerations, different modelling processes are reviewed to indicate the best for the study.

1.4.2 Temperature effect on uranium recovery

Section 1.3.6 mentioned that temperature has a great effect on the leachability of uranium slurry. The different studies that considered varying temperature to test this effect are discussed and the findings obtained from the researchers are investigated. Each study had different parameters that were kept constant to best evaluate the effect of temperature. These parameters are also reviewed to fully understand the uranium recovery process.

Lottering et al. [6] focused on uranium leaching at two different temperatures. To clearly investigate the effect, the manganese dioxide concentration was kept at 4 kg/tonne and the sulphuric acid concentration at 16 kg/tonne. The first mixture was tested at a temperature of 40°C, resulting in an 85% uranium extraction, whereas when the temperature was increased to 60°C, 90% of the uranium was recovered. This resulted in a 5% increase in uranium dissolution with a 20°C temperature increase.

Gilligan and Nikoloski [31] investigated the influence of temperature over a five-hour period during which the sulphuric acid concentration was kept constant at 0.25 mol/L. Leaching the mixture at 25°C resulted in a 30% uranium recovery after five hours, but increasing the mixture to 52°C

increased the uranium recovery to 68%. Lastly, a 96°C mixture temperature reported a 98% uranium recovery.

When Gilligan and Nikoloski [35] discussed the effect of sulphuric acid concentration, they placed more focus on temperature since it had a greater effect. The study observed, for example, that a 10°C increase from 52°C had a similar effect on the uranium recovery than increasing the acid concentration fourfold. This study clearly showed the importance of slurry temperature when uranium undergoes leaching.

Zakia et al. [30] varied the leaching temperature from 25°C to 90°C. Their study emphasised the importance of leaching improvement where temperature was concerned. The samples were tested with an aggressive sulphuric acid concentration of 200 g/L with four hours of leaching. The uranium extraction result was 60% for a temperature of 30°C, whereas increasing the temperature to 80°C improved the uranium extraction to 98.5%. The study concluded that 80°C is the optimum temperature for the leaching specimen since increasing the temperature to 90°C results in a constant uranium extraction, which does not increase the extraction.

Madakkaruppan et al. [2] also investigated high leaching temperatures that ranged from 35°C to 95°C, while keeping the sulphuric acid concentration constant at 38 g/L. After 90 minutes of leaching, the uranium recovery tested at 35°C yielded a 42% extraction, while increasing the temperature to 75°C improved the uranium recovery to 72%. When the temperature was tested at its maximum, namely at 95°C, the recovery yielded an 80% extraction. As the study investigated the early stages of recovery, only 90 minutes were documented.

The studies have consistently shown that increasing the mixture temperature enhances both the slurry leaching rate and uranium extraction. Figure 9 depicts the incremental increase in uranium dissolution where the temperature of the mixture is concerned.

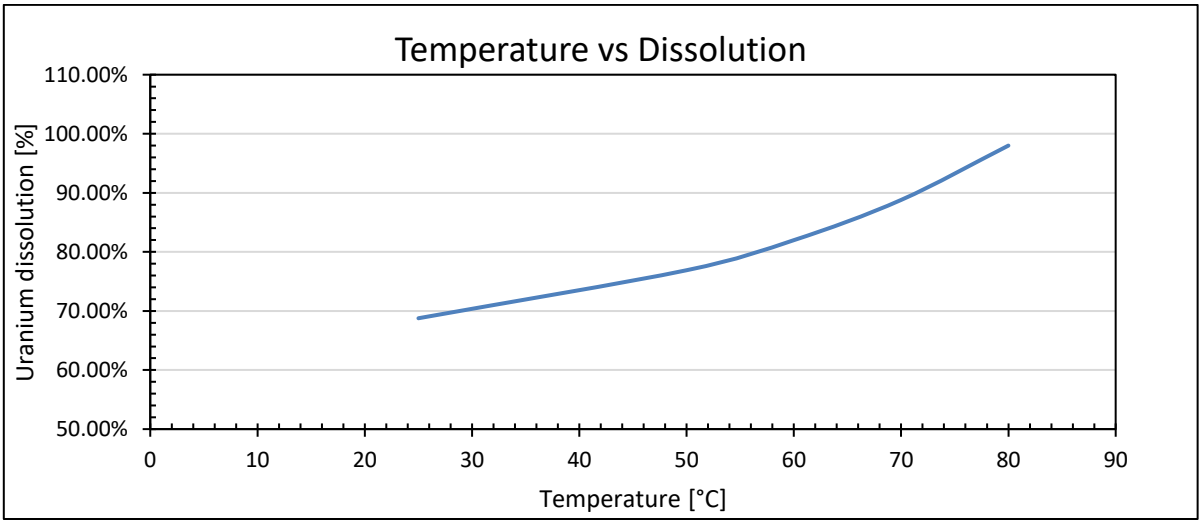

Figure 9: Effect of temperature on uranium dissolution [5]

Figure 9 depicts the relationship between uranium extraction and uranium temperature. Figure 9 clearly indicates that lower temperatures result in lower uranium extraction and higher temperatures result in higher uranium extraction. Increasing the leaching temperature (slurry) has a greater effect on the amount of uranium extraction than the effect if sulphuric acid is increased. However, it is still crucial to know that sulphuric acid is an important aspect to investigate when doing an uranium leaching study [6, 29]. The following section describes the potential heat sources being operated in the industry.

1.4.3 Potential heat sources available

Background

This section discusses the conventional heating equipment and methods currently being used in the industry along with modern technology that reduces the energy usage at different mines. The different equipment to be discussed includes boilers, photovoltaic systems, heat pumps and mining compressor systems. Renewable energy is considered as one of the most promising solutions towards alleviating the energy demand in this specific industry and needs to be investigated. The results are as follows [36]:

Boilers

The industry and power plants typically use boilers to generate steam from water, depending on the requirements, as well as electricity [37]. Boilers assist with other heating purposes, such as space heating for industrial buildings or providing hot water for industrial use, which contribute to heating-related savings [8, 38]. Different studies have been conducted to determine the application of different boilers and the effect thereof.

Almost every major industry uses a steam boiler system. These systems consume approximately 37% of the fossil fuel being burned by United States industries. Steam production is essential in different industries and they allocate different proportions to fossil fuel consumption: 81% is devoted to pulp and paper; 23% to refining petroleum; 57% to food processing; and 42% to chemical industry [39]. The study conducted by Einstein et al. [39] reviewed the energy consumption of boilers used by industry and determined an estimated 6.1 quad (6.4 EJ), resulting in nearly 66 MtCO2e (million tonnes of carbon dioxide equivalent emissions).

Another application for a boiler is converting electricity to heat. Although electric boilers are popular for these applications, they encounter a high amount of heat loss due to radiative losses. The study conducted by Manni et al. [40] investigated the performance of an electrode boiler, which resulted in the boiler achieving an efficiency of 97%. The boiler had the potential of converting 1 444 Wh of electricity to 1 404 Wh of thermal energy, heating the fluid being pumped

through the boiler to 55°C. This warm fluid could heat the air leaving the system to approximately 40–45°C.

The negative side of using boilers is that they experience substantial energy losses and have high running costs. Different heat losses are experienced when a boiler is operational, including convection, radiative, fly ash and blow-down, leading to 20–30% of heat loss [41]. Since boilers are used in large industries, the energy consumed during operation is high [42]. There are methods to ensure that boilers perform efficiently, but some industries do not have proper procedures to account for heat losses in the boiler. This further affects the financial aspect of plant operations as more energy is used to account for heat losses [42]. Demand-side management is an implemented strategy that assists with energy flexibility [42].

Saidur et al. [43] analysed the energy utilisation of a boiler system. The study featured the factors through which the energy being converted could be lost. There is potential for heat recovery with such boiler systems; however, if it is not utilised, the boiler system could result in a high expenditure and lead up to a 22.5% energy loss.

Photovoltaic source

Since the mining industry accounts for a large portion of energy consumption, the importance of other technologies, such as renewable energy, has been increasing. As the energy demand grows along with increased production and materials required, it also increases the need for the renewable energy sector to lower energy costs with an added benefit of lowering carbon emissions [36]. Solar energy is one of these technologies [44, 45]. Solar energy can be converted to the required electrical or thermal energy needed for different applications [46]. Renewable energy is being introduced in different industries, as well as the mining industry [47].

Choi and Song [47] focused on photovoltaic systems at 19 different operating and abandoned mines across the world. The mine of interest was Thaba Mine in Limpopo, South Africa. This chrome mine is one of the largest chromium reserves in the country. CRONIMET Mining Energy AG installed a 1 MW photovoltaic system, which has been operating since 2012. This is the first utility-scale, off-grid photovoltaic system in the country. It accounts for all the mining operations and generates about 1.8 GWh of electrical energy annually.

The mining industry in Chile faces extreme challenges with energy demand, which results in energy costs accounting for 20–40% of the mines' total operating costs. These mines represent the world's largest reserves for copper and lithium. Solar energy is popular in Chile due to high energy prices. From January 2011 to May 2017, the mining industry has grown its renewable energy potential from 591 MW to 3 793 MW. Since then, Chile has been the largest producer of solar energy in Latin America [44]. The study concluded with a comparison of different

technologies that clearly shows that solar photovoltaic systems have the lowest electricity generation cost. This is evident in Figure 10, which compares different systems in industry.

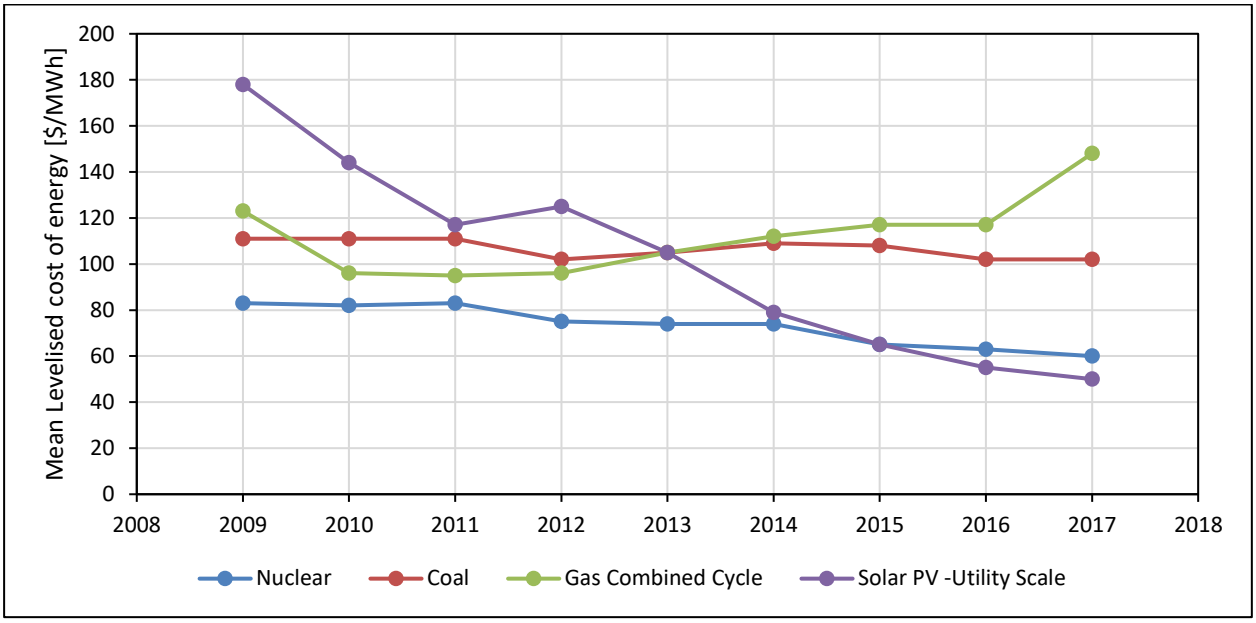

Figure 10: Comparison between technologies based on average levelised cost of energy [44]

Globally, the installation of renewable energy projects has increased from 42 MW to 3 397 MW annually in the years from 2008 to 2019. It is clear that there has been an increase in the renewable energy sector and mostly since 2018 and from 2019, hybrid systems are being installed that accounts for smooth variability [48].

Heat pumps

A heat pump is a device that increases the temperature of a substance from a lower temperature to a higher temperature. It could be used to increase a waste heat source to a useful temperature. This waste heat, which is usually rejected into the atmosphere, could be used to reduce energy costs since it could replace purchased energy. The typical applications for heat pump systems vary between industries; for example, the pharmaceutical industry heats process water and the wood production industry dehumidifies and dries lumber.

Heat pumps could reduce energy costs and lead to cost savings because they use waste heat to increase temperature and deliver that increased heat cheaper than the cost of fuel [49]. This is especially favourable when the heat output could replace energy such as boiler steam, hot water preparation or even space heating [50]. M-Tech industrial [51] compared a heat pump and direct electrical heating for gold mine change house water heating. The study reviewed the typical conditions for flow usage and water temperatures. The study reported that a typical person in a change house uses between 35 and 42 litres of water at 60°C [51]. The payback period calculated for a heat pump, by including the time-of-use tariffs, network demand charge, rates and taxes, for

a normal electrical heating system was around two years with R250 000 annual operating cost savings. Figure 11 shows the break-even point for the heat pump for normal conventional systems [51].

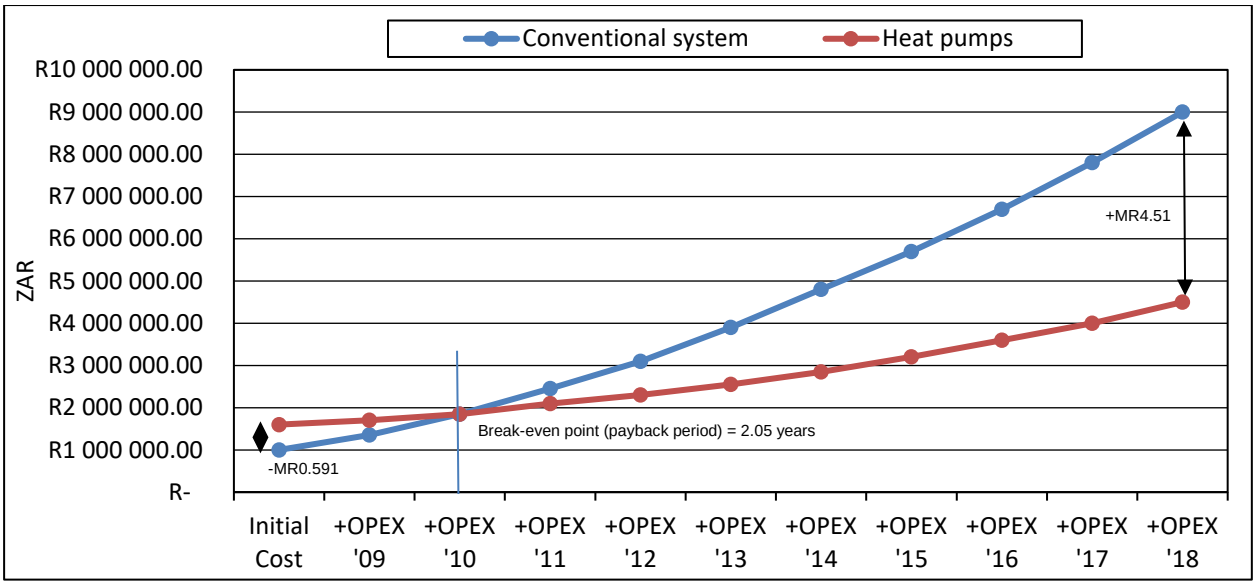

Figure 11: M-Tech heat pump study break-even point [51]

Figure 11 represents the break-even point for the heat pump system under normal operations, as conducted by M-Tech industrial [51]. The figure shows that at Year 2 after project implementation, the cost of normal operations outweighs the heat pump cost, resulting in a payback period of 2.05 years. Compressor waste heat is discussed next.

Compressor waste heat

For compressed air to be supplied for mine production, there needs to be a compressed air system to meet the required demand. This compressed air system can be used as a ring-feed system or a standalone system [52, 53]. For a single standalone compressor, only a compressor house with a different combination of compressors is necessary, whereas a ring-feed system is a bit more complex and includes different compressors in different compressor houses [52].

A typical industrial air compressor converts 80–93% of electrical energy consumption into heat. This poses a possibility to recover the heat and use it on another part of the mine. The heat recovered from such a system can range typically from 50% to 90% [54]. A typical method to utilise the recovered heat is to use it as a source for water heating, industrial process heating, space heating or boiler makeup heating [55]. Industrial drying and space heating use the heated ambient air that passes through the aftercooler system and lubrication cooler, which extracts the heat. A general guideline is that 15 kW (50 000 Btu/hour) is usable for 100 cfm of air and achieves recovery efficiencies of 80–90% [54].

Another aspect is water heating. Water can be heated by using an aftercooler (heat exchanger), using the cold water to cool the compressed air, which results in warm water for other applications. Figure 12 shows a typical aftercooler for decreasing the temperature of hot compressed air, which uses the heated water for heating applications. This hot water could be used for many purposes on mines, namely laundries, heat pumps, cleaning processes or boilers [54].

Figure 12: Compressor aftercooler [54]

De Villiers and Grobler [12] investigated methods for change house water heating. Change houses use calorifiers with resistance heating elements; however, the electrical consumption is very high. The authors introduced waste heat from mine compressors to recover the heat for change house heating purposes. The heat was recovered through an aftercooler with a heat exchange process, heating the water at the change house. The study focused on the factors that affect the energy consumption of the system. A baseline electrical consumption was calculated to determine when the most energy was being used. From the baseline, the authors compared the electrical usage and thermal energy usage. The study calculated a 0.551 MW reduction in power consumption on a daily average, which directly translated to a 13.22 MWh electrical energy consumption reduction per day [12].

The warm water recovered from the aftercooler being used to heat the change house water also needs to undergo a heat exchange process. This usually happens through any typical heat exchanger best suited for the application [54]. Since the medium that needs to be heated is uranium slurry, the ideal heat exchanger is a spiral heat exchanger [56]. The heat exchanger consists mainly of initial expenditure involved for the system, whereas savings are obtained from the running costs since there are no costs involved. Figure 13 depicts the working principle of a spiral heat exchanger. More detail regarding the spiral heat exchanger is given in Appendix A.

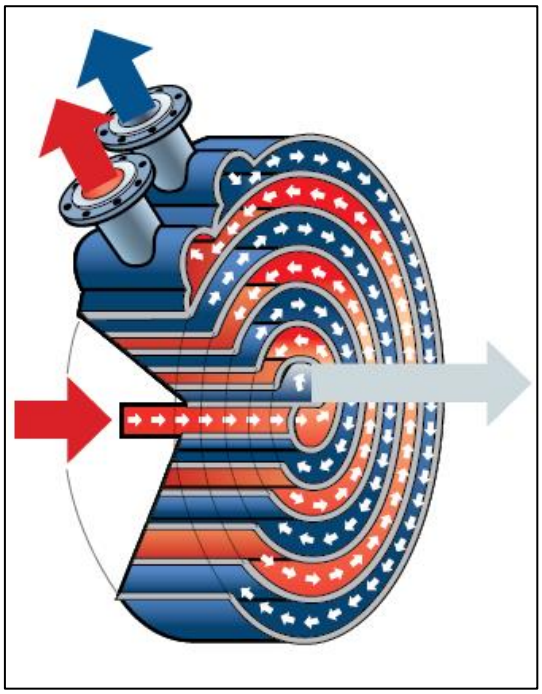

Figure 13: Spiral heat exchanger [57]

Conclusion

The different heating potential sources focused on the amount of heat available and typical applications of the system. The boilers that were investigated produced sufficient heat that could be used for industry applications. However, a significant amount of electricity is required to convert the electrical power to thermal heat, which leads to high electricity usage.

Photovoltaic systems have the lowest operating costs, but the input cost could be high and the storage replacement cost is high, such as a battery storage system. Heat pumps proved more effective than normal electrical heating since waste heat could be introduced to assist with energy costs. Compressor waste heat proved very useful since it captures the heat already being generated and wasted. Although using waste heat has certain expensive initial expenditure, no running costs are involved due to the heat recovery system.

Analysing all these different methods, the most promising method seems to be a compressor waste heat recovery system since compressors produce large amounts of heat, and with such a system, the heat could be recovered and used daily. The only extra expenditure required for the system is a heat exchanger to exchange the heat obtained from the compressors and use it to assist with other process heating, such as chemical plants.

1.4.4 Energy and processing modelling

Different industries comprise complex processes, which can be inefficient if not well maintained or designed. To aid with such processes, several technologies have been developed. The most relevant methods contributing to the study are discussed.

Since the system being used in the study comprises of different mediums through which the energy is transferred, a viable way to obtain accurate answers is through simulations. Different studies have been conducted to test the accuracy of different simulation packages compared with real-life industries [58]. In this section, these studies are discussed briefly to assess the viability of the different simulation packages that could be used to assist with real-world problems regarding efficiency of designing and maintenance.

To accurately simulate mining or plant operations, the following packages could be used [59, 60]:

- Flownex.
- KYPipe Gas.
- Computational Fluid Dynamics (CFD).
- MATLAB.
- Process Toolbox (PTB).

Flownex

Zubair et al. [61] used Flownex software to analyse the behaviour of an emergency core cooling system in a reactor during the early stages of a loss of coolant accident. This is an important simulation since insufficient cooling of such a reactor, or system failure, can lead to a core meltdown. The simulation was conducted successfully and accurate results that were well in agreement with the safety analysis report of the United States Nuclear Regulatory Commission were obtained.

KYPipe Gas

Another study analysed the flow rate in a gas pipeline using KYPipe Gas simulation software. The study resulted in accurate simulations that could be used to analyse the gas pipeline flow [62].

Computational Fluid Dynamics

CFD is a simulation tool used in a variety of industries [63]. Xia and Sun [63] analysed the application of CFD in the food processing industry. CFD was used to design specific equipment that was required during these operations, and it also predicted certain stages during food

processing. CFD as a simulation tool accurately assisted in the early stages of new conceptual designs and for more detailed developments [63].

Furthermore, a CFD analysis was done on the cement industry to aid with the design of a calciner, which is a vital part of carbon dioxide emissions during plant operations. A mathematical model of such a process had been developed and validated before it was used in the CFD simulation software to accurately support this design. Results obtained from the simulations aided with gaining an in-depth understanding of all the different reactions that occur during the process. Understanding the process can further assist with an optimised design for the operations to aid with carbon dioxide reductions [64].

MATLAB

McLean et al. [60] used MATLAB in their study to construct a model to simulate heat recovery for the mining and mineral processing industry. The model aimed to recover heat that was being rejected into the atmosphere, reducing the environmental impact and operational cost. The study successfully concluded with a 42% reduction in carbon dioxide emissions and a 20% reduction in cooling tower emissions, which aid global warming and human toxicity potentials.

Process Toolbox

The investigations conducted by Nell [65] and Nell [66] focused on simulation packages for water systems and compressed air systems, respectively. Nell [65] investigated the reliability of mining dewatering systems by using simulation software to aid with identifying risks and solutions. PTB simulation software was used during the study and accurately simulated a replica of the case study used for the dewatering system. The simulation resulted in an error of 4.2% and prevented previously encountered problems.

Nell [66] analysed compressed air where drilling time in the mining sector was concerned. The compressed air system required for the drilling operations was developed and simulated on PTB simulation software to address the related problems. The study concluded with a simulation error of less than 2%, which resulted in a 20% drilling rate increase due to identifying the obstructions in the compressed air system obtained through the simulation model.

1.5 Need for the study and objectives

Gold and uranium production in South Africa has been decreasing over the past years due to several challenges. The mining sector is experiencing significant financial pressure and current operations need to be optimised to assist operational standards and yield profit margins. The

current process needs to reduce operating costs [15] and improve the efficiency of production; therefore, there is a need to optimise the process.

The uranium recovery process is reliant on the temperature of the slurry. Heat is normally supplied using electricity, which has proven to be expensive when used for heating purposes such as boilers. There is a need to identify energy in the form of heat that is being wasted through mining equipment. The industry wastes 27–29% energy, which can be obtained and reused [67]. Ideally, this heat must be recovered as waste heat since the heat is already being generated and is available. Therefore, the objectives are:

- Develop and verify a current operational heat recovery model.
- Develop and verify a current operational heat source model.
- Develop and verify an empirical model for uranium leaching analysis.
- Integrate the verified models.
- Conduct a feasibility study.

1.6 Dissertation overview

This dissertation started by giving a basic overview of the mining industry focusing on the uranium recovery process. It further discussed the different parameters affecting this process, focusing on the effect of temperature. Knowing that temperature has a great effect, different heat sources were analysed to investigate the potential thereof. To visualise heat potential, different simulation packages were discussed.

This dissertation's main objective is to show that the struggling mining industry has the opportunity to recover heat that is being produced already to improve the efficiencies of uranium plants.

Chapter 1: Introduction

This chapter provided background on the mining industry and highlighted that uranium is a by-product of gold mining. The most common uranium extraction process was discussed to analyse the different factors that could assist with uranium recovery and identify which factors could be used to improve the process.

The importance of temperature was discussed during the first section of the literature review. A few potential heat sources were listed along with heat possibilities. The literature review further investigated the different methods for simulating and predicting the behaviour of a system by analysing different simulation software packages and comparing the accuracy thereof. It highlighted the ideal way of increasing the efficiency of uranium production, which is by heating the mixture and integrating an existing heat source for this purpose.

Chapter 2: Methodology

During this chapter, the method is discussed to assist with the objectives of the study. It describes the steps to construct and verify a current heat recovery system with the aid of simulations. It highlights the steps to identify a heat source that could be used for potential heat recovery. This chapter further discusses the method needed to verify the dissolution data used for the investigation to quantify the benefit of such a system.

Chapter 3: Results and discussion

During this chapter, the results obtained from the methodology to construct and verify a current heat recovery model are discussed. The results obtained from the heat source system that could be used to integrate with the heat recovery are also discussed. Furthermore, the financial benefit of integrating the identified heat source with the heat recovery system is analysed. This chapter concludes with the validation of the study, which describes all the objectives and whether they were completed.

Chapter 4: Conclusion

This chapter summarises the entire dissertation and concludes the research. It further provides recommendations for future possibilities that align with the investigation of heat recovery systems.

CHAPTER 2 – METHODOLOGY

2.1 Preamble

In Chapter 1, a literature review was conducted to analyse previous research regarding a variety of factors that affect uranium processing. The research that was conducted to form part of the basis of this methodology includes the following:

- Different parameters affecting uranium recovery.
- Different heat sources that form part of heat recovery systems.
- Simulation methods that form part of the industry.

This research is used to develop a methodology for constructing, evaluating, and analysing the application of heat recovery systems in the uranium process. The methodology is developed to address the need for the study, as mentioned in Section 1.5.

Figure 14 shows a brief depiction of this methodology process that consists of five steps. First, the current heat recovery system is investigated, whereafter a simulation model is developed. This model is verified with actual data obtained from a system inspection. To verify the simulation model, a replica of a heat recovery system is represented that could be used as a basis for other heat recovery systems [65].

Second, a system containing a heat source that could be used for recovery purposes is investigated. As in Step 1, this heat source is verified to obtain an accurate simulation replica [68].

Third, a chemical plant with the potential of forming part of a heat recovery system is investigated. Since the plant being investigated is a uranium plant, an empirical model is developed and verified to ensure the accuracy of the system data [6, 12].

Fourth, the verified models obtained from Step 1 and Step 2 are integrated. This ensures the maximum possible accuracy for investigating the proposed heat recovery system for recovering the heat from a heat source to improve uranium recovery.

Fifth, the verified data obtained in Step 3 and the integrated model obtained from Step 4 are used to analyse the effect of heat recovery and conduct a feasibility study [69].

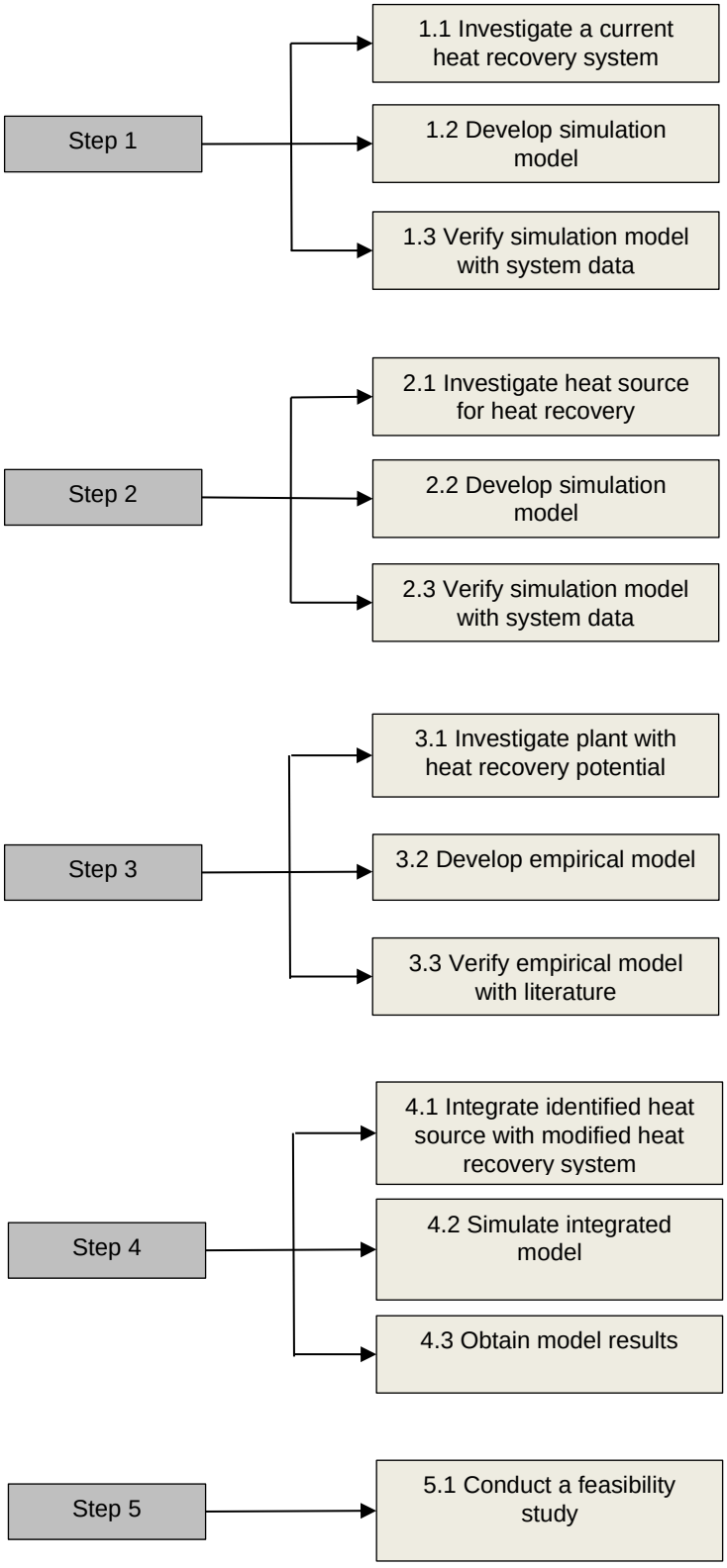

Figure 14: Simplified steps of the methodology

The following section discusses Step 1 of the developed methodology in Figure 14.

2.2 Heat recovery system

Step 1 in Figure 14 is to investigate a current heat recovery system, develop a simulation, and verify this simulation with system data. This section discusses the investigation procedure and model construction of a heat recovery system. Figure 15 shows an overview of the methodology.

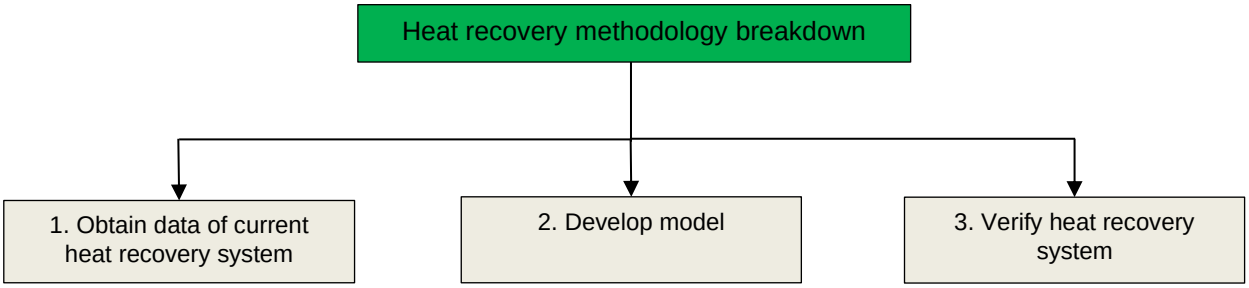

Figure 15: Heat recovery methodology breakdown

The goal of the methodology in Figure 15 is to derive a generic procedure for obtaining a verified heat recovery simulation model. Each step is discussed in this section.

2.2.1 Obtain data

As observed in Step 1 in Figure 15, Maré et al. [70] concluded that the best first step for understanding a system is to construct an overview of the system being investigated and to identify the availability of data. Doing this ensures that all the necessary components that affect this process are obtained, such as the interaction between the heat source and the equipment used to recover the heat.

Generally, the system layout should be acquired through system inspection to understand the current system, and if possible, obtain any system data. Obtaining a general layout of the system is an important step that contributes to model development, where the layout is integrated with the simulation software [65]. System inspection entails doing a walkthrough of the site, which is at the installed location of the current system, to understand the working flow of the process. Ideally, the easiest way to gather data is through sensors that have been installed to monitor different systems and their components. This is not always possible since the system could be quite new, which is not yet equipped with sensors, or people neglect to monitor the system or maintain instrumentation. Figure 16 describes the process for obtaining the data from the system [65].

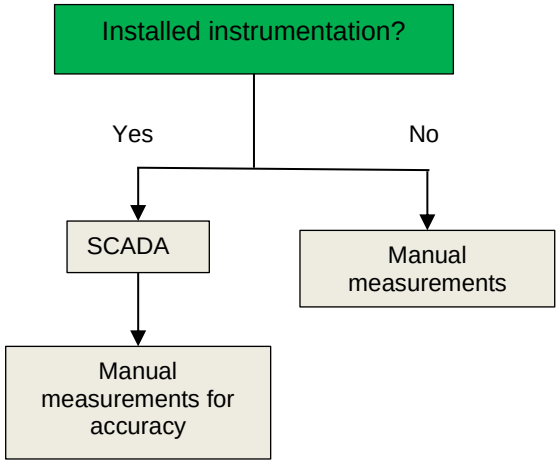

Figure 16: Data collection methods [68]

Referring to Figure 16, if there are any sensors installed, they could assist with monitoring measurements. This data is read at constant intervals and is transferred to the main network, known as the supervisory control and data acquisition (SCADA) system [69]. The SCADA system monitors the processes remotely and is useful since adjustments can be made on the SCADA that controls the system as even alarm triggers can be programmed. An entry is given an address in the system. Each address is known as a tag name, which could assist people accessing a specific search or for reporting [65]. For this investigation, typical readings to be obtained include water flow readings, water pressure readings and water temperature readings.

If no instrumentation is installed, the data should be collected by means of equipment designed for such purposes. Since most heat recovery systems consist of an air-to-water heat recovery system [10], data is collected using the main equipment shown in Table 1. These measurements ensure that all the water flows and temperatures are correct to quantify the effect of the heat exchanger in such a system.

Table 1: Equipment for data collection [71]

Equipment	Measurement	Unit
Ultrasonic flow meter	Water flow	L/s or m^3/s
Ultrasonic thickness gauge	Pipe thickness	mm
Infrared thermometer	Water temperature	°C
Pressure gauge	Water pressure	kPa

Table 1 describes the components typically used to measure water properties [71]. An ultrasonic flow meter and thickness gauge are typically used to measure the water velocity and flow in a pipe. According to Rahmat et al. [71], water probe sensors improve the accuracy of water flow and temperature readings; however, if there are no installed probe sensors, an infrared

thermometer is typically used to measure water temperature. This gives a good indication of the water properties in a pipe.

An important aspect to consider is that a thermometer only measures the surface temperature of a pipe, so the water temperature in the pipe may differ slightly from the measured temperature [72]. Along with collecting the data, the different components affecting the system should also be inspected. These components must be known to construct an accurate simulation model. Table 2 shows the typical components that could be encountered in a system.

Table 2: Components in system [73]

Components	Measurement	Unit
Pipes	Diameter Length Cladding	mm m m
Compressors	Power Flow Discharge temperature Discharge pressure	kW kg/s °C kPa
Pumps	Power Flow Head Efficiency	kW L/s m %
Cooling towers	Duty Water flow Airflow Dam volume	kW L/s kg/s m^3
Heat exchanger (Aftercooler)	Type Designed duty	– kW

Table 2 lists the different components to be investigated. The data obtained from this investigation is crucial since it contributes to the verification of the system, but this data must be accurate. Manual measurements, using the equipment in Table 1, should also be conducted on the relevant components, which consist of sensors for ensuring accurate data. The instrumentation should be verified within an accuracy range of 10% [65].

These steps must be followed to ensure accurate data of the system is collected as the results obtained from the simulation model need be compared with the data obtained from the system investigation. Once the data has been obtained accurately, the following part of this methodology can commence, namely, to discuss all the steps that should be taken to develop the simulation model for the heat recovery system.

2.2.2 Develop model

As observed in Step 2 in Figure 15, the following step is to develop the model. With an understood concept of a heat recovery system and identified data points, a model can be constructed to simulate the process. The process to develop this model is discussed in this section.

Firstly, simulation software should be considered for model development. Section 1.4.4 discussed the different simulation packages that are used often. Studies concluded that Flownex and KYPipe Gas do not have the ability to view real-time data through an interface, and KYPipe Gas is not suitable for compressible fluids [59, 66]. The studies reviewed in Section 1.4.4 concluded that PTB was the preferred package to use since it has a variety of integrated thermodynamic properties and has been proven to be an effective simulation program, which uses a drag and drop interface to communicate to the components [65, 66, 70]. Although CFD is also a popular software package since it aids with the predesigning of integrated systems, PTB is used for this study as it focuses on the heat recovery from mining equipment, which is a thermodynamic system, and accounts for different losses such as heat from pipelines and pressure during pipe bents. An overview of the procedure that should be followed to develop a model is shown in Figure 17 [66].

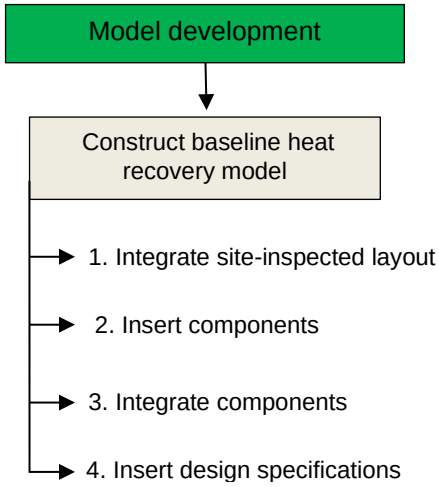

Figure 17: Baseline heat recovery model development

Figure 17 shows that the first step is to integrate the layout of the system. This site-inspected layout is constructed using the data collected and procedures, as mentioned in Section 2.2.1. The different components acquired from the data collection are inserted in the precise location for maximum accuracy by using a satellite view of the surface and placing each component where it is supposed to be [73].

Accurately simulating the model requires inserting all the components that influence the system, as observed in Step 2 in Figure 17. When these components have been inserted, the following

step is to integrate these components by connecting each node and pipe in the system to ensure correct flow direction [73].

Lastly, the typical design specifications are inserted. From Table 2 in Section 2.2.1, this entails inserting all pump and pipe sizes, specifying the heat exchangers and aftercooler according to their designed duties, and ensuring the boundaries represent the correct temperature and pressure. When all these steps have been followed, the model should be ready for simulation and should depict the current heat recovery system. The following step in Figure 15 describes the process that should be followed to verify the simulation model. It is discussed in the upcoming section.

2.2.3 Verify system

As observed by Step 3 in Figure 15, the following step is verifying the simulation model. Using the steps to develop the model, a representation of the actual heat recovery system should be obtained. Figure 18 shows an overview of the procedure for verifying the simulation model [73].

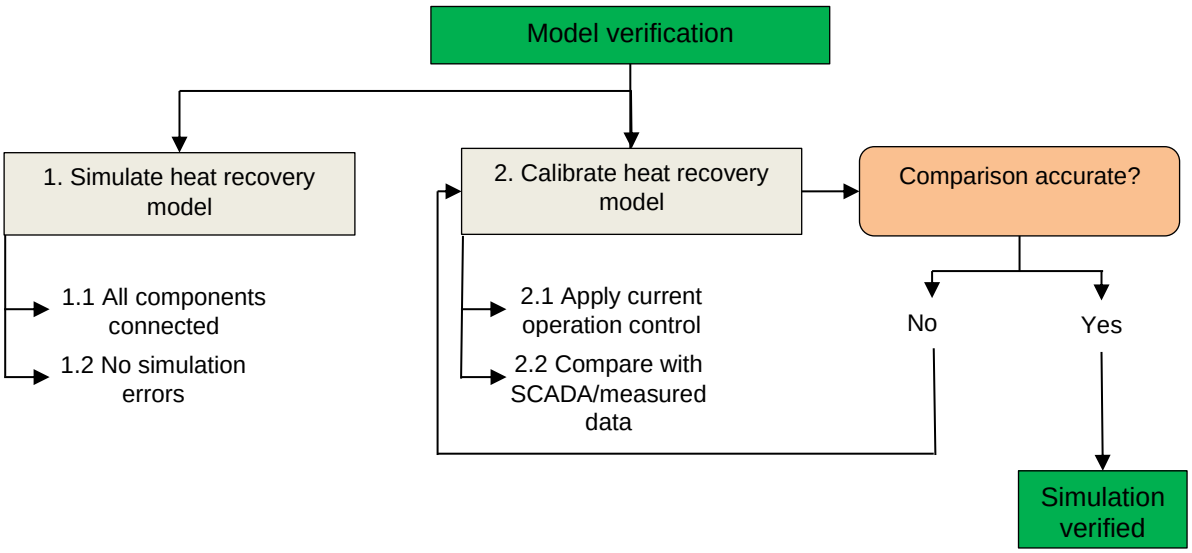

Figure 18: Verification of heat recovery model

Figure 18 clearly describes all the steps for ensuring that the model is verified, and if not, which steps should be repeated. The first step is to ensure a working simulation model. The simulation parameters are set to the initial conditions and boundaries. When simulating the model, the model should run to show that all the components are connected and there should be no errors. This is a prerequisite for the calibration and verification of the model since without a working model, calibration cannot be done [66]. After a successful simulation run, it is important to compare the obtained results with the actual data collected from the site audit, as outlined in Section 2.2.1. This step is crucial for ensuring that the simulation represents the real-world process accurately.

Step 2, as described in Figure 18, describes the process for ensuring an accurate simulation. The first subtask is to apply the current operation control systems. This typically includes the pumping schedule, demand usage at places, such as change houses, valve statuses, and ambient conditions, such as the air temperature, humidity, and pressure.

After the control system or philosophy has been applied, the next step is to compare the simulated results with the SCADA system or measured readings. These readings should be retrieved from reporting data and from the tag values, which can be selected specifically for the period of investigation. The comparison between the results of the heat recovery model and actual data should be within an accuracy range of 10%, which is the minimum deviation required for an accurate simulation [65, 66].

The simulation is verified once the results are within a 10% range of the SCADA or measured values. If not, Step 2 should be reviewed to ensure all controls and components are correct. This process should be repeated until the simulation is verified. This procedure outlined in Section 2.2 is designed to obtain a verified model of a current working heat recovery system that could be used as a baseline for other heat recovery projects.

The next section discusses the development of a methodology for investigating a system, which contains a heat source, and the construction of the dedicated simulation model.

2.3 Heat source system

Section 2.2 discussed the procedure to develop a generic method for investigating a heat recovery system and developing a model to replicate the true system. This was the first step, with the second step in Figure 14 being to investigate and develop a methodology that could be used for a system that contains a heat source, which may form part of a heat recovery system.

In this section, some of the steps described previously (refer to Section 2.2) remain the same, but the focus shifts to identifying and simulating a heat source that can be used for potential heat recovery. An overview of the methodology procedure is shown in Figure 19.

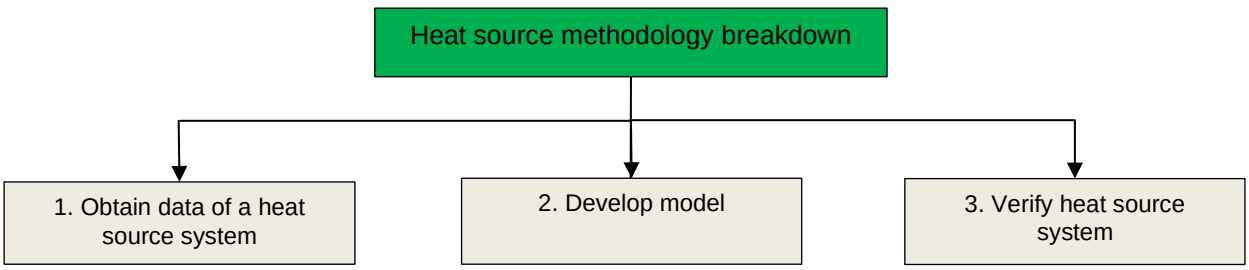

Figure 19: Heat source methodology breakdown

The goal of the methodology in Figure 19 is to derive a generic procedure that could be used to obtain a verified heat source simulation model. Each step is described in this section.

2.3.1 Obtain data

As observed in Section 2.2.1, the best first step is to inspect and investigate the location of the heat source to create an overview of the system. Once a verified heat recovery model has been obtained, the important factors to consider include the source of heating equipment, accessibility of this source, and possibility of being used for heat recovery.

Section 2.2.1 showed that a site inspection should be done to obtain the layout of the possible heat source. In addition to exploring the heat sources, other factors, such as accessibility, infrastructure and data locations, should be examined to enhance the precision of the ultimate simulation.

Figure 16 illustrated the typical methods for collecting data, which is usually done with sensors that read the values to the SCADA system. If not possible, data should be collected manually using the designed equipment for such purposes. The equipment typically used for water measurements include an ultrasonic flow meter, ultrasonic thickness gauge, and infrared thermometer as shown in Table 1. The typical components for a heat source system are similar to Table 2 and are shown in Table 3.

Table 3: Components in heat source system [73]

Components	Measurement	Unit
Pipes	Diameter Length Cladding	mm m m
Compressors	Power Flow Discharge temperature Discharge pressure	kW kg/s °C kPa
Pumps	Power Flow Head Efficiency	kW L/s m %
Cooling towers	Duty Water flow Airflow Dam volume	kW L/s kg/s m^3

Table 3 lists the different components and data that could be required in the investigation to ensure that an adequate system is investigated with the potential to form part of a heat recovery system. Once accurate data has been obtained, the methodology procedure can commence, which discusses all the steps required to develop the simulation model for the heat source system.

2.3.2 Develop model

Once all the data has been obtained as discussed in Section 2.3.1, the model development can begin as shown in Step 2 in Figure 19. This process is discussed in this section.

The aim of the methodology is to create a simulation model that replicates the actual heat source system and determines its heat potential. Section 2.3.1 outlined the process for obtaining the necessary information during the site inspection, which is shown in Figure 20. The green highlighted section represents the necessary information to be obtained for the simulation model.

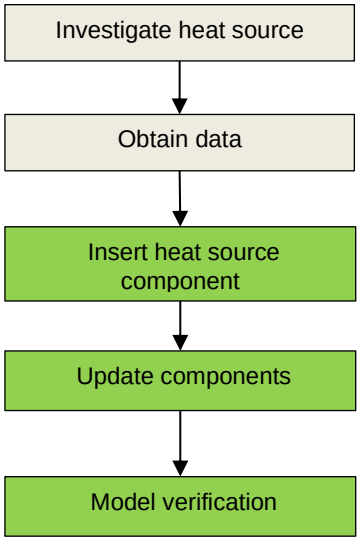

Figure 20: Heat source model process flow

Figure 20 clearly shows the construction process of the heat source model. The heat source on the mine must be investigated and constructed to replicate the actual system. Using the procedure as outlined in Figure 20, the model can be developed once all the data has been obtained. Figure 17 in Section 2.2.2 listed the basics steps for developing a model that shows the heating potential. The steps are similar, but instead of simulating a complete heat recovery system, only the heat source along with its components are simulated and verified. Figure 21 shows these steps and process.

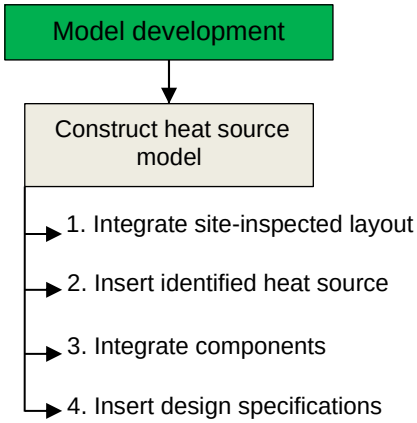

Figure 21: Heat source model development

Referring to Figure 21, all the components that could influence the system should be collected from the site inspection to ensure that the system can be simulated with complete accuracy. These components mainly include the compressor sizes, amount of heat available, the cooling performances, such as those for the cooling towers, and the pumps available for transferring the fluid.

As seen in Figure 21, the first step is to integrate the new site-inspected layout. The data collected from the audit is used to ensure that the pipe layout and different components are accurate. These components typically include cooling towers, pumps, dams, and compressors, which should all be in their correct location.

Once the layout has been updated to reflect the heat source system, the integration of all these components commences. This involves connecting each node and pipe in the system to ensure the correct flow direction. The design specifications as mentioned in Section 2.2.2 should be considered and applied as well. Once all the steps have been completed (refer to Figure 21), the simulation should reflect the real-world operations.

Lastly, once the simulation is solving without any errors, it should be verified to quantify the heat potential that could be used. The verification steps are similar to Figure 18 in Section 2.2.3, with the only difference being that the heat source system is not yet a working heat recovery system, which will be simulated accordingly.

The following step, as observed in Figure 19, describes the process for verifying the simulation model, which is discussed in the upcoming section.

2.3.3 Verify system

As observed in Step 3 in Figure 19, the following step is verifying the simulation model. As mentioned in Section 2.2, once these steps have been completed, the model should represent

the actual heat recovery system. Figure 22 only represents an overview of the verification procedure since it is similar to the steps for the heat recovery verification, as described in Section 2.2.3. The system should simulate within a 10% accuracy range [65, 66].

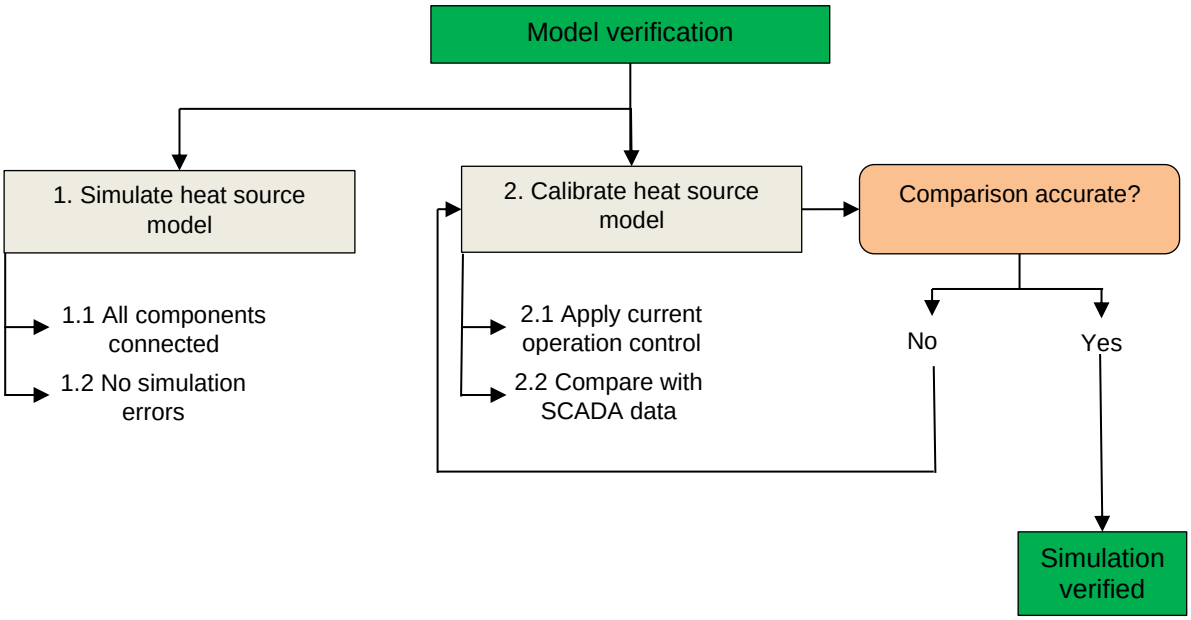

Figure 22: Verification process of heat source model

Once the simulation model is considered accurate and verified, the heat being generated can be quantified. This should represent the potential that can be used for other aspects, such as a heat recovery system, as discussed in Section 2.2.

The development of a methodology for constructing an empirical model is discussed in the following section. This model is used to verify the chemical plant data obtained from the investigation.

2.4 Empirical model

Sections 2.2 and 2.3 discussed the steps for developing the methodologies for obtaining verified heat recovery and heat source systems, respectively. Once both systems have been verified, the simulations can be modified and integrated to simulate potential heat recovery systems accurately. As mentioned, a heat recovery system needs to have at least two main components, namely a heat source and demand (refer to Section 2.2) to which the recovered heat is applied [12].

The demand for this study is a chemical plant. Data should be collected, an empirical model developed, and the results verified. Figure 23 shows the methodology adopted in this section.

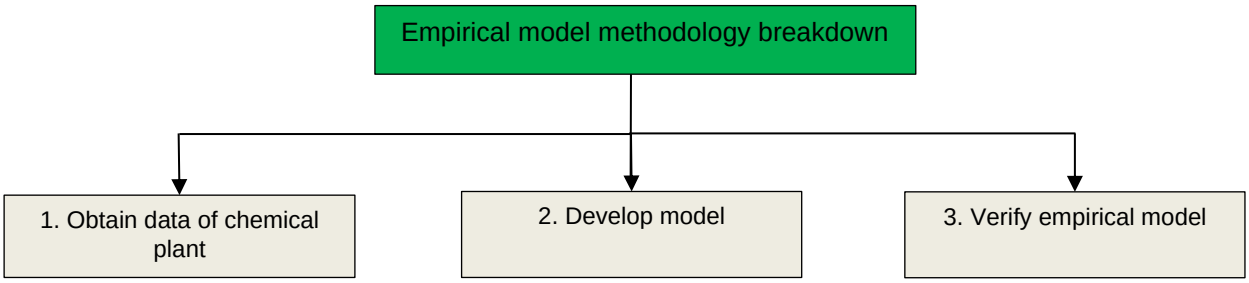

Figure 23: Empirical methodology breakdown

Each step in the methodology breakdown in Figure 23 is discussed in this section to ensure all the aspects affecting the system is covered.

2.4.1 Obtain data

Referring to Section 2.2.1, the first step is to investigate the system to be used for heat recovery. If the type of plant considered for heat recovery integration is unknown, it should first be identified, followed by a plant investigation. Typical aspects to consider when choosing a plant is ensuring that there is clear potential for heat recovery, which justifies an investment. It should further be accessible for integration with industrial operations such as mines [74]. Table 4 lists different aspects that should be investigated before identifying a potential plant.

Table 4: Basic information needed to identify heat recovery application [74]

Components	Type
Plant	Chemical Mining Manufacturing
Infrastructure	Pipes size Pumps size Cooling units Heat exchangers Dam size

Once all the aspects as listed in Table 4 have been considered, the system is investigated further to obtain the relevant information that forms part of the analysis. Since the heat recovery system will be integrated with a chemical plant, Table 5 lists the specific aspects that should be reviewed.

Table 5: Different factors that may influence chemical processing [5, 6, 30]

Factors	Unit
Temperature [5, 6, 30]	°C
Acid concentration [5, 6, 30]	kg/tonne
Leaching rate [5, 6, 30]	hours

Factors	Unit
Ore grade [5, 6, 30]	g/tonne
Chemical density [5, 6, 30]	kg/m^3

Once the information in Table 4 and Table 5 have been obtained, the next step according to Figure 23 is to develop the empirical model. This model is used to analyse the behaviour of the chemical processes of the plant, which is discussed in more detail in the following section.

2.4.2 Develop model

Once all the mentioned data have been obtained (Section 2.4.1), the empirical model is developed. This model analyses the behaviour of the processes at the chemical plant, for example, the leaching process.

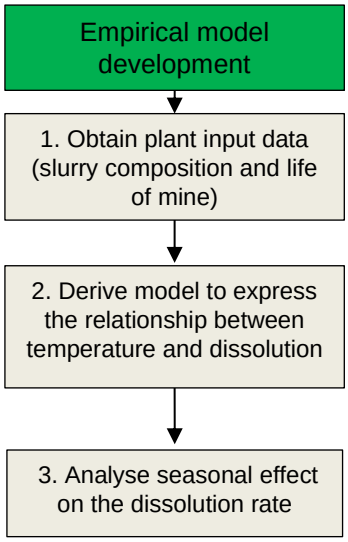

Figure 24: Empirical model process flow

The first step in Figure 24 is to obtain the plant input data. As outlined in Section 1.3.6, this typically entails obtaining certain parameters that affect the chemical processes and some general data as discussed in Section 2.2.1.

The second step in Figure 24 is to derive an empirical model that expresses the relationship between certain aspects, such as temperature, and chemical process, namely dissolution. Referring to the literature review conducted in Section 1.4.2, several studies were investigated to derive a relationship between these two aspects.

The third step in Figure 24 entails analysing the expression for different seasons throughout the year. As outlined in Section 1.4.2, varying temperatures affect the chemical processes differently. During the year, different seasons experience different temperatures, which is important data when analysing a dynamic model.

When all these steps have been followed, the model can be used to test different aspects affecting the chemical processes. The next step in Figure 23 describes the process to be followed to verify this model, which is discussed in the following section.

2.4.3 Verify system

Once the empirical model has been developed, the model should represent the processes pertaining to the chemical plant. Section 1.4 noted that the best technique for ensuring that these processes are correct is by verifying the models. An overview of the verification procedure is shown in Figure 25.

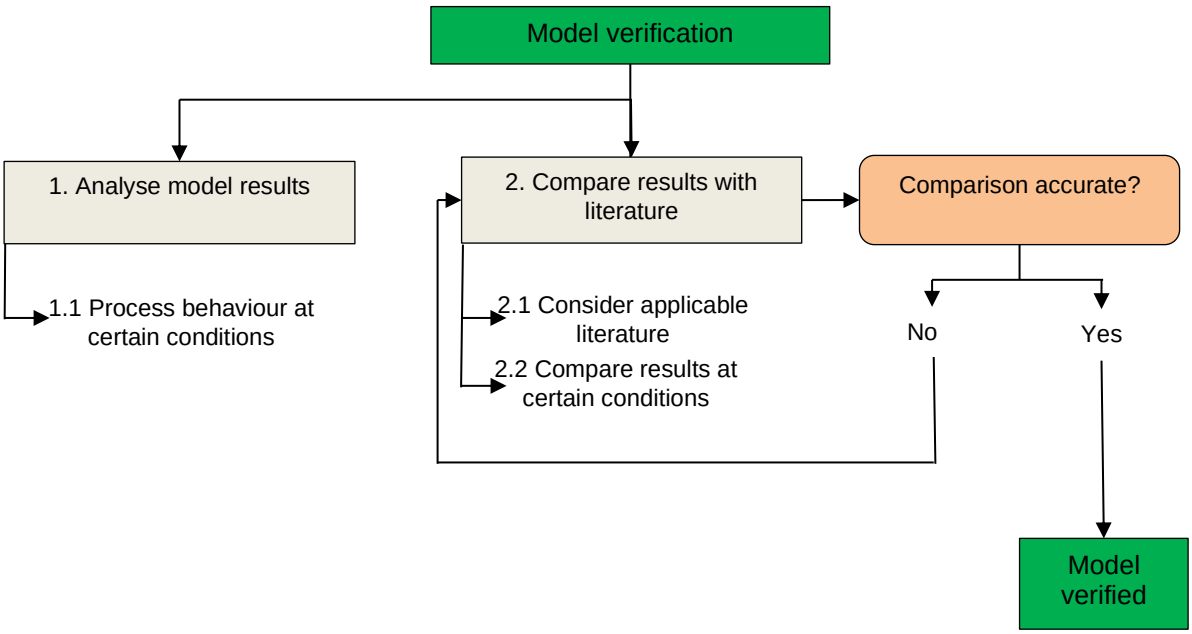

Figure 25: Verification procedure of empirical model

Figure 25 clearly describes the procedure that must be followed to verify the model. First, the results obtained from the model developed, as described in Section 2.4.2, should be analysed. These results should describe the process behaviour at certain conditions, for example, investigating the leaching process under given temperatures or different leaching concentrations, as indicated in Section 1.4.

Once the results have been analysed, the following step is to compare these results with literature relating to the study. The literature for this comparison was reviewed during the literature review in Section 1.4. Comparing the results with actual research ensures trustworthy and accurate results that can form part of the final model integration [62, 66].

If the comparison is accurate or deviate with accurate reasons (scaling in pipes may influence readings), the model is verified; however, if the comparison is inaccurate, the results should either be re-analysed or be recompared with literature more relevant to the plant being investigated.

This process should be repeated until there is a clear correlation between the results and research conducted.

Once the previously described models in Sections 2.2–2.4 have been verified, an integration process of these models needs to be developed. This ensures accurate information and models that can be used to simulate possible heat recovery scenarios. This process is discussed in the following section.

2.5 Model integration

Using the methods discussed in Sections 2.2 and 2.3, a verified current working heat recovery model should have been obtained and simulated along with an identified heat source that could form part of a heat recovery system. Integrating these models establishes a solution model for using the identified heat source to simulate potential heat recovery models for other mines or plants. The model as described in Section 2.4 highlighted that a feasibility analysis should also be conducted, but the solution model must be developed first.

The fourth step in Figure 14 is to integrate the heat source model with the modified heat recovery system. The reason for referring to a “modified heat recovery system” is because the simulation model used for the current working heat recovery system may not be the same for every application, thus the model should be updated with the desired requirements. The integrated model will be referred to as the “solution model” henceforth. Figure 26 shows the process.

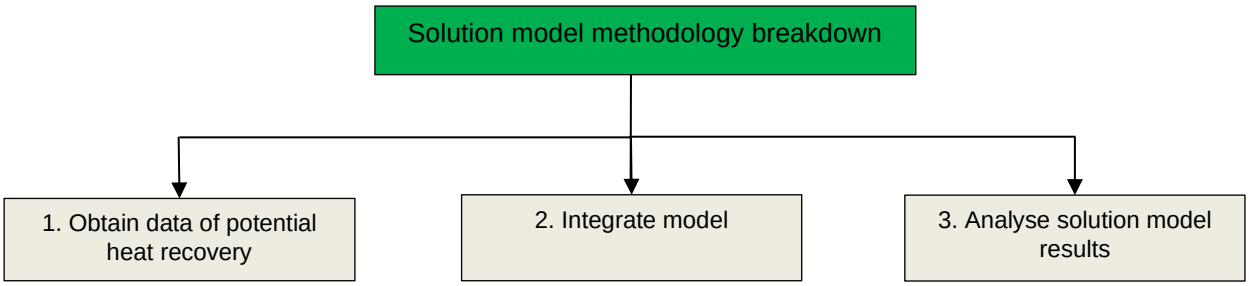

Figure 26: Solution model methodology breakdown

Each step regarding the investigation and modification of a potential heat recovery system, as seen in Figure 26, is discussed in this section.

2.5.1 Obtain data

Referring to Section 2.2.1, the first step is to investigate the location where the system is planned to be implemented. This location should be where the heat source system that needs improvement is currently in operation in the chemical plant.

Section 2.2.1 mentions that the infrastructure should be assessed and any data locations that could be used to increase the accuracy of the simulation should be investigated. This typically entails investigating which infrastructure could be used to integrate the systems and, if not available, which could be added. Aspects typically considered include components, such as pipes, pumps, and accessibility between locations. This is further discussed in the feasibility analysis for this study.

As mentioned in Section 2.4, a heat recovery system consists of at least two main components, namely the heat source and the demand that uses the supplied heat from the source. Thus, an overview of this process should be obtained. The steps were discussed in Section 2.2.1, which should be similar to the heat recovery system explained.

Once accurate data has been obtained, the simulation model for the potential heat recovery system can be modified and integrated. The steps are discussed in the following section.

2.5.2 Modify and integrate model

Once all the data has been obtained as mentioned in Section 2.5.1, the model modification can begin. The model to be changed has to simulate the solution model, which consists of the identified heat source and the identified plant for implementation. Figure 27 depicts the process flow used to modify and simulate the solution model.

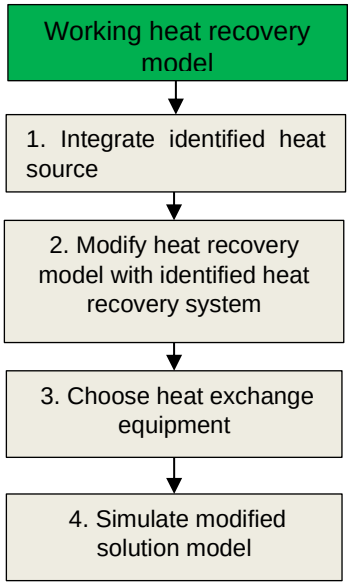

Figure 27: Solution model process flow

Step 1 in Figure 27 is to integrate the identified heat source that was investigated, developed and verified in Section 2.3 with the working heat recovery model developed in Section 2.2. The integration of these models ensures that a working verified simulation model is used along with a

working verified heat source, which allow for accurate simulations to quantify the heat available for recovery.

Step 2 in Figure 27 describes the modification process of the heat recovery model and the information obtained in Table 4 should be used. This ensures that the heat recovery potential from the heat source and identified heat recovery system are accurate.

Section 2.2.2 discussed the steps for ensuring an accurate simulation. These basic steps entail integrating the new inspected layout into the modified model to ensure all the components are in the correct and accurate locations.

Step 3 in Figure 27 is to choose the type of heat exchange process and equipment that could be used for this system. Section 1.4.3 noted that when heat must be transferred from one medium to another, a heat exchanger is the ideal approach [56, 57]. A heat exchanger is thus selected for the simulation process since knowing the optimal heat duty for the heat exchange process should improve the simulation accuracy.

Step 4 in Figure 27 describes the last step before the results can be obtained. Once again, the nodes, pipes, and other systems in the simulation software need to be connected to ensure the flow directions are correct.

If all the design specifications have been followed, the simulation should be ready. Once the simulation solves without any errors, the results obtained should be analysed to view the impact of the heat recovery system. The discussion to analyse the results obtained from the solution mode follows.

2.5.3 Obtain system results

As observed in Step 3 in Figure 26, the next step is to analyse the results of the solution model. A solution model that simulates potential heat recovery aids with the designing process of such a system. It is further favourable to observe whether the system could be beneficial to current processes.

As mentioned in Section 2.2.3, the prerequisite for a working simulation model is to ensure that the model simulates without any errors. Once the model simulates without any problems, the heat recovery results can be obtained and analysed. This is important since it provides a representation of how much heat can be added to a heat recovery system from an existing heat source.

Once the system results have been obtained and analysed, they are used for the preplanning processes, such as doing a feasibility study to determine whether there are financial benefits to

implementing the project. This heat recovery can be used to analyse the different parameters affecting the chemical processing, as reviewed in Section 1.4.3 [62]. The financial aspect is discussed in the following section.

2.6 Feasibility study

Sections 2.2 to 2.5 clearly describe the methods for analysing different scenarios to obtain an accurate and trustworthy heat recovery simulation. The results obtained from the simulations are used to assess the feasibility of implementing the system [9]. If the efficiency of the chemical plant improves by using a heat recovery model, the benefit should be quantified to calculate the financial benefit. Figure 28 summarises the necessary steps for conducting a feasibility analysis.

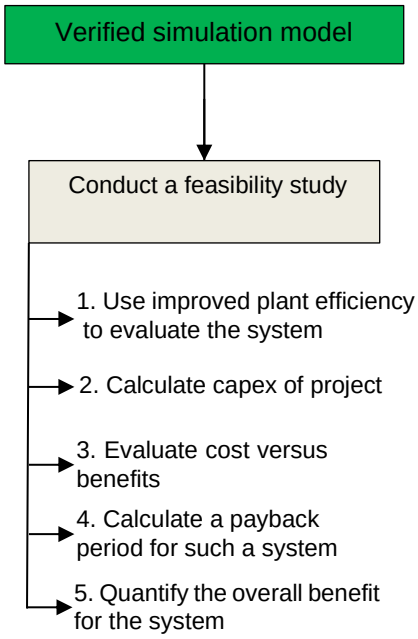

Figure 28: Feasibility analysis flow diagram [9]

Using the flow diagram in Figure 28, a feasibility analysis is conducted to obtain a good indication of the feasibility of the project. Referring to Step 1, if there is an efficiency increase, it should be analysed to obtain a benefit for a certain period, typically the life of mine period. Step 2 in Figure 28 evaluates the capex of the project, which entails all the initial costs for obtaining the infrastructure and equipment [75].

Step 3 and Step 4 in Figure 28 refer to the steps for evaluating the cost versus benefit of the simulated system. The result of comparing the cost versus benefit usually quantifies the payback period. This payback period represents a value by which the benefit surpasses the cost of the project, which is usually measured in years [75]. Once the payback period has been quantified, an overall benefit, as seen in Step in Figure 28, is quantified to assign a certain financial indication

of the project's feasibility, which is determined by the mining personnel. More about the calculations is discussed during Chapter 3.

Once all the steps described in this section have been followed and discussed, an overall conclusion is completed to describe all the processes used to construct the system and analyse the impact on the chemical plant. This conclusion and the validation of the study are discussed in the following section [76].

2.7 Conclusion

A thorough methodology was developed that clearly described each step of investigating a heat recovery and heat source system, by which a digital replica was obtained to simulate the behaviour and potential of such systems. The methodology was described to achieve an empirical model for analysing the effect of the different parameters affecting chemical processing. The methodology can be applied to any heat recovery system since it was developed to be generic. The methodology investigated the previous models used, as mentioned in Section 1.4, and the necessary steps required to construct these systems.

The first part of the process to achieve the study objectives, as discussed in Section 1.5, was to investigate and simulate a current heat recovery system. This entailed identifying a current working system and using the procedure to obtain an accurate simulation model that represented the process of the heat recovery system, as outlined in Section 2.2.

The next section of the methodology consisted of investigating a heat source through which heat could be recovered. The construction and development of the simulation model were discussed, which should depict the actual heat available to use. The final part of Section 2.3 discussed the verification process that should be used for the simulation model.

Section 2.4 discussed the method for constructing an empirical model for analysing the data obtained from the chemical plant. This result has to be verified, which was discussed in the section. Ensuring a verified empirical model should assist with analysing the effect of temperature on the process since the chemical plant could be part of the heat recovery process.

Lastly, the integration of the systems, as outlined in Section 2.2 and 2.4, was discussed, which represented the solution heat recovery model, as seen in Section 2.5. This is a combination of the heat recovery and heat source model, with the integration of the chemical plant. The heat recovery integration could be used to simulate potential heat recovery systems. The chapter concluded with a methodology that should be used to conduct a feasibility study, as discussed in Section 2.6.

The final part of this dissertation is to validate the study by referring to the objectives as mentioned in Section 1.5. The next chapter describes the case studies used to apply the methods as discussed in this chapter. The results of these system are listed and discussed, and the verification of the study is shown.

CHAPTER 3 – RESULTS

3.1 Preamble

Chapter 2 discussed the methodology for investigating different heat systems and constructing simulation and empirical models that represent a replica of the real-world operations. It further discussed the verification procedure to be followed. The derived methodology focuses on the process for integrating these verified models, which can be used to conduct a feasibility study for a potential heat recovery system. The process determines whether the project would be feasible and the extent of a benefit that could be expected.

In this chapter, the results obtained from the applied methodology are discussed. Firstly, the methodology is applied to a mine with a current heat recovery system and the simulation obtained is verified. Secondly, the results obtained from the heat source model are discussed and verified. Thereafter, the results obtained from the empirical model are discussed and the data obtained from the chemical processing plant is evaluated. Lastly, these models are integrated to simulate the potential of a heat recovery system to recover heat from the mine compressors and use this heat at the uranium plant. This chapter concludes with the feasibility study and validation.

As discussed in Section 1.5, the methodology aims to address the following objectives:

- Develop and verify a current operational heat recovery model.
- Develop and verify a current operational heat source model.
- Develop and verify an empirical model for uranium leaching analysis.
- Integrate the verified models.
- Conduct a feasibility study.

3.2 Case study background

3.2.1 Current heat recovery system

For confidentiality, the name of the mine containing the heat recovery process is omitted in this dissertation and is referred to as ‘Mine A’.

Mine A has a change house water heat recovery system, which recovers the heat from aftercoolers of the compressors and uses it to heat the water at the change house. The methodology developed in Section 2.2 was used to investigate the heat recovery system, develop a simulation model, and verify the model with the investigated results.

3.2.2 Current heat source

For confidentiality, the name of the mine containing the heat source is omitted in this dissertation and is referred to as ‘Mine B’.

Mine B has a large compressor system that contributes to a ring feed that supplies compressed air to Mine A and Mine B. The methodology developed in Section 2.3 was used to investigate the heat source, develop a simulation model, and verify the model with the investigated results.

3.2.3 Chemical plant for heat recovery

For confidentiality, the name of the chemical plant to be used as a potential heat recovery system is omitted in this dissertation and is referred to as ‘Plant X’.

Plant X applies the leaching processes discussed in Section 1.3. The case study forms part of the process developed in Section 2.4. The results obtained from the verified systems from the different case studies were used to conduct a feasibility study for determining the benefit and potential of the heat recovery system.

3.3 Current heat recovery system results

3.3.1 Data obtained

Recalling the process discussed in Section 2.3.1, the best step is to investigate the site and obtain data relevant to the system that is needed for a site layout. Mine A has two compressors supplying the compressed air demand underground for mining purposes. The first compressor is a 4.8 MW Sulzer compressor supplying 17 kg/s of compressed air at maximum guide vane angle. The second compressor is a 10.3 MW VK100 compressor supplying 33.5 kg/s also at maximum guide vane angle. Generally, both compressors are running during the drilling shift, whereas only one compressor could be running outside the drilling shift, depending on demand. Table 6 summarises the running operations of Mine A.

Table 6: Mine A compressor operating conditions

Time frame	Sulzer	VK	Total
Drilling shift	ON	ON	2
Outside drilling shift	ON or OFF	ON or OFF	1 or 2

As mentioned in the case study background in Section 3.2.1, Mine A has a surface heat recovery system that recovers the heat from the compressors in Table 6 to assist with change house water heating. Figure 29 shows a schematic of this process.

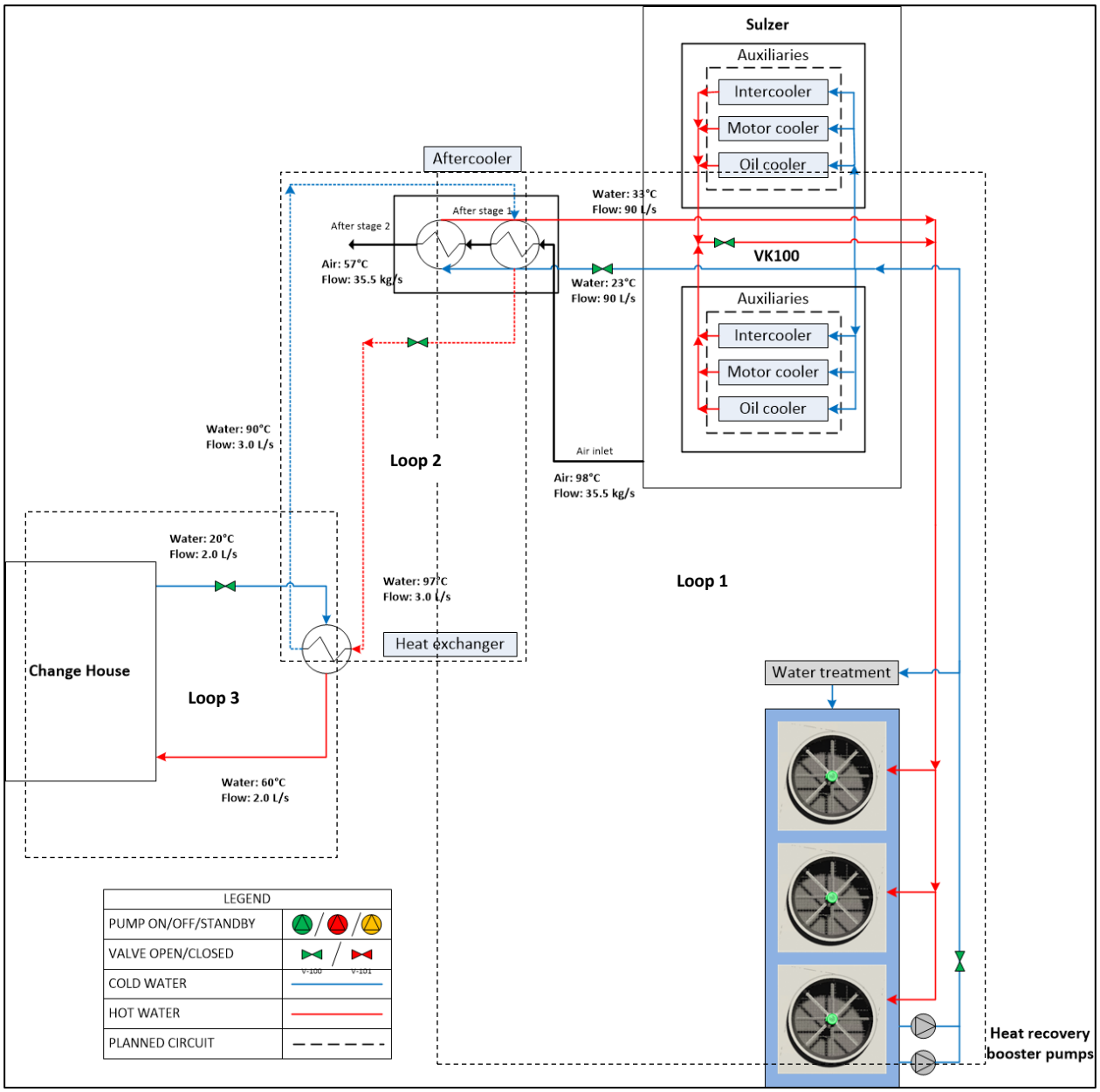

Figure 29: Detailed layout of Mine A heat recovery system

The data obtained was allocated to the system specifications and processes. The site audit provided good insight into the operating conditions regarding the heat recovery system. Figure 29 displays the values obtained using the measurement equipment, as discussed in Section 2.2.

Figure 29 indicates three closed loops in the layout. Loop 1 is the water circuit that cools the air through the aftercoolers by using the cooling towers to remove the heat from the water. Loop 2 is the water circuit that also cools the air; however, it captures the heat from the air and uses it to heat the water at the change house. Loop 3 is the water used at the change houses that is heated by the water circuit in Loop 2. These are all closed loop systems as the water used in Loop 2 is treated differently to prevent scaling in the pipes [12].

To understand the process as observed in Figure 29 more clearly, a brief description follows. The compressors at Mine A increase the pressure of the ambient air for underground mining demands. Increasing the pressure increases the temperature of the air as well [59, 66]. This compressed air needs to be cooled by a compressor aftercooler before it is supplied underground through the mineshaft. The type of aftercooler in use employs double-stage cooling. This simply implies that the water circuit from the cooling towers (Loop 1) does not mix with the water supplied to the change houses (Loop 2).

The first stage of cooling uses the water in Loop 2 to initially lower the temperature of the compressed air. The temperature of the water in Loop 2 returning from the change houses has decreased as it has exchanged its heat with the change house water in Loop 3 (heating the change house water), which is used to cool the compressed air. Since the water from Loop 2 has a higher temperature than the water from Loop 1, the compressed air temperature does decrease; however, not as much as the water from Loop 1, since Loop 2 has the first contact with the hot compressed air. The colder water from the cooling towers in Loop 1 is the second stage that cools it to adequate temperatures for mining demand. Both compressors discharge the compressed air into a single column that leads to the aftercooler. The heat is captured by the water as energy, which is used to supply the heat to the change house used by employees.

For more clarity on Figure 29, a table was constructed to explain the heat transfer between the different mediums. Table 7 depicts the measured values obtained from the aftercooler system on Mine A. The aftercooler serves as a heat exchanger that exchanges heat between mediums, such as the heat from the compressed air that is exchanged with the colder water.

Table 7: Aftercooler heat recovered data on Mine A

	Measured	
	Aftercooler Stage 1	**Aftercooler Stage 2**
Water fluid flow (L/s)	5.0	90.0
Hot airflow (kg/s)	35.5	35.5
Cooling duty (kW)	8 000.0	13 000.0
Cold fluid temp in (°C)	93.0	26.1
Cold fluid temp out (°C)	96.9	33.3
Hot fluid temp in (°C)	97.7	93.8
Hot fluid temp out (°C)	93.8	55.0

Table 7 indicates the different mediums along with the temperature effect thereof. Looking at Stage 1 of the aftercooler, the colder fluid in this case is the water returning from the change house, which is seen as the cold fluid since it is the colder medium of the first stage of cooling.

The hot fluid is the compressed air that is at 97.7°C at the discharge of the compressors and inlet of the aftercooler. The air is cooled to around 93°C, which heats the water to 97°C.

The second stage consists of the most cooling as the colder fluid is the water from the cooling towers that are designed to cool the compressed air temperature significantly. The air is further cooled to 55°C by the second stage and is used by the mining demands. Table 7 mainly shows which type of aftercooler is used and how the heat is recovered and distributed. The important aspect is the distribution of the heat and what effect it has on the demand, namely the change houses. This is summarised in Table 8.

Table 8: Change house heat exchanged data on Mine A

	Measured
	Change house
Water fluid flow (L/s)	2.0
Hot fluid flow (L/s)	5.0
Cooling duty (kW)	9 000.0
Cold fluid temp in (°C)	20.0
Cold fluid temp out (°C)	60.0
Hot fluid temp in (°C)	96.4
Hot fluid temp out (°C)	93.5

Table 8 shows that the cold fluid is the water that is heated at the change house side for employees (Loop 3), whereas the hot fluid is the heated water that flows from the first stage at the aftercooler (Loop 2). The hot fluid has significantly higher temperatures than the cold fluid since it is in constant contact with the heated compressed air. The heat exchanger is a plate heat exchanger that uses the hot fluid to heat the cold fluid from 20°C to 60°C. The desired temperature is maintained by using valves in the change house [12]. The following section describes the heat recovery model that was developed in the simulation software.

3.3.2 Heat recovery model results

As mentioned in Section 2.2, PTB was used as simulation software. Recalling the steps in Figure 17, the layout had to be integrated with the simulation software along with the components and design specifications. Using the schematic process in Figure 29 and these abovementioned steps, a clear layout of the simulation was constructed as shown in Figure 30.

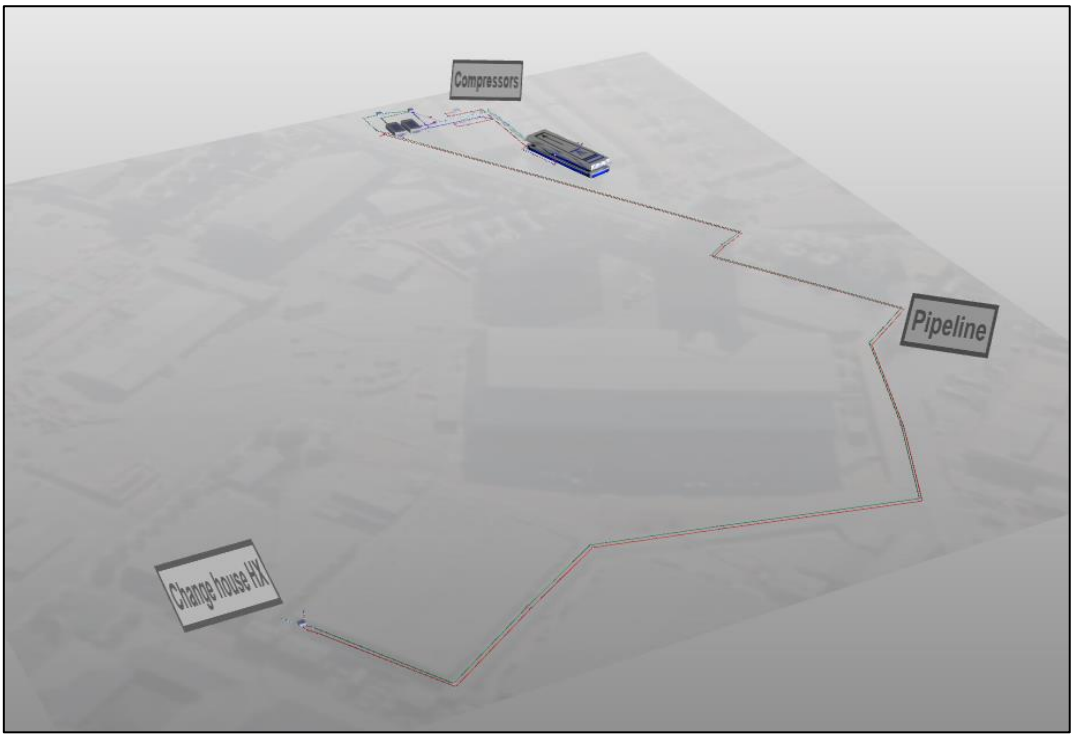

Figure 30: Mine A heat recovery simulation model

Figure 30 displays the PTB simulation constructed for the heat recovery system of Mine A. The important sections are the change house heat exchanger (HX), which represents Loop 3, the pipelines to and from the change house, which is Loop 2 and, lastly, Loop 1, which is the compressors along with its cooling towers. The water is transferred through cladded pipes from the aftercooler to the change houses, which reduces the temperature drop over the 1 250 m pipe length. A plate heat exchanger is installed at each change house. For more details, including the components, please refer to Appendix A.

3.3.3 Verification of Mine A simulation

The simulation represented in Figure 30 was ready for simulating the heat recovery system. Referring to Figure 18, the first step was to simulate the model without any errors, whereafter the model had to be calibrated and the measurement controls applied. The operating conditions of the heat recovery system on Mine A were known and the different temperature and flow rate data was obtained, which was used for the model simulation.

Once the model had been calibrated, it represented a replica of the heat recovery system of Mine A. The results from the simulation are shown in Table 9 and Table 10, respectively, showing the results of the aftercooler stages and the change house heat exchange process.

Table 9: Aftercooler heat recovered results on Mine A

	Simulated	
	Aftercooler Stage 1	**Aftercooler Stage 2**
Water fluid flow (L/s)	5.0	90.0
Hot airflow (kg/s)	35.5	35.5
Cooling duty (kW)	7 600.0	12 500.0
Cold fluid temp in (°C)	92.4	24.8
Cold fluid temp out (°C)	96.0	32.6
Hot fluid temp in (°C)	97.7	92.5
Hot fluid temp out (°C)	92.6	58.4

Table 10: Change house heat exchanged results on Mine A

	Simulated
	Change house
Water fluid flow (L/s)	2.3
Hot fluid flow (L/s)	5.0
Cooling duty (kW)	8 750.0
Cold fluid temp in (°C)	20.0
Cold fluid temp out (°C)	57.8
Hot fluid temp in (°C)	95.4
Hot fluid temp out (°C)	91.8

Table 9 and Table 10 represent the simulation results of the heat recovery system. The results are listed in the same format as the data obtained from the site inspection as shown in Table 7 and Table 8. This data was used to determine the accuracy of the model, which is important since it represents the relationship between the simulation and real-world operations.

Better representations are shown in Figure 31 to Figure 33. These figures represent column graphs to visually display the difference between the simulated results and the data from the site audit. The comparison between the simulated and gathered data of the first stage of the aftercooler is shown in Figure 31, the second stage of the aftercooler in Figure 32, and the change house in Figure 33.

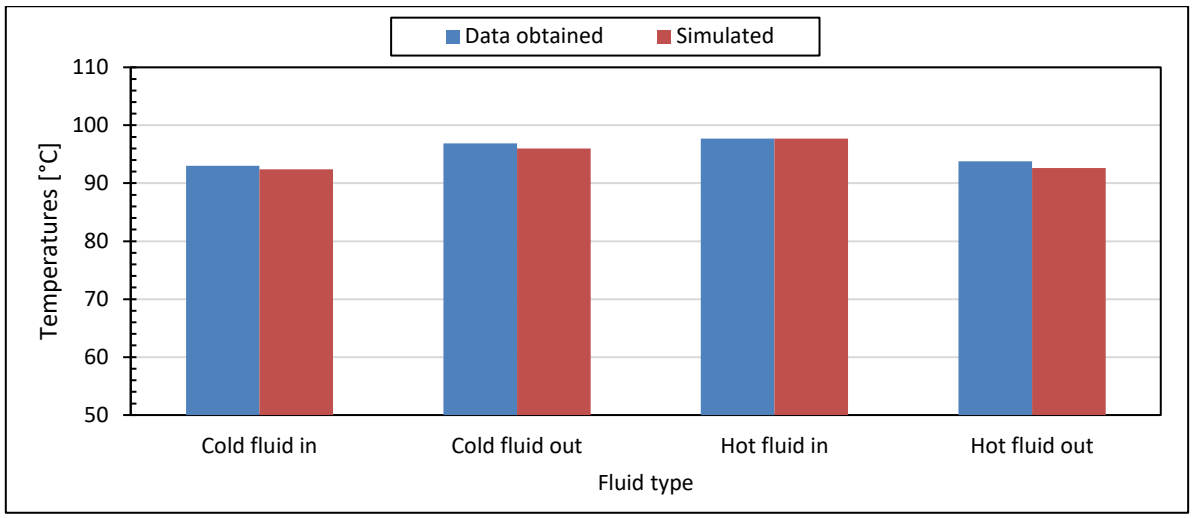

Figure 31: Stage 1 aftercooler temperature comparison

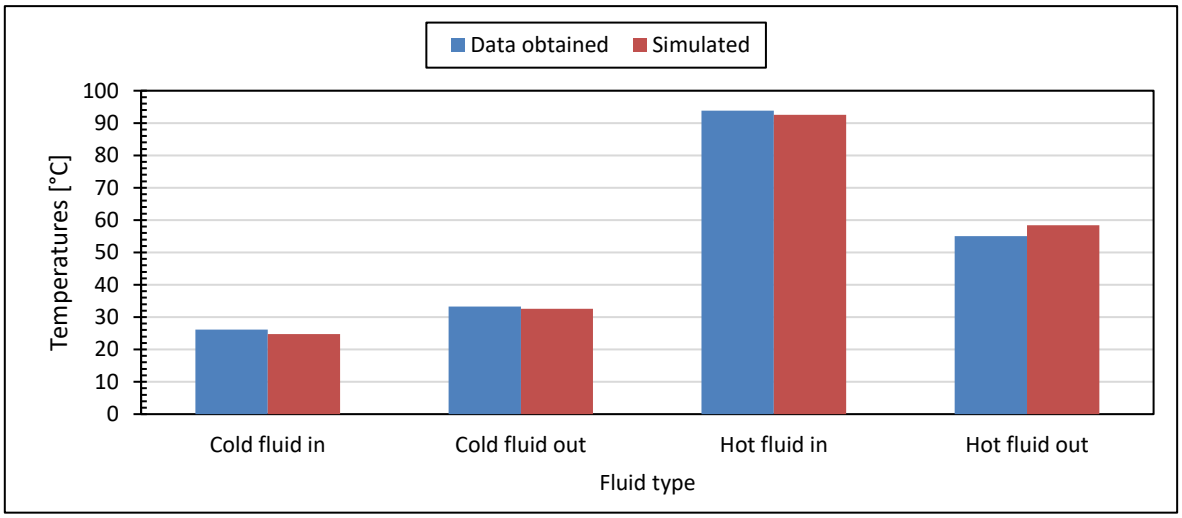

Figure 32: Stage 2 aftercooler temperature comparison

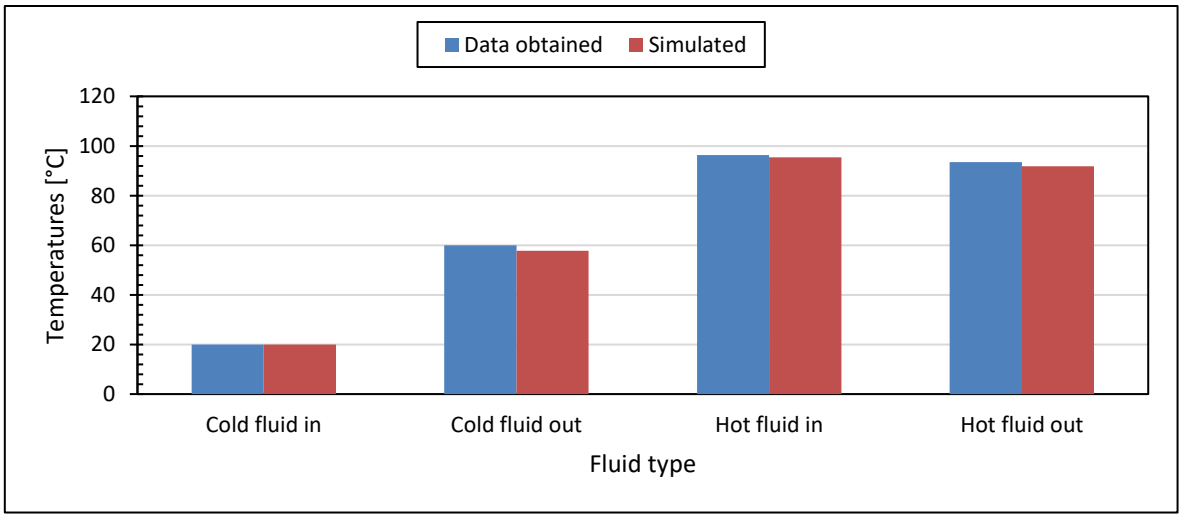

Figure 33: Change house heat exchanger temperature comparison

Using the data obtained in Table 7 and Table 8 and comparing it with the results presented in Table 9 and Table 10, the accuracy of the model compared with the system was calculated. If the model result in the verification parameters, as mentioned in Section 2.2.3, the model could be used for other simulations.

Comparing the simulated results discussed in this section with the data obtained from Section 3.3.1, the model simulated with 97.19% accuracy. This percentage satisfied the requirements of keeping a simulation error of less than 10% [65, 66]. The accuracy of the model ensured that it could be used for other simulations of the same process and the results obtained could be trusted.

As mentioned in Section 2.2.3, once the heat recovery simulation has been verified, the following step was to investigate a heat source for the heat recovery system. The results obtained from the methodology developed to investigate the heat source are discussed in the following section.

3.4 Heat source system results

3.4.1 Data obtained

Referring to Section 2.3.1, the first step was to investigate and obtain a heat source on the mine that could be used for a heat recovery system. As mentioned in Section 3.2.1, the compressors located at Mine B were used for the investigation. Mind B had three 5.9 MW compressors, each supplying 15–17 kg/s of compressed air at maximum guide vane angle. During the drilling shift, all three compressors were running. Depending on the demand requirements, one or two compressors generally ran outside the drilling shift. Table 11 lists the typical compressor combinations for *normal* operations.

Table 11: Mine B compressor operating conditions

Time frame	GN Compressor 1	GN Compressor 2	GN Compressor 3	Total
Drilling shift	ON	ON	ON	3
Outside drilling shift	ON or OFF	ON or OFF	ON or OFF	1 or 2

As mentioned in Section 1.4.3, compressors use a cooling circuit to cool compressor components as they produce heat during operation. Figure 34 illustrates the water-cooling circuit of Mine B's compressors when all three compressors are running.

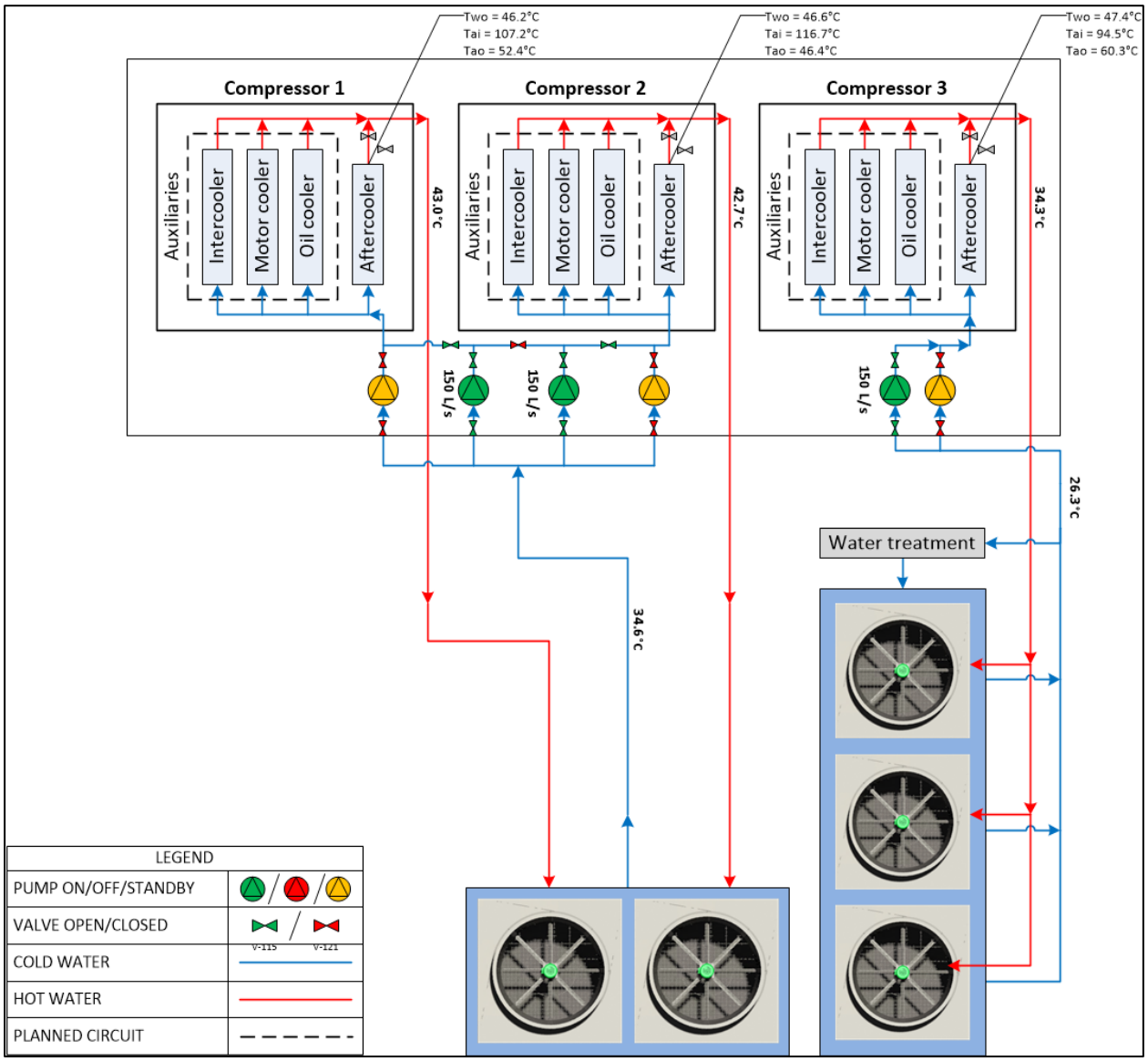

Figure 34: Mine B compressor water-cooling circuit

Figure 34 depicts the data along with the flow of the process. The site audit provided good insight into the operating conditions of the compressor circuit. Figure 34 displays the readings obtained using the measurement equipment as discussed in Section 2.3. The cooling towers are primarily used to cool down the return water from the aftercooler and auxiliaries (namely, the intercooler, motor cooler and oil cooler) at an average water flow rate of 150 L/s and a ΔT of 9°C for each compressor. The cooled water leaving the cooling tower is pumped to each compressor. Thereafter, the heat generated from the auxiliaries is cooled with the water since it produces heat during operation. This warm water flows to the cooling towers where it is cooled with ambient air. This loop repeats itself consistently, with the flow rate varying depending on the compressor demand.

To provide more clarity regarding the layout in Figure 34, the data obtained is shown in Table 12. It displays the results for each compressor's aftercooler process of Mine B as operated in winter conditions. The data from summer conditions are shown in Table 13.

Table 12: Winter heat source data obtained of Mine B

	Winter compressor data		
	Compressor 1 Aftercooler	**Compressor 2 Aftercooler**	**Compressor 3 Aftercooler**
Cold fluid flow (L/s)	25.5	25.6	25.7
Hot fluid flow (kg/s)	15.0	15.0	15.9
Cooling duty (kW)	2 090.0	2 100.0	2 290.0
Cold fluid temp in (°C)	19.5	19.56	19.7
Cold fluid temp out (°C)	39.0	38.9	39.1
Hot fluid temp in (°C)	95.0	95.0	95.0
Hot fluid temp out (°C)	75.0	75.0	75.5

Table 13: Summer heat source data obtained of Mine B

	Summer compressor data		
	Compressor 1 Aftercooler	**Compressor 2 Aftercooler**	**Compressor 3 Aftercooler**
Cold fluid flow (L/s)	25.5	25.6	25.7
Hot airflow (kg/s)	15.0	15.0	15.9
Cooling duty (kW)	2 025.0	2 025.7	2 229.6
Cold fluid temp in (°C)	25.4	25.4	25.2
Cold fluid temp out (°C)	43.7	43.75	45.1
Hot fluid temp in (°C)	95.0	95.0	95.0
Hot fluid temp out (°C)	75.6	75.5	77.1

Table 12 and Table 13 represent the cold fluid flow which is the cold water from the cooling towers. This cold fluid is used in the aftercooler to cool down the hot fluid, which is the pressurised air of the compressors. The aftercooler used at Mine B differs slightly from Mine A since it employs only one-stage cooling, but the principle of the aftercooler stays the same, namely, to cool the compressed air. The compressed air enters the aftercooler at 95°C and leaves the system at a temperature between 75°C and 77°C. This heat is captured by the water and is transferred to the cooling towers where it is dissipated into the atmosphere. The water leaving the aftercooler vary between 39°C and 45°C, depending on the season.

The following section describes the heat source that was developed in the simulation software.

3.4.2 Heat source model results

As mentioned in Section 2.2, PTB simulation software was used to construct a replica of the compressed air system, which is shown in Figure 34. The steps to integrate the layout with the simulation model were already discussed in Section 2.3.2. The process ensured that a replica of the current compressor system was simulated. Figure 35 shows the PTB simulation system.

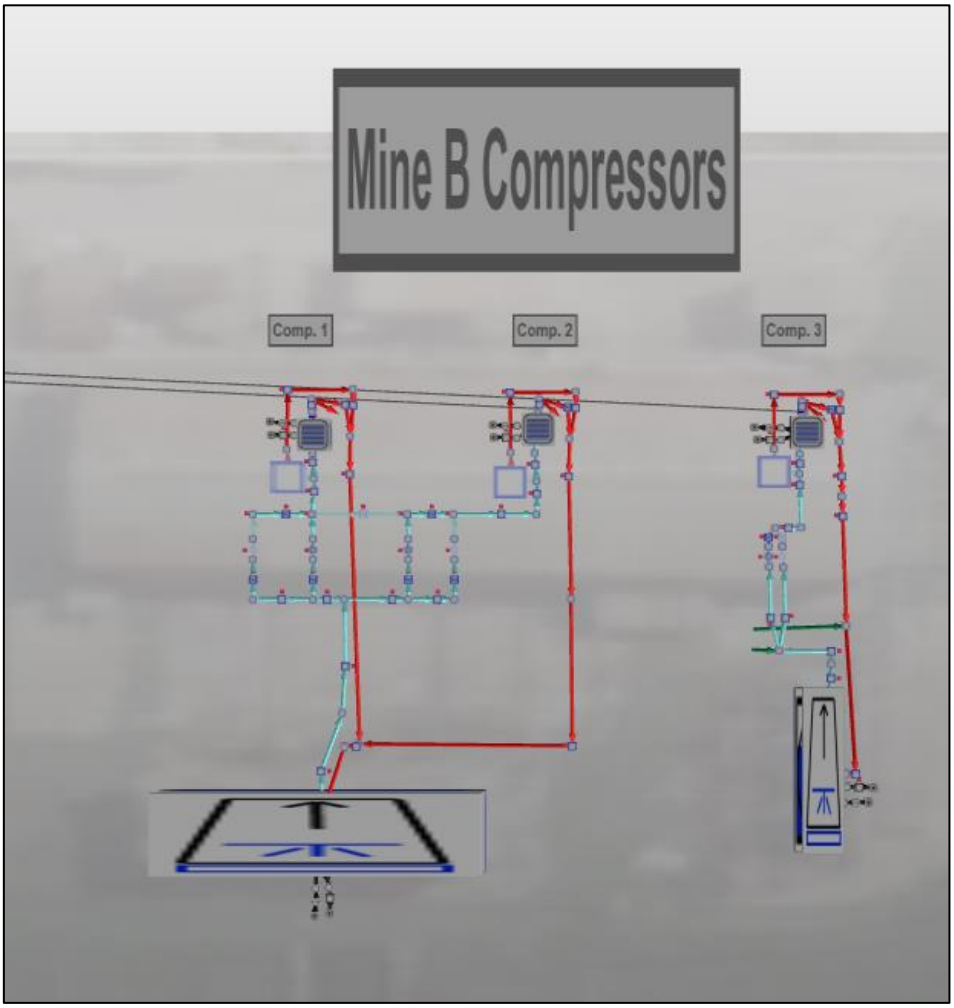

Figure 35: Mine B compressor simulation system

The results obtained from the simulation, as observed in Figure 35, were compared with the actual data obtained from the audits as mentioned in Section 2.3.2. This ensured that the model simulated the temperature difference correctly, including the correct flow during the operating conditions to quantify the heat available that could be used for a heat recovery system.

The following section discusses the results obtained from the simulation and the verification accuracy of the model.

3.4.3 Verification of Mine B simulation

The simulation model in Figure 35 was ready for simulation. As stated in the methodology, the simulation had to solve without errors and apply the measurement controls. Knowing the operating conditions of the compressed air system on Mine B, the simulation was run to determine whether a replica of the actual compressor system was obtained. A replica could only be obtained once the model had been calibrated, as described in the steps in Section 2.3.3.

The results from the simulation for winter and summer conditions are shown in Table 14 and Table 15, respectively.

Table 14: Simulation results of Mine B compressor system during winter conditions

	Baseline winter simulation model		
	Compressor 1 Aftercooler	**Compressor 2 Aftercooler**	**Compressor 3 Aftercooler**
Cold fluid flow (L/s)	26.8	26.5	26.5
Hot fluid flow (kg/s)	15.0	15.0	15.9
Cooling duty (kW)	2 101.8	2 100.9	2 304.4
Cold fluid temp in (°C)	19.6	19.5	19.2
Cold fluid temp out (°C)	38.3	38.5	40.0
Hot fluid temp in (°C)	95.0	95.0	95.0
Hot fluid temp out (°C)	75.7	75.7	76.1

Table 15: Simulation results of Mine B compressor system during summer conditions

	Baseline summer simulation model		
	Compressor 1 Aftercooler	**Compressor 2 Aftercooler**	**Compressor 3 Aftercooler**
Cold fluid flow (L/s)	26.8	265	26.5
Hot airflow (kg/s)	15.0	15.0	15.9
Cooling duty (kW)	2 035.2	2 034.2	2 232.3
Cold fluid temp in (°C)	25.3	25.3	25.0
Cold fluid temp out (°C)	43.5	43.7	45.2
Hot fluid temp in (°C)	95.0	95.0	95.0
Hot fluid temp out (°C)	76.9	76.9	77.3

The values in Table 14 and Table 15 give the results obtained from the simulation in Figure 35. The cold fluid in each case was the water used to cool the aftercooler, whereas the hot fluid was the compressed air from the compressors. Using the data obtained in Section 2.5.1 and

comparing it with the results obtained from the simulation model, the accuracy of the model compared with the system could be quantified.

Figure 36 and Figure 37 compare the temperatures between the data and simulation of the aftercooler at Compressor 3 during winter and summer conditions. The rest of the graphs are given in Appendix C. These figures represent a column graph to visually display the difference between the simulated results and the data from the site audit.

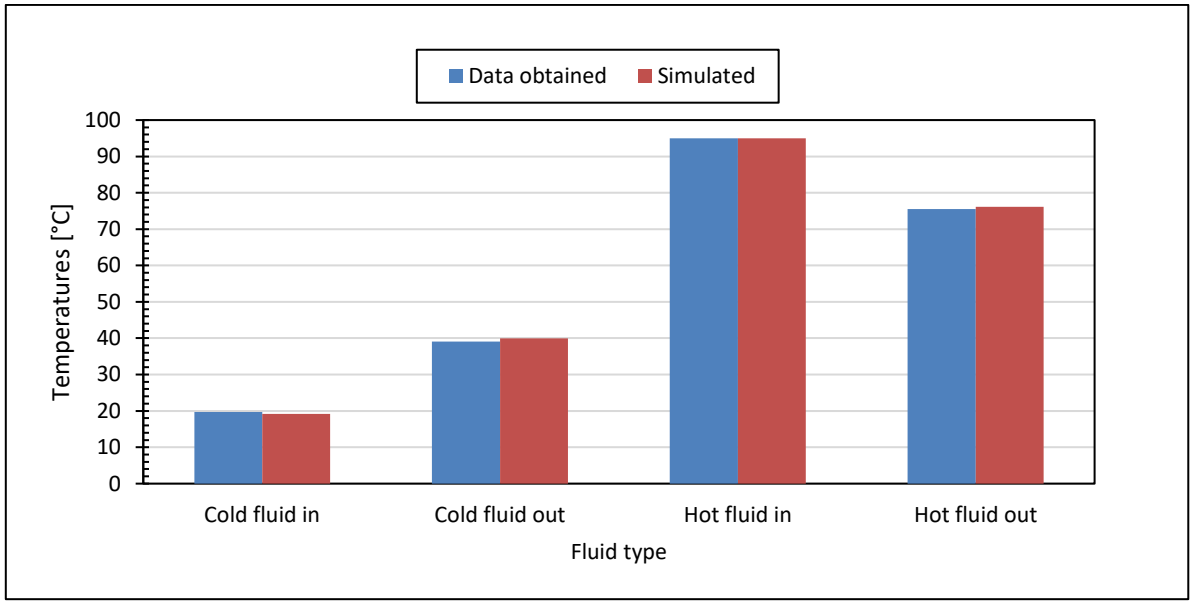

Figure 36: Compressor 3 aftercooler winter temperatures comparison

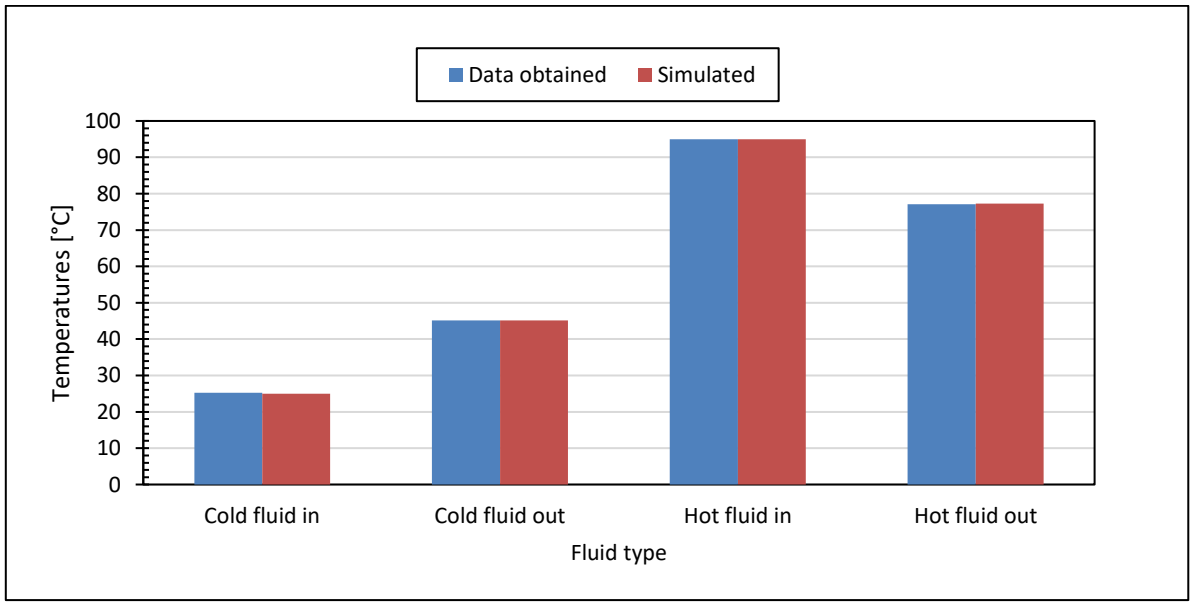

Figure 37: Compressor 3 aftercooler summer temperatures comparison

Figure 36 and Figure 37 clearly show the accuracy of the comparison between the simulation and the data acquired. The results for the aftercoolers of Compressor 1 and 2 are given in Appendix C. Using the data obtained as discussed in Section 3.4.1 and comparing it with the data gathered from the simulation, the accuracy of the model compared with the system could be calculated.

The comparison between the simulated results from this section and the data obtained from Section 3.3.1 demonstrated that the model simulated with a 96.33% accuracy. This percentage satisfied the requirements of obtaining a simulation error of less than 10% [65, 66]. Achieving such a high accuracy indicated the reliability of the simulation since it almost replicated the results obtained from the real-world operations.

As mentioned in Section 2.3.3, once the results of the heat source model had been verified, the next step was to construct and develop an empirical model to verify the data obtained from the chemical plant. The results obtained from the investigation are discussed in the following section.

3.5 Empirical model results

3.5.1 Data obtained

Referring to Section 2.5.1, the first step in the investigation is to obtain the data through a site inspection to verify the empirical model. The audit data of the plant, referred to as Plant X, is shown in Table 16. The overall dissolution calculations were based on these design parameters. The table provides the dissolution for both summer and winter seasons, density and flow rate. The data in Table 16 was used as input parameters for the potential heat recovery model.

Table 16: Plant X audit data of the leaching process

Parameter	Min.	Max.	Avg.
Specific heat of slurry (kJ/kg.K)	–	–	3.2
Mass flow of slurry (tonnes/hr)	166.0	240.0	203.0.
Mass flow of slurry (kg/s)	46.1	66.7	56.4
Sulphuric acid concentration (kg/tonne)	–	–	130
Density (kg/m^3)	1 500.0	1 500.0	1 500.0
Uranium price (R/kg)	1 400.0	1 900.0	1 650.0.

Parameter	Min.	Max.	Avg.
Winter – at time of study			
Slurry incoming temperatures	12.0	24.0	19.0
Slurry temperatures after reagent addition (sulphuric acid = exothermic reaction)	15.0.	25.0	220
Leach dissolution	–	–	47.0%
Overall dissolution	–	–	60.0%
Winter – with boilers			
Slurry incoming temperatures	12.0	24.0	19.0
Slurry temperatures after reagent addition (sulphuric acid = exothermic reaction)	38.0	45.0	50.0
Leach dissolution	–	–	47.0%
Overall dissolution	–	–	73.0%
Summer – at time of study			
Slurry incoming temperatures	28.0	34.0	30.0.
Slurry temperatures after reagent addition (sulphuric acid = exothermic reaction)	30.0	40.0	33.0
Leach dissolution	–	–	47.0%
Overall dissolution	–	–	65.0%
Summer – with boilers			
Slurry incoming temperatures	28.0	34.0	30.0
Slurry temperatures after reagent addition (sulphuric acid = exothermic reaction)	50.0	60.0	56.0
Leach dissolution	–	–	75.0%
Overall dissolution	–	–	80.0%

Table 16 lists the results of the data required as mentioned in Section 2.5.1. The specific heat capacity of slurry, as measured by mining personnel, is 3.2 kJ/kg.K, which is lower than the heat capacity of water. The average mass flow rate of slurry is around 60 kg/s and the density is 1 500 kg/m^3. Data from the decommissioned boiler was obtained from daily audits when the boiler was still operational, which is shown in Table 16.

Plant X has different numbers of ore tonnes that are being treated each year, which are planned and updated each year by the mining personnel. The result is shown in Table 17 along with how much ore is currently being treated, how much will be treated, and how much uranium is expected

to be recovered from these processes. This table was used to calculate the mass flow required to treat the required tonnage, which is known to influences the slurry temperature [5].

Table 17: Life of mine plan of Plant X

Financial year	Planned tonnes treated	Planned uranium delivered (kg)
2021/2022	1 465 877	274 905
2022/2023	1 565 144	288 889
2023/2024	1 566 435	306 729
2024/2025	1 395 140	337 441
2025/2026	998 196	269 957
2026/2027	735 203	195 627
2027/2028	350 479	104 372
2028/2029	182 607	56 755
2029/2030	95 605	42 161

The life of mine is important since it typically gives a good indication of the confidence the plant has regarding its system. If the life of mine is short, it usually represents that the plant will not be operational much longer. This could be used as guidance when designing the future aspects of a system. The results obtained from the empirical model are discussed during the following section.

3.5.2 Empirical model results

Referring to Section 2.4.2, the first step towards obtaining the model was to obtain all the plant input data as shown in Section 3.5.1. Secondly, the relationship between the slurry dissolution and temperature had to be quantified. The empirical model was constructed using Microsoft Excel by obtaining a relationship between the slurry temperature and the dissolution rates. The results obtained are discussed in this section.

The life of mine obtained from the site inspection was used to calculate the mass flow needed to satisfy the projected tonnage treated for the upcoming years. The trend at which the slurry mixture could be heated for the tonnes treated, as shown in Table 17, at different slurry inlet temperatures is shown in Figure 38.

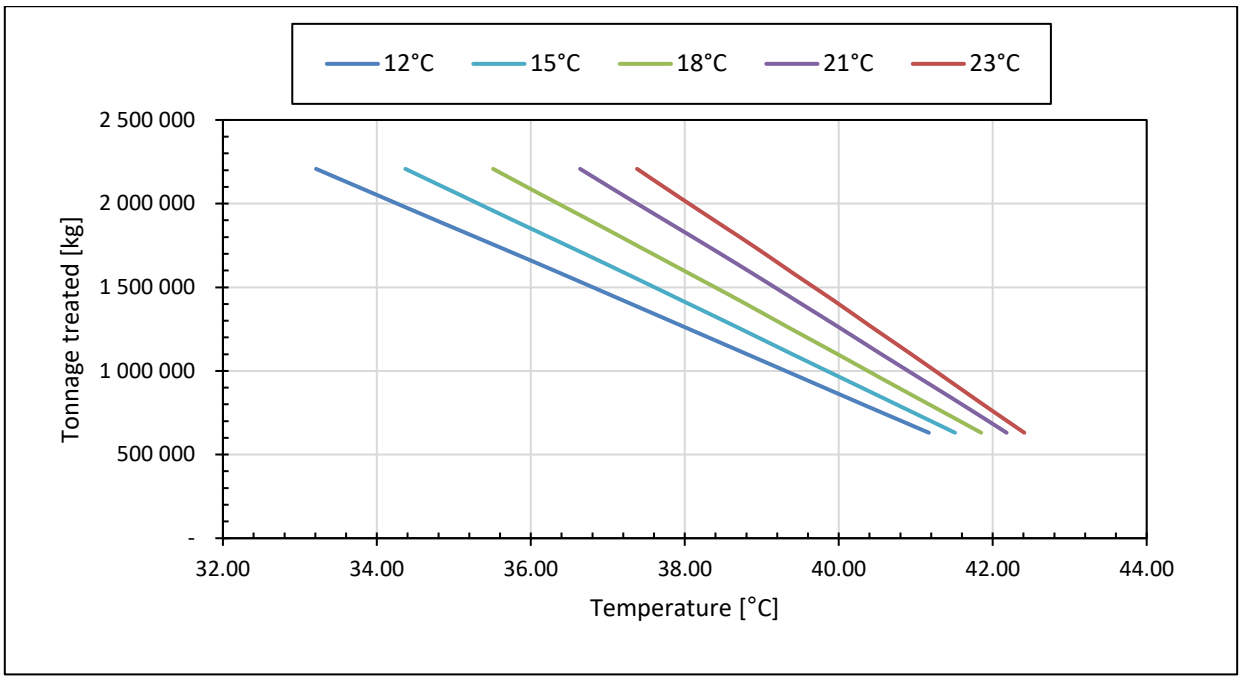

Figure 38: Outlet slurry temperature for different tonnages treated at different slurry inlet temperatures

Figure 38 depicts the effect that the total tonnage treated has on the temperature of the mixture. The fewer tonnes treated, the higher slurry temperature is achieved since there are fewer particles that receive the same heat supplied from the compressors to heat the slurry to a certain point. This figure was constructed to show the effect of treating different tonnages because as the life of mine progresses, different temperatures could be obtained. Warmer ambient conditions lead to a faster slurry temperature increase as the water temperature supplied from the compressors is also warmer. This is seen in the results of the heat source in Section 3.4.3.

Figure 39 depicts the relationship between the total tonnes treated to recover uranium slurry at different inlet temperatures, which represent seasonal changes in temperature.

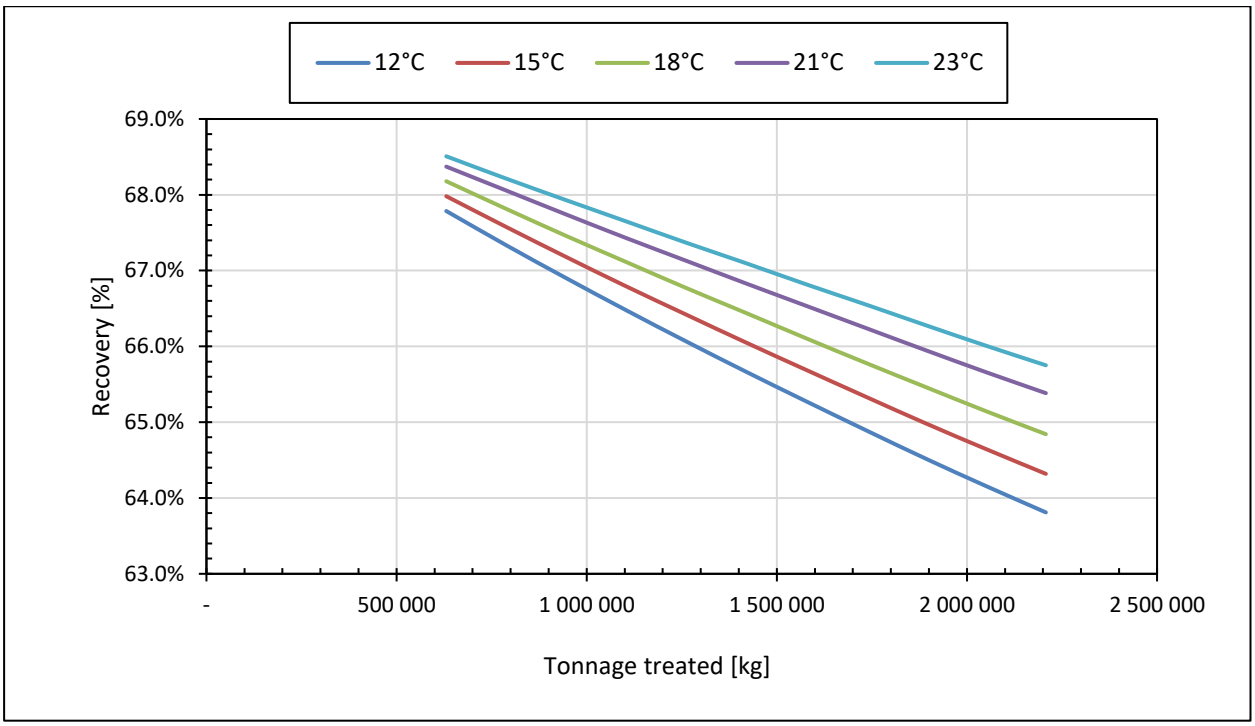

Figure 39: Uranium recovery for different tonnages treated at different inlet temperatures

It is clear in Figure 39 that if the tonnes treated increase, the slurry mass flow also increases to manage the same amount of slurry, since they are directly proportional. In turn, the increase in the mass flow implies that the slurry mixture's temperature will decrease. This is due to the increase in the mass of the mixture being treated for the same amount of time, which will not heat the mixture as much as a smaller volume treated at the same time.

Figure 39 further shows the effect for different inlet temperatures. A higher inlet temperature increases the recovery obtained for the same number of tonnes treated compared with other inlet temperatures. It clearly indicates that when treating minimal tonnes, the recovery rates of uranium at the different inlet temperatures are grouped more closely together. This is simply due to the sulphuric acid concentration that influences the process, as mentioned in the literature review in Section 1.4.2. If the amount of sulphuric acid used during leaching and the temperature increases, the mixture starts to extract the most out of the combination between the two variables.

Figure 40 shows the relationship between the inlet temperature for the recovery for different tonnes treated. As known from literature, uranium recovery increases as the slurry temperature increases; however, for clarity, it was done on different tonnage being treated for recovery to incorporate the life of mine.

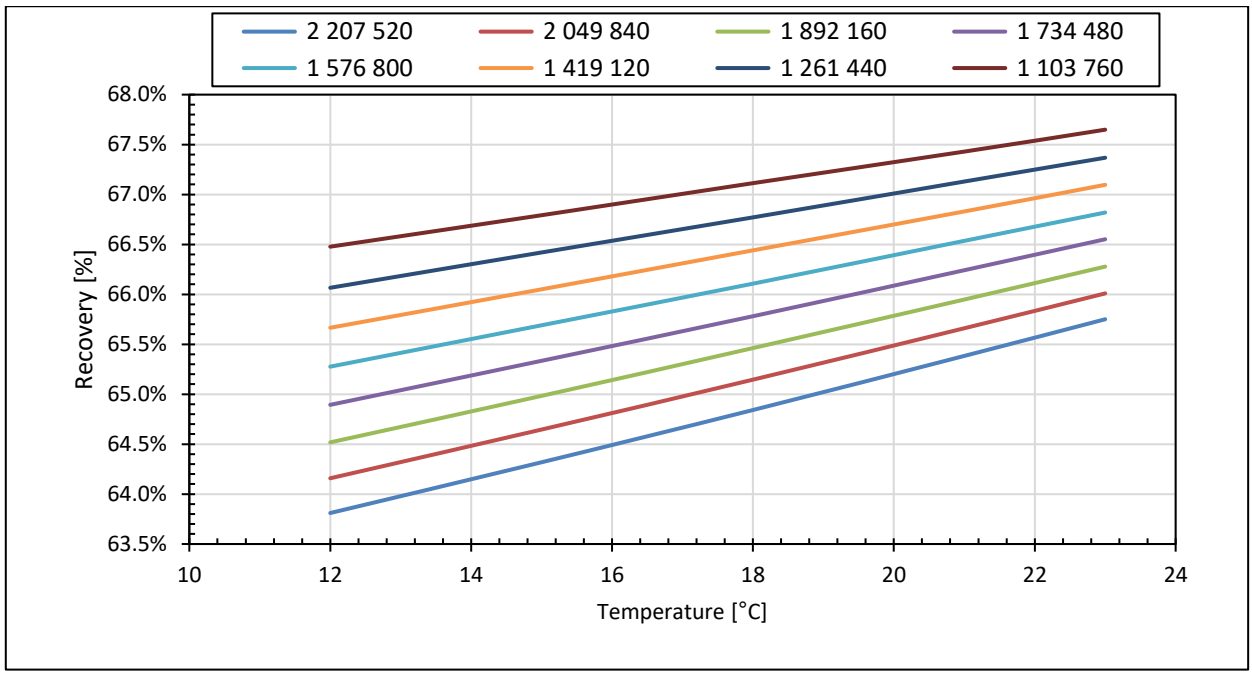

Figure 40: Uranium recovery for different inlet temperatures at different tonnages treated

Figure 40 corresponds with literature that states that an increase in temperature results in an increase in the recovery of uranium slurry [6, 31, 33, 35]. Figure 40 assumes that the inlet slurry temperature is the same as the ambient air conditions. Making this assumption eliminates other variables such as heat loss due to conduction of the pipes. It emphasises the variable being controlled, namely the number of tonnes treated. Every line represents a scenario that could be used to monitor how much uranium could be recovered at certain temperatures while moving along the life of mine of the plant.

The results obtained in Figure 40 again illustrates that if fewer tonnes are treated in Plant X, the heat that could be applied would result in a higher recovery since the mixture would be heated more effectively. The analysis was done for slurry inlet temperatures ranging from 12°C to 23°C. Figure 40 is an important figure for demonstrating the importance of temperature during the process.

When the mixture is at 12°C, the extraction lines are further apart from the other lines obtained from the tonnes treated than the extraction rates at 23°C. This emphasises that if the temperature of the mixture is higher, a better extraction could be achieved in comparison with the tonnes treated. When the temperature is high, the variability of the treated tonnes does not have such a great impact as when the temperature is low.

The results obtained in this section enable an analysis of the possibilities that could happen once the uranium dissolution process is heated. The verification procedure, as discussed in Section 2.4.3, is discussed in the following section.

3.5.3 Verification of the empirical model

The results of the relationship between the slurry inlet temperature and slurry mixture extraction regarding the life of mine of the plant were discussed in Section 3.5.2. The results confirmed the statement from Section 1.4, namely that when the temperature of the slurry mixture increases, the extraction does as well. In this section, the temperature and dissolution values are verified.

The relationship between temperature and dissolution was represented on a single graph at a certain year of the life of mine to only demonstrate the relationship between the two factors. Figure 41 depicts the slurry mixture temperature versus the overall dissolution of the mixture at a constant slurry inlet temperature.

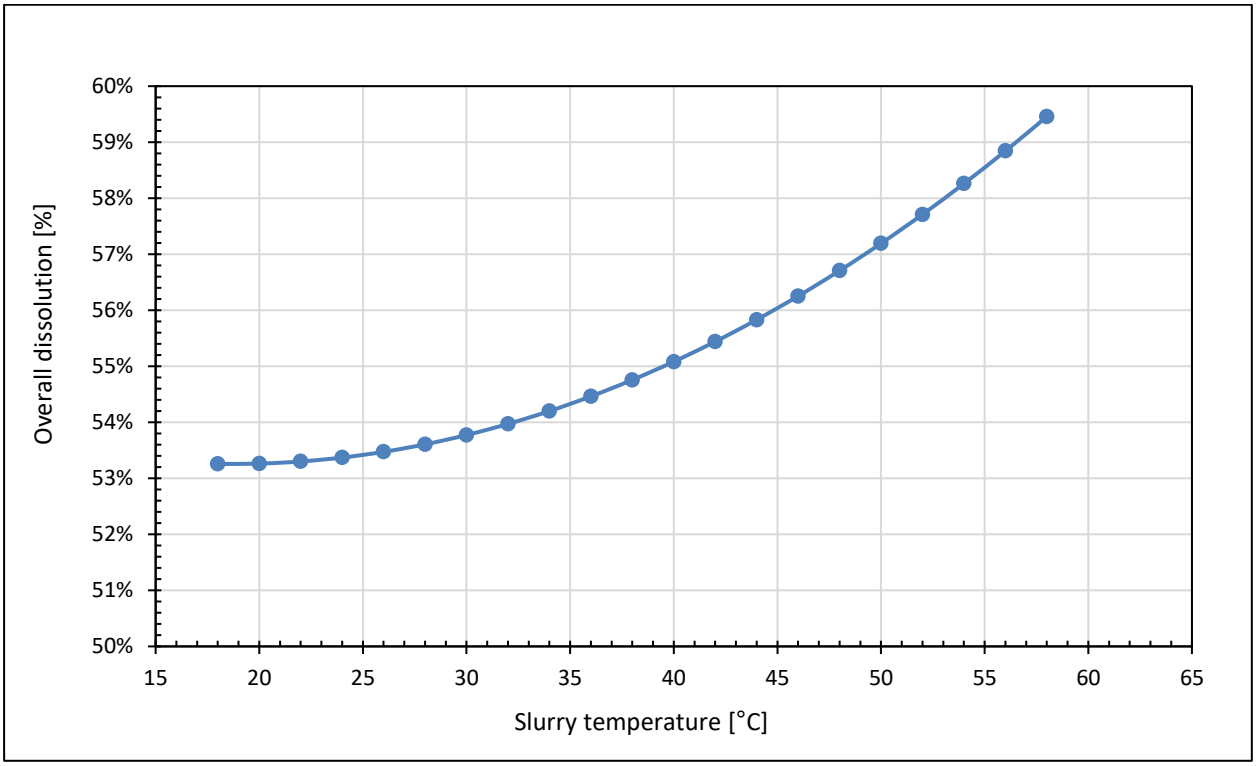

Figure 41: Overall dissolution vs slurry temperatures at Plant X

Figure 41 clearly shows that if the slurry temperature could be increased, more uranium could be recovered since the dissolution rate would increase. The purpose of the heat recovery model is to recover heat already being generated and rather use it to assist with the uranium recovery at Plant X. This uranium dissolution data had to be verified, which was done by comparing it with the literature reviewed on the uranium leaching process (refer to Section 1.4.2).

Different studies used various factors that influence the uranium process as shown in Table 16. However, studies that investigated similar acid concentrations than used in South Africa were used to verify the results. From the data obtained it was determined that Plant X used 13 kg/tonne,

Lottering et al. [6] used 16 kg/tonne, and Gilligan and Nikoloski [31] used 25 kg/tonne. These studies were compared with Plant X as shown in Figure 42.

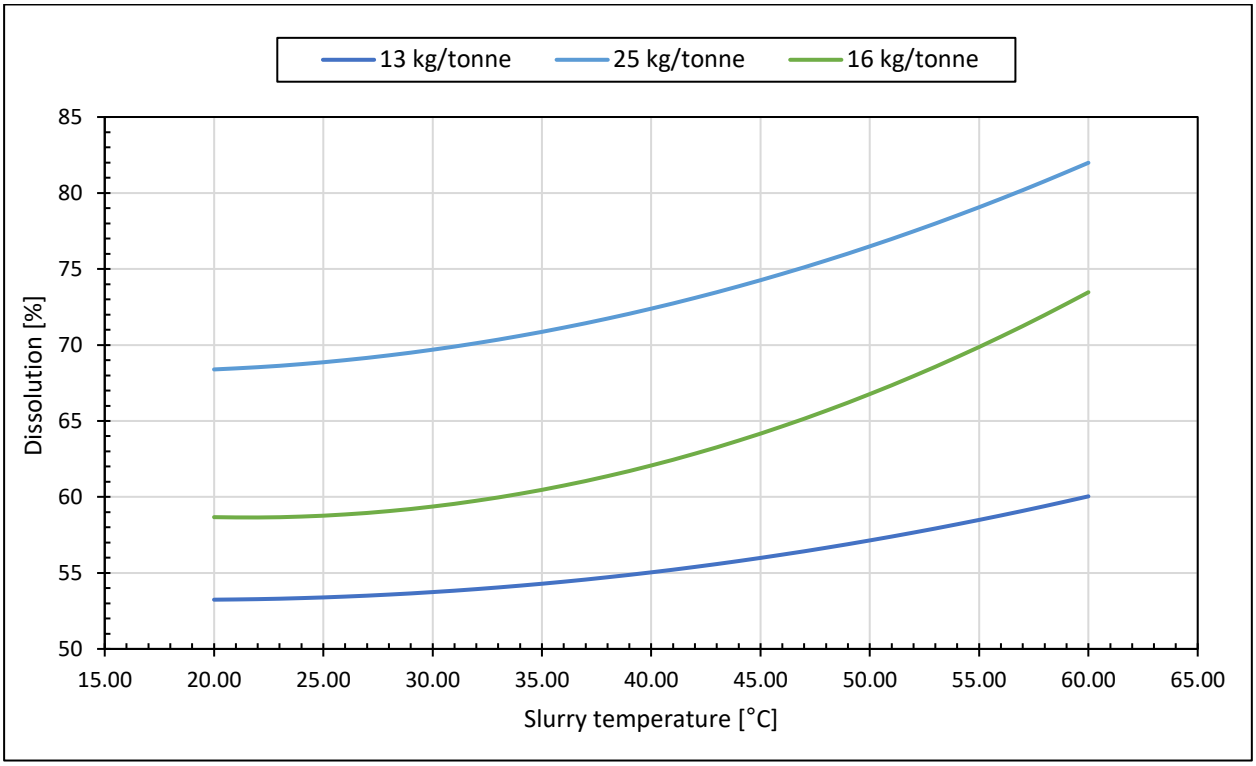

Figure 42: Verification of dissolution graph

Figure 42 demonstrates the different dissolution rates for the different temperatures at different sulphuric acid concentrations. Recalling from Sections 1.3.6 and 1.4.2, the first aspect that influences uranium extraction is the type of ore being treated. From Reynolds et al. [34] it is clear that between uraninite to coffinite, brannerite is the most difficult uranium refractory for recovering uranium, which is also the type of ore at Plant X. Studies on brannerite minerals being treated to recover uranium clearly concluded that brannerite is the most difficult ore being used [6, 29, 34].

Another aspect discussed during the literature review was the acid concentration used during the extraction process [3, 5, 6, 29, 30, 34]. Although acid concentration had a significant effect, the effect was not as great as the temperature for such an application, as was discussed in Section 1.3.6. The 13 kg/tonne line depicted in Figure 42 represents data obtained from the operations at Plant X, which used brannerite minerals with a 13 kg/tonne sulphuric acid concentration. Comparing this line with the 16 kg/tonne and 25 kg/tonne lines, respectively, it clearly had the lower concentration of the two rates. Lottering et al. [6] investigated the leaching process at a 16 kg/tonne of acid concentration, whereas Gilligan et al. [29] investigated a 25 kg/tonne concentration. The lower concentration of sulphuric acid ran on a lower line than the rest of the concentrations, which ran on the higher lines. The important aspect to conclude from Figure 42 is that the results of the 13 kg/tonne line had the same trend as the other two lines obtained from

literature. This clearly showed that the results of the empirical model were accurate since the results represented the 13 kg/tonne line.

Most aspects affecting the process were kept constant throughout the literature to analyse the effect of the temperature to verify the uranium extraction rates. The heat recovery rates at different sulphuric acid concentrations were compared since the model had to be verified with a factor that influenced the extraction rates other than the effect of temperature. Although other factors do affect the process, such as manganese oxide, the studies that were reviewed concluded that the concentrations were typically the same.

Once the empirical model had been verified and deemed accurate, it was used to analyse different possibilities at Plant X. This plant had the potential to form part of a heat recovery system since there were mining equipment that produced heat and there was a clear increase in uranium extraction when the temperature of the mixture increased. The following section discusses the integration of the verified models.

3.6 Model integration

3.6.1 Data obtained

Once all the models had been verified, they were integrated to simulate the heat recovery potential of the system. As mentioned in Section 2.5.2 and Figure 27, the uranium plant had to be integrated with a heat recovery system.

The integrated layout shown in Figure 43 was created using the heat source layout of Mine B as seen in Figure 34 and the data obtained from the site inspection. Some values in Figure 29 were used as parameters for the simulation to ensure that the model simulated with the required accuracy.

Figure 43 represents the layout and integration of the solution model, which is the integration of the uranium plant with the compressors at Mine B. It follows the same concept as the heat recovery on Mine A. The water leaving the compressor aftercoolers usually flows to the cooling towers, as observed in Figure 29, and this heat is dissipated into the atmosphere. Instead of the warm water being pumped to the cooling towers, the water could rather be redirected towards Plant X.

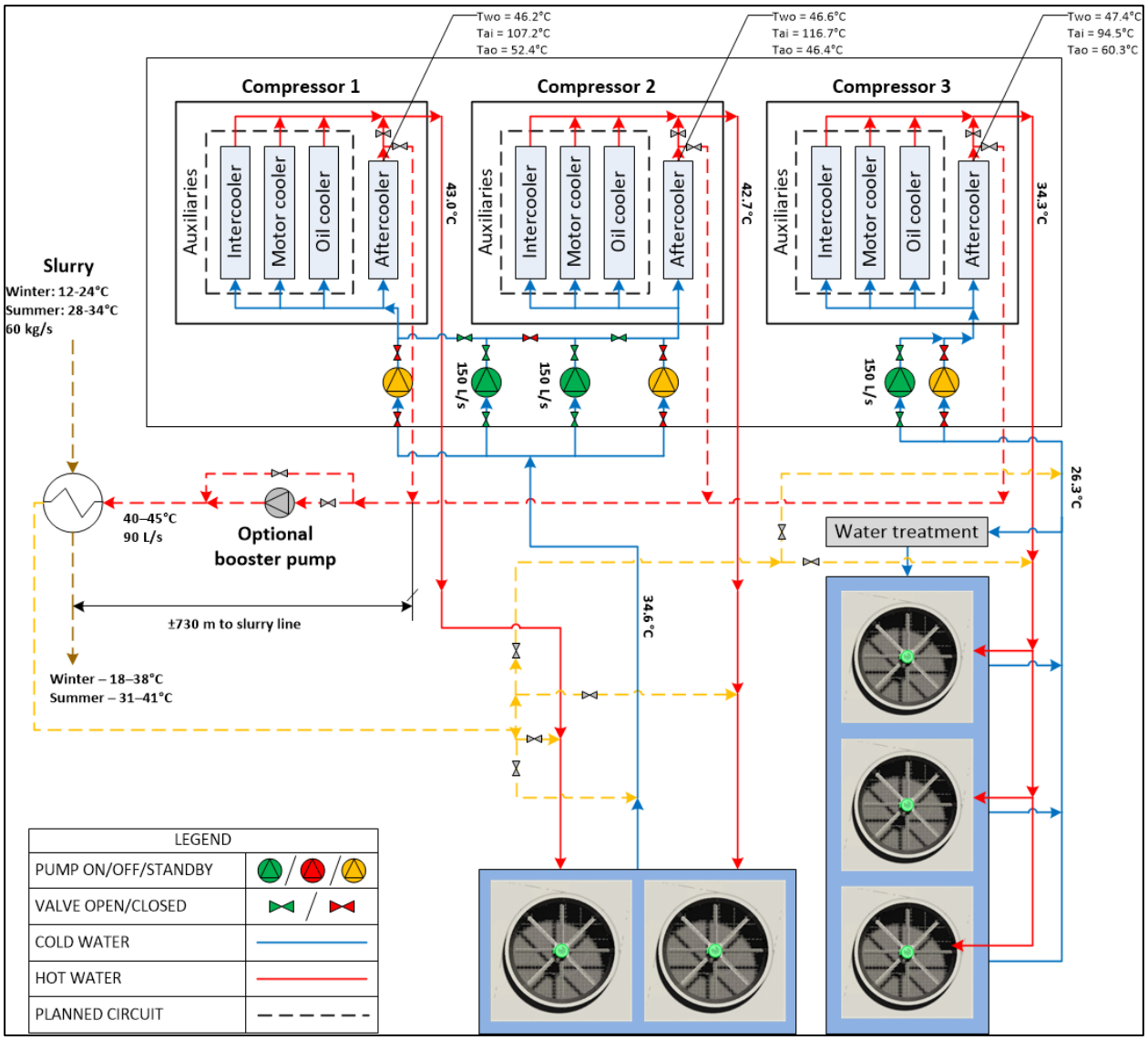

Figure 43: Solution model heat recovery layout

The water is pumped through cladded pipes as in Mine A to reduce the heat loss through pipes subjected to the environment. Currently, the uranium-carrying slurry being transferred to Plant X is subjected to atmospheric conditions, which keep the slurry at a lower temperature. In the slurry feed line, a spiral heat exchanger is inserted to transfer the heat from the warm water to the colder uranium slurry, compared with the heat transfer from the warm water to the change house in Section 3.3.

Since the integrated layout of the solution model was constructed as shown in Figure 43, the simulation model could be developed, which is discussed in the following section.

3.6.2 Solution model integration results

Referring to Section 2.5.2, the next step was to modify the simulation model and integrate the necessary components. Using the solution model layout as shown in Figure 43, the simulation

was modified using the PTB software. Figure 44 shows the simulation layout for the heat recovery system.

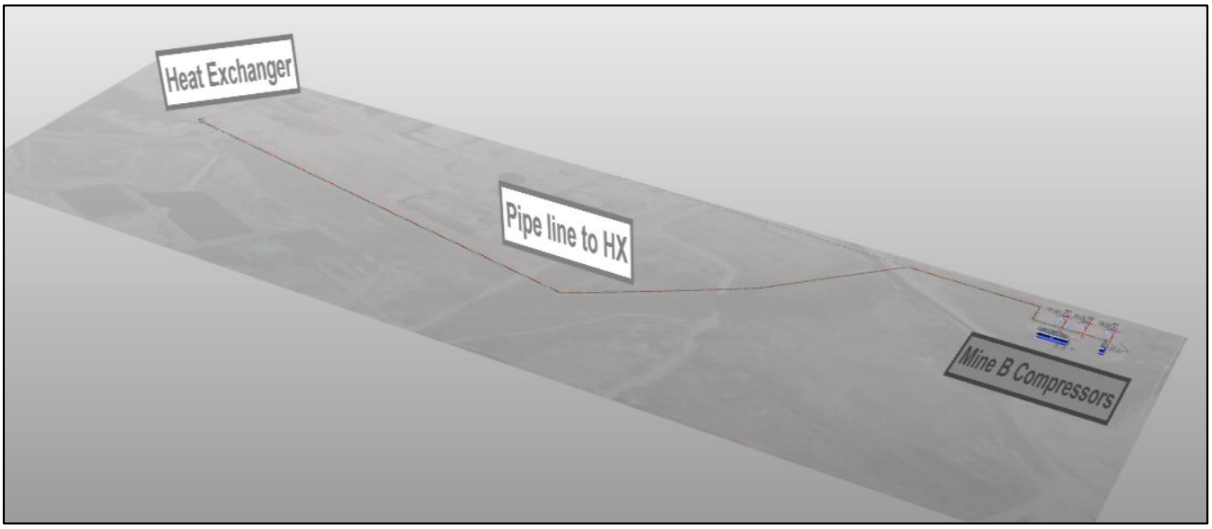

Figure 44: Mine B heat recovery proposed layout

Figure 44 displays the simulation obtained from PTB. It recovers the heat at the compressors at Mine B, transfers it through the pipeline to the heat exchanger, and exchanges the heat at the heat exchanger situated at Plant X. The results obtained from the simulation is analysed during the following section, starting with optimal duty results used for the heat exchanger.

3.6.3 Results of solution model

As mentioned in Section 2.5.3, the heat recovered from a heat source needs to be transferred and exchanged through a system. A heat exchanger could be used for such a purpose. The working principles were discussed in the literature review in Section 1.4.3.

Figure 27 showed that the next step after modifying and integrating the system is to choose the type of heat exchange equipment. A spiral heat exchanger was chosen for the application due to its reduced fouling, simplified maintenance, increased heat transfer, and being compact in size with still great heat transfer capabilities [56]. The design of the spiral heat exchanger makes it ideal for dirty and highly viscous liquids. The heat exchanger has the potential of achieving an approach temperature of 2°C and one of its greatest advantages is the self-cleaning effect [77].

Using the data obtained from the design specification, as indicated in Appendix A, the heat exchanger potential was simulated to determine which conditions would be ideal for the heat recovery system. The effect of the heat exchanger during different seasons throughout the year was simulated. The results of the heat transfer potential during winter and summer conditions are shown in Figure 45 and Figure 46, respectively.

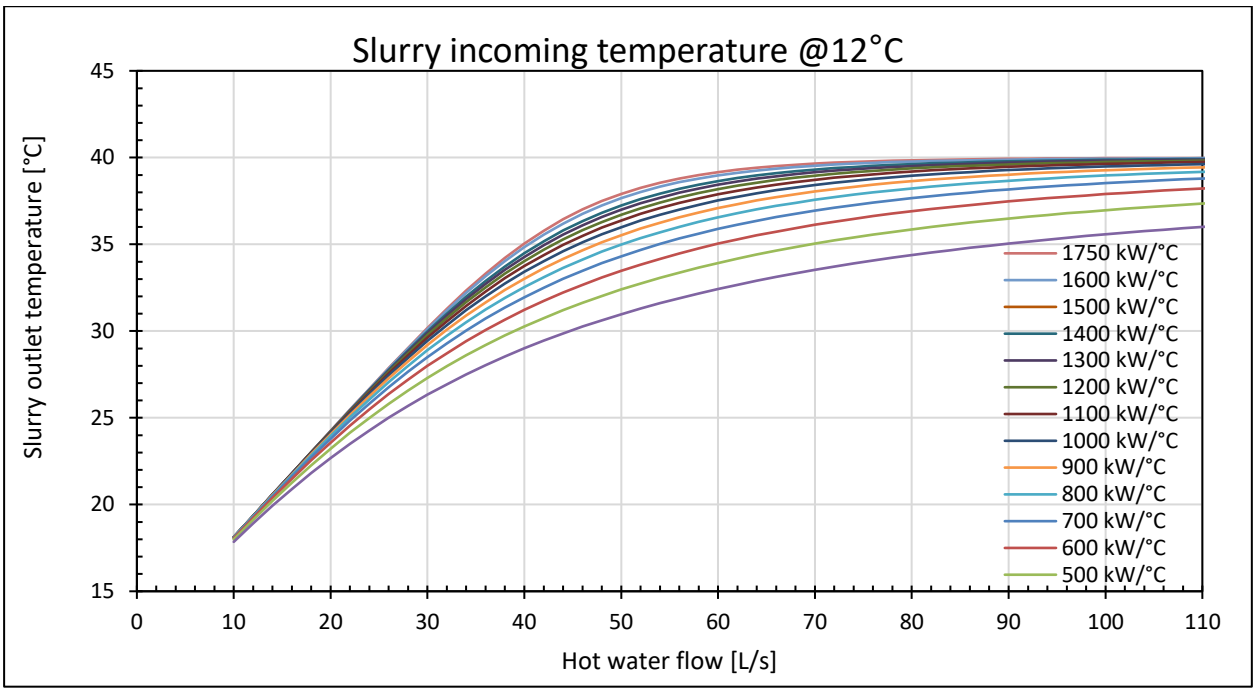

Figure 45: Heat exchanger potential at different water flow rates during winter conditions

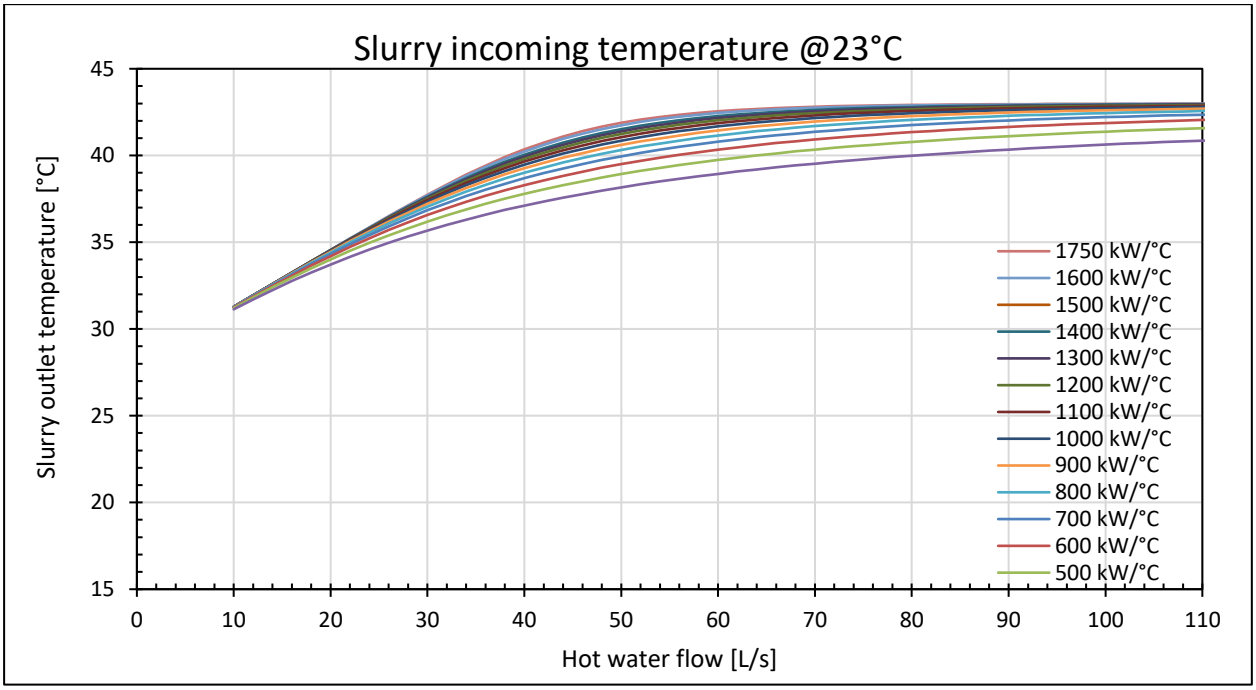

Figure 46: Heat exchanger potential at different water flow rates during summer conditions

Figure 45 and Figure 46 explain the behaviour of the heat exchanger. As the flow rate of the hot water increased, it caused a significant increase in slurry outlet temperatures. Most temperatures started to converge between 60 L/s and 70 L/s. As the average water flow entering the heat exchanger was 90 L/s, as mentioned in Section 3.6.1, convergence was possible.

The higher overall heat transfer coefficient of the heat exchanger, represented by the lines in Figure 45 and Figure 46, resulted in higher temperatures being achieved faster. Using the data

obtained from the simulations in Figure 45 and Figure 46, it was determined that 1 750 kW/°C was the ideal heat transfer coefficient to be used as the duty for the heat exchanger. This ensured that the heat exchanger in the simulation model for the heat recovery would be accurate. The modified simulation model, as shown in Figure 44, was ready for simulation with a heat exchanger duty of 1 750 kW/°C.

The different scenarios simulated for the solution model are summarised in Table 18. The four scenarios were simulated for winter and summer conditions, at 12°C and 23°C, respectively.

Table 18: Heat recovery scenarios for Solution model

Scenarios	Description
Scenario 1	Heat recovered from one compressor running
Scenario 2	Heat recovered from two compressors running
Scenario 3	Heat recovered from all three compressors running
Scenario 4	Heat recovered from just the aftercoolers

Table 18 shows all the simulated scenarios. Scenario 1 to 3 recovered heat from the different aftercoolers of different compressors, which were combinations of Compressor 1 to 3. Scenario 4 recovered the heat from all the aftercoolers of the three compressors, which resulted in a higher temperature as discussed in the following tables.

Table 19 shows the results for Scenario 1. The tables showing the results follow the same layout as Table 12, with the only change being the slurry heat exchanger column that was inserted to analyse the heat pickup from the different scenarios.

Table 19: Results for Scenario 1 at winter conditions

	Scenario 1 – Winter			
	Compressor 1 aftercooler	Compressor 2 aftercooler	Compressor 3 aftercooler	Slurry heat exchanger
Cold fluid flow (L/s)	27.9	26.6	26.5	67.0
Hot fluid flow (kg/s)	15.0	15.0	15.9	90.6
Cooling duty (kW)	2 107.1	2 103.1	2 304.4	3 812.5
Cold fluid temp in (°C)	19.3	19.3	19.2	12.0
Cold fluid temp out (°C)	37.4	38.3	40.0	25.6
Hot fluid temp in (°C)	95.0	95.0	95.0	26.5
Hot fluid temp out (°C)	75.6	75.7	76.1	16.4

Referring to Table 19, the cold fluid is the slurry subjected to ambient conditions with a flow rate of 67 L/s according to the design specifications (see Appendix A), whereas the hot fluid is the recovered hot water from the compressors at Mine B. The winter temperature was assumed to be the same as the slurry temperature, which was 12°C. Recovering heat from one compressor increased the slurry temperature to 25.6°C, which we knew from literature would increase uranium recovery [2, 5, 6, 23, 30, 34]. The heat recovered from one compressor and the rest of the compressors still used the water-cooling circuit, as observed in Figure 34.

Table 20 and Table 21 show the results for Scenario 2 and Scenario 3, respectively.

Table 20: Results for Scenario 2 at winter conditions

	Scenario 2 – Winter			
	Compressor 1 aftercooler	**Compressor 2 aftercooler**	**Compressor 3 aftercooler**	**Slurry heat exchanger**
Cold fluid flow (L/s)	27.1	26.9	26.5	67.0
Hot fluid flow (kg/s)	15.0	15.0	15.9	92.3
Cooling duty (kW)	2 118.3	2 117.5	2 304.4	4 754.7
Cold fluid temp in (°C)	18.1	18.1	19.2	12.0
Cold fluid temp out (°C)	36.8	36.9	40.0	29.0
Hot fluid temp in (°C)	95.0	95.0	95.0	30.0
Hot fluid temp out (°C)	75.4	75.4	76.1	17.7

Table 21: Results for scenario 3 at winter conditions

	Scenario 3 – Winter			
	Compressor 1 aftercooler	**Compressor 2 aftercooler**	**Compressor 3 aftercooler**	**Slurry heat exchanger**
Cold fluid flow (L/s)	27.0	26.7	26.8	67.0
Hot fluid flow (kg/s)	15.0	15.0	15.9	92.5
Cooling duty (kW)	2 107.3	2 106.4	2 272.5	5 465.3
Cold fluid temp in (°C)	19.1	19.1	21.9	12.0
Cold fluid temp out (°C)	37.8	37.9	42.2	33.7
Hot fluid temp in (°C)	95.0	95.0	95.0	35.0
Hot fluid temp out (°C)	75.6	75.6	16.7	19.4

Table 20 and Table 21 show that the slurry temperature entering Plant X after the heat exchanger could reach temperatures of 29.0°C and 33.7°C, respectively. This is a good increase since the slurry temperature during winter conditions is usually 12°C and could possibly multiply the temperature by 2.

After determining the winter results for Scenario 1 to Scenario 3, the same three scenarios were repeated for summer conditions. Table 22, Table 23 and Table 24 show the results for the three scenarios simulated during summer conditions.

Table 22: Results for Scenario 1 during summer conditions

	Scenario 1 – Summer			
	Compressor 1 aftercooler	**Compressor 2 aftercooler**	**Compressor 3 aftercooler**	**Slurry heat exchanger**
Cold fluid flow (L/s)	27.8	26.5	26.6	67.0
Hot fluid flow (kg/s)	15.0	15.0	15.9	91.0
Cooling duty (kW)	2 016.1	2 011.6	2 232.8	2 911.5
Cold fluid temp in (°C)	27.2	27.2	25.0	23.0
Cold fluid temp out (°C)	44.6	45.3	45.1	33.3
Hot fluid temp in (°C)	95.0	95.0	95.0	34.0
Hot fluid temp out (°C)	77.2	77.2	77.3	26.4

Table 23: Results for Scenario 2 during summer conditions

	Scenario 2 – Summer			
	Compressor 1 aftercooler	**Compressor 2 aftercooler**	**Compressor 3 aftercooler**	**Slurry heat exchanger**
Cold fluid flow (L/s)	27.1	26.9	26.5	67.0
Hot fluid flow (kg/s)	15.0	15.0	15.9	92.3
Cooling duty (kW)	2 024.5	2 023.6	2 232.4	3 884.1
Cold fluid temp in (°C)	26.3	26.3	25.0	23.0
Cold fluid temp out (°C)	44.2	44.3	45.2	36.9
Hot fluid temp in (°C)	95.0	95.0	95.0	37.7
Hot fluid temp out (°C)	77.0	77.0	77.3	27.7

Table 24: Results for Scenario 3 during summer conditions

	Scenario 3 – Summer			
	Compressor 1 aftercooler	Compressor 2 aftercooler	Compressor 3 aftercooler	Slurry heat exchanger
Cold fluid flow (L/s)	27.0	26.7	26.8	67.0
Hot fluid flow (kg/s)	15.0	15.0	15.9	93.1
Cooling duty (kW)	2 017.6	2 016.7	2 187.9	4 985.8
Cold fluid temp in (°C)	26.9	26.9	28.4	23.0
Cold fluid temp out (°C)	44.7	44.9	48.0	40.8
Hot fluid temp in (°C)	95.0	95.0	95.0	41.8
Hot fluid temp out (°C)	77.1	77.1	77.9	29.0

Table 22, Table 23 and Table 24 demonstrate the potential of the uranium slurry temperature yield. From an ambient temperature of 23°C, the hot water recovered during these scenarios had the potential of heating the slurry to 33.3°C, 36.9°C and 40.8°C, respectively.

Table 25 and Table 26 display the simulation results for Scenario 4 for winter and summer conditions, respectively.

Table 25: Heat recovery results from only the aftercooler during winter

	Only aftercooler – Winter			
	Compressor 1 aftercooler	Compressor 2 aftercooler	Compressor 3 aftercooler	Slurry heat exchanger
Cold fluid flow (L/s)	30.2	30.0	29.6	67.0
Hot fluid flow (kg/s)	15.0	15.0	15.9	89.8
Cooling duty (kW)	2 114.2	2 113.5	2 304.4	6 529.7
Cold fluid temp in (°C)	19.3	19.3	20.1	12.0
Cold fluid temp out (°C)	36.0	36.2	38.7	35.3
Hot fluid temp in (°C)	95.0	95.0	95.0	36.9
Hot fluid temp out (°C)	75.5	75.6	76.2	19.5

Table 26: Heat recovery results from only the aftercooler during summer

	Only aftercooler – Summer			
	Compressor 1 aftercooler	Compressor 2 aftercooler	Compressor 3 aftercooler	Slurry heat exchanger
Cold fluid flow (L/s)	30.2	30.0	29.6	67.0
Hot fluid flow (kg/s)	15.0	15.0	15.9	89.8
Cooling duty (kW)	2 028.3	2 027.5	2 213.9	5 394.0
Cold fluid temp in (°C)	26.8	26.8	27.3	23.0
Cold fluid temp out (°C)	42.9	43.0	45.2	42.2
Hot fluid temp in (°C)	95.0	95.0	95.0	43.6
Hot fluid temp out (°C)	77.0	77.0	77.0	29.2

Table 25 and Table 26 show that the water leaving the compressor had a slightly higher temperature than the slurry outlet temperature after the heat exchanger. The temperature entering the uranium plant was 35.3°C and 42.2°C, respectively. This difference between these two temperatures was below 2°C, which was correct according to the approach's design specifications.

The results obtained from the solution model simulation clearly demonstrated the effect of the heat recovery system. Using the heat recovered from the compressors had a clear impact on the temperature of the uranium after the heat exchanger. To provide more clarity relating the effect, Figure 47 compares the slurry outlet temperatures obtained from the simulation.

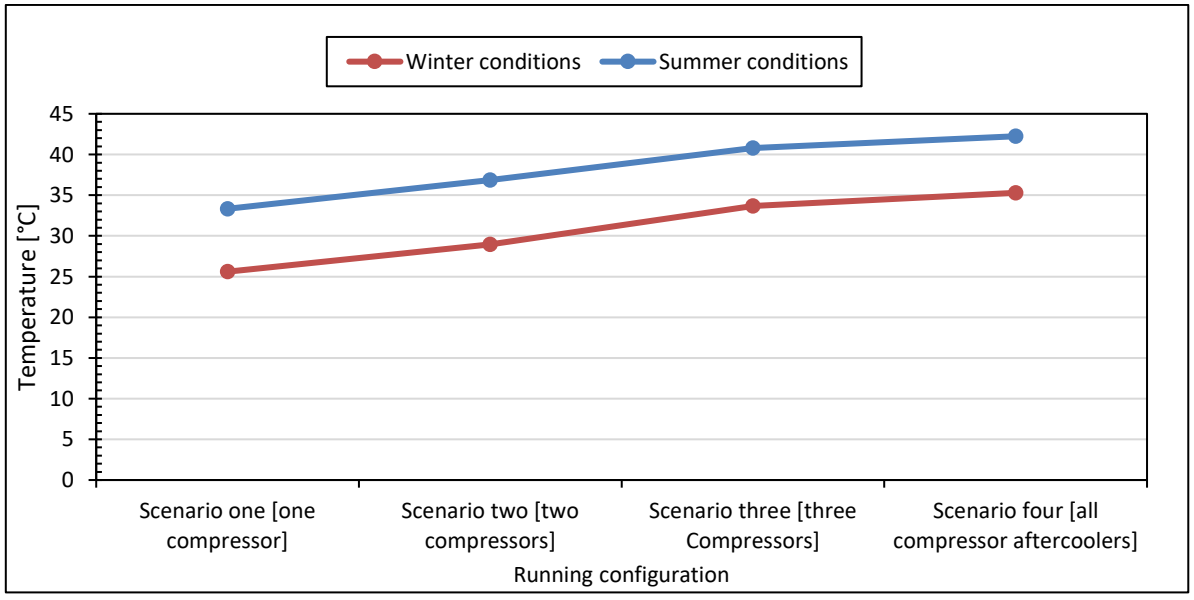

Figure 47: Slurry outlet temperature from the different heat recovery combinations at winter and summer conditions

Figure 47 clearly highlights the effect between winter and summer conditions for the respective running configuration scenarios that were running constantly. There was a temperature increase each time another compressor was added to the heat recovery circuit, which resulted in the best heat recovery being obtained during drilling shifts when all three compressors were running.

Since all the previous models had been verified to ensure the accuracy of the solution model, the results obtained in this section could be used to conduct a feasibility study to estimate the possible revenue versus expenditures for the system. The feasibility study is discussed in the next section.

3.7 Feasibility study of the heat recovery system

The effect of heat recovery was studied in Section 3.6, which concluded that slurry temperature clearly increases by using the heat recovered from Mine B. An important aspect to consider was how much this heat increase could benefit production financially. This was quantified by conducting a feasibility study. Recalling the steps from Section 2.6, the first step was to investigate all the costs involved in such a project. The capex of the project included the quoted price for the heat exchanger and the pipe prices per size and length. Table 27 shows the capex of the project [78].[1]

Table 27: Cost analysis of heat recovery [78]

Component	Price	Quantity	Total
Heat exchanger	R3 000 000	1	R3 000 000
Control valves	R43 000	8	R344 000
Piping to heat exchanger (250 mm)	R18 639	81	R1 509 764
Piping from heat exchanger (200 mm)	R15 154	81	R1 227 467
Cladding to heat exchanger (per metre)	R824	730	R601 243
Total (incl. 20% labour)			**R8 m²**

The quantities were obtained from recommendations in price lists and the layout obtained from the site inspection. Using the information obtained in Table 27, the yearly costs and benefits were calculated and inserted into Table 28.

Table 28: Yearly costs and benefits

Years	Yearly costs	Yearly benefits
1	R8 960 000.00	R1 883 505
2	R1 008 000.00	R2 890 429

[1] Cost estimate issued by Zonke Engineering on 19 May 2021.
[2] The exact value may vary with a 10% contingency.

Years	Yearly costs	Yearly benefits
3	R1 058 000.00	R7 913 099
4	R1 111 000.00	R10 880 205
5	R1 166 000.00	R10 470 950
6	R1 225 000.00	R14 156 910
Total:	**R14 528 000.00**	**R48 195 098**

The calculations were done with an initial cost of R8 000 000[3] for the heat exchanger and its components, such as pipes and valves. A monthly maintenance cost of 1% of the total capex was added for redundancy to maintain the heat exchanger and implications such as broken pipes [75]. This resulted in R80 000 monthly, and 5% was used for yearly inflation to estimate the expenditures yearly toward the end of the life of mine [79]. The benefit values were quantified by using the amount of uranium treated, the temperature increase of the uranium slurry, and a uranium price of R1 700/kg [80]. The expected increase in the slurry temperature, which leads to a higher dissolution rate, resulting in higher uranium recovery, was multiplied by R1 700/kg to determine the opportunity cost in terms of revenue.

Using the values from Table 28, the life of mine and the solution model simulation, a breakdown of the benefit was compiled for different year groups. Figure 48 and Figure 49 show the benefits for Year 1 and Year 2, respectively. The resulting years are shown in Appendix D.

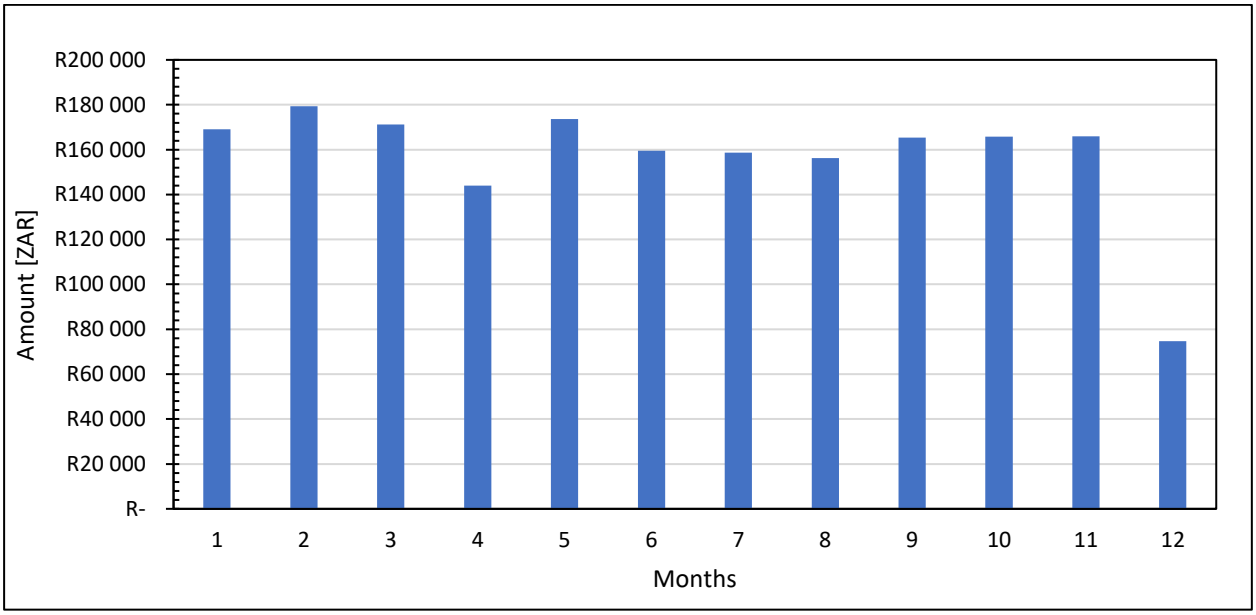

Figure 48: Monthly benefit for Year 1 of solution model

[3] Cost estimate issued by Zonke Engineering on 19 May 2021.

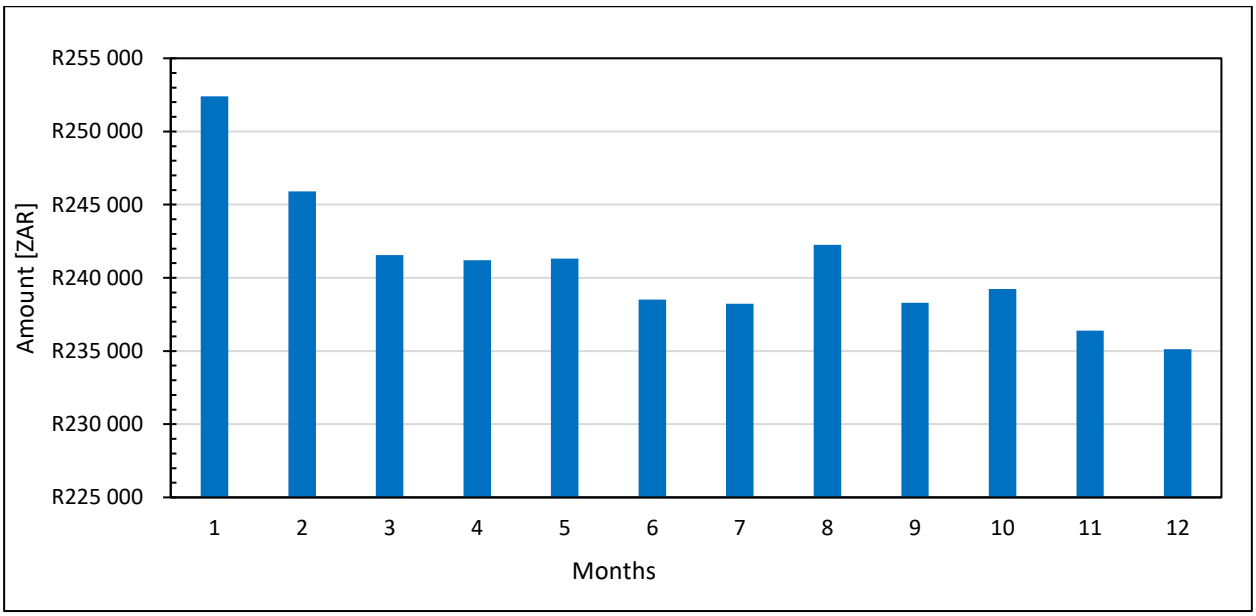

Figure 49: Monthly benefit for Year 2 of solution model

Recalling the results of the empirical model in Section 3.5 it was concluded that each year group treated different uranium tonnes, which resulted in different yields of uranium. It was investigated further to depict each year with monthly tonnes treated. Figure 48 and Figure 49 show the dynamic change in the benefit. This variability is due to the different tonnes being treated in the first year of the project as the same amount of ore was not treated each month. It is important to remember that this is still less than the initial capex of the project shown in Table 28; however, the benefit will outweigh the cost over time. This payback period is discussed later in this section.

Figure 49 depicts Year 2 of the project and the benefit that could be obtained. The benefit for Year 2 is more than Year 1 since fewer tonnes were treated, resulting in a warmer mixture (refer to Section 3.5.2). Figure 48 and Figure 49 show that a smaller benefit was obtained for Month 12, which is December, since the mine from which the ore was received underwent maintenance and did not supply for a time [66]. An important aspect to consider is that these calculations were based on the planned life of mine, which is a prediction of what the benefit should be since the models had been verified.

Using the same data as in Figure 48 and Figure 49, the payback period of the project was calculated. Calculations were done to quantify the total cost of the project including maintenance and inflation and to quantify the benefit of the project, which included the yearly benefit and the different tonnages treated. Figure 50 shows the cost for the solution model versus the cumulative benefit.

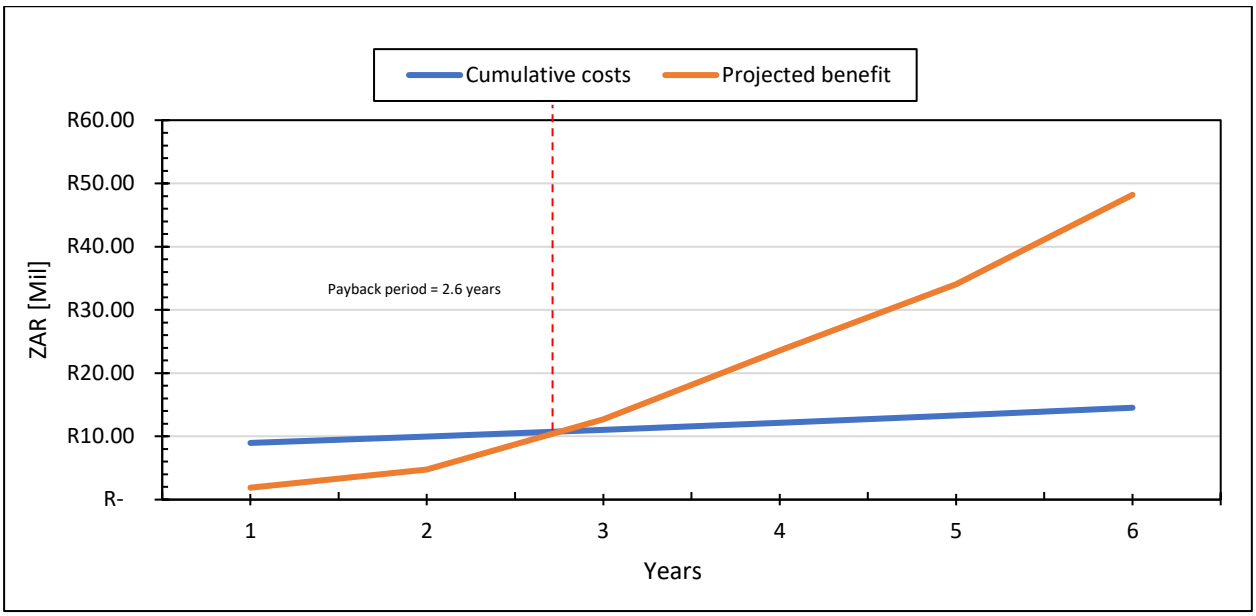

Figure 50: Heat recovery break-even point for six years

Figure 50 represents the total cumulative cost versus benefit for the solution heat recovery model. The substantial benefit from a heat recovery project is that mostly just the installation expenditure is expensive since there are no running costs. Monthly maintenance costs were included for redundancy using the values obtained from Table 28.

The red dashed line in Figure 50 indicates the payback period for this project, which was an estimated 2.6 years. More tonnes are processed during the first part of the life of mine, which leads to a colder mixture than in Year 3 to Year 6. This trend was discussed extensively in Section 3.5. The cumulative benefit line takes around 2.6 years to cross the cost line. The cost line is not a straight line as it includes monthly expenditure due to maintenance. However, since no electricity cost is needed for the project, as for boilers and heat pumps, the yearly expenditure is not much. This proves that the best option for the heat recovery application is to use the compressor waste heat obtained from Mine B and using a heat exchanger at Plant X.

The cumulative revenue obtained from the six years of available data used to determine the effect of the heat recovery project compared to the normal operating conditions at Plant X, is depicted in Figure 51.

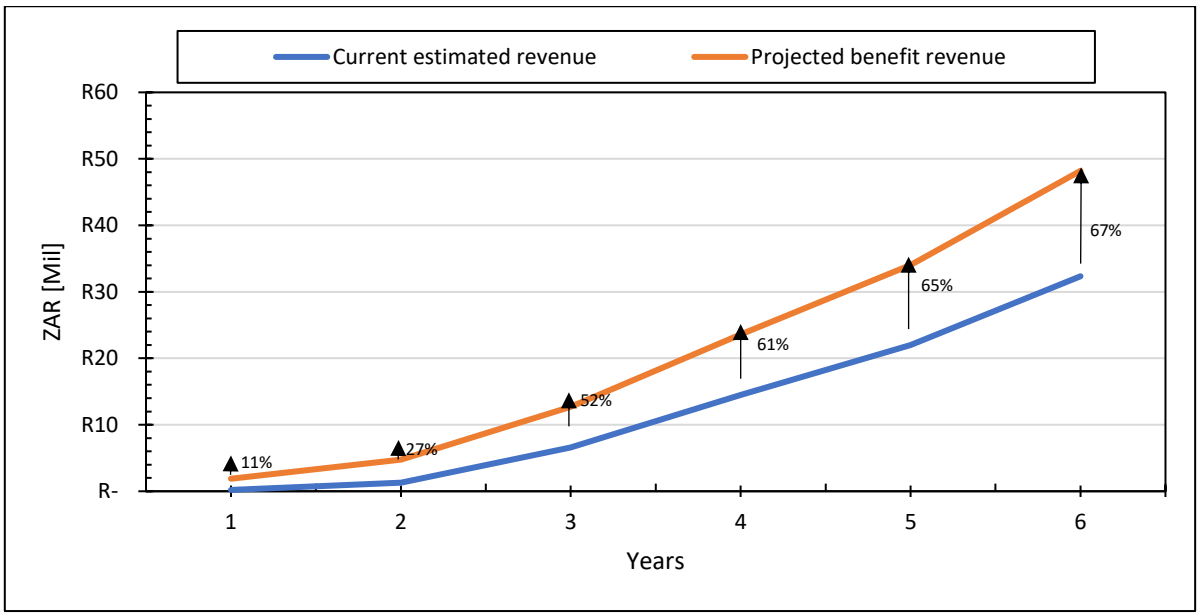

Figure 51: Normal operations revenue versus its heat recovered benefit

Figure 51 depicts the current operations at the uranium plant versus the projected benefit should the heat recovery be implemented each year. The figure shows that the current benefit after six years is an estimated R16m. The findings were calculated using a uranium price of R1 700/kg. A percentage increase is also listed in Figure 51, which depicts the higher increase obtained from the heat recovery model each year since the benefit increases each year (refer to Section 3.5.2) and the operational cost remains low.

The heat generated by the compressors was assumed to be the same every year, which implies that the heat exchanger at the uranium plant has the same amount of heat available to heat the slurry. Although the first year already shows a benefit, the tonnes treated are quite high according to the life of mine, thus the slurry will not be heated as much as when fewer tonnes are treated, as shown in Figure 48 and Figure 49. This is mainly due to the predicted decrease in tonnes treated towards the end of the life of mine, which enables a warmer mixture during the leaching process, resulting in the increasing gap between the benefit and revenue shown in Figure 51.

The results of the study were discussed and analysed in detail throughout this chapter. The last step is to validate the study by evaluating the study objectives mentioned in Section 1.5. The validation and conclusion of the study are discussed in the following section.

3.8 Validation and conclusion

3.8.1 Validation of the study

A crucial step in a study is to ensure that the study objectives have been achieved. Recalling from Section 1.5, the successes of the objectives can be summarised as:

- Develop and verify a current operational heat recovery model, which was completed successfully in Section 2.2 and Section 3.3.
- Develop and verify a current operational heat source model, which was completed successfully in Section 2.3 and Section 3.4.
- Develop and verify an empirical model for uranium leaching analysis, which was completed successfully in Section 2.4 and Section 3.5.
- Integrate the verified models, which was completed successfully in Section 2.5 and Section 3.6.
- Conduct a feasibility study, which was completed successfully in Section 2.6 and Section 3.7.

The methodology that was developed can be used in most industries where heat from a working system can be recovered to improve and evaluate a system, such as a uranium plant. These simulations may be used to aid with a prefeasibility and concept study before an actual project is implemented.

3.8.2 Conclusion

The generic methodology developed was implemented successfully in various cases. These case studies were included to successfully investigate a working heat recovery system and verify its simulation accuracy. The next step was to investigate a heat source that had potential to be integrated with a heat recovery model, whereafter the simulation results were verified. The third step was to derive an empirical model to analyse the data obtained from the uranium plant, which was completed successfully. Lastly, the verified models had to be combined to investigate the simulation model used to assess the improved performance of such a system.

The solution model was used to assess the performance of a uranium plant and simulate possible improvements to the system. To assess the uranium plant, a feasibility study was included to determine whether the heat recovery system was feasible. The payback period of the solution model was calculated to be around 2.6 years with great additional benefits.

Using all the steps mentioned in the study, a clear and accurate understanding of such a system's performance was obtained and quantified. This indicates that should this methodology be used to assess other aspects, it will be successful. The following chapter concludes the study by discussing the overall conclusion of this dissertation, which includes a summary and recommendations that could assist with future studies.

CHAPTER 4 – CONCLUSION

4.1 Summary

Mining in South Africa encompasses various mineral extraction processes, including the retrieval of uranium from leaching slurry at gold processing plants. Heating is necessary to increase the temperature and hasten the uranium leaching process. However, declining ore quality coupled with high electricity pricing tariffs in South Africa has led to reduced efficiency of uranium plants.

The current method to extract uranium was conducted at normal ambient temperatures. Other heating methods available to assist with the process have been proven to be energy intensive, leading to an increase in energy consumption that outweighs the yield it provides. Therefore, there was a need to develop a method for investigating a heat source that could form part of a heat recovery system to increase the efficiency of a chemical plant. This could ensure an increase in in the yield of the uranium extraction and reduce operational costs.

Thus, the study objectives were to:

- Develop and verify a current operational heat recovery model, refer to Section 2.2 and Section 3.3.
- Develop and verify a current operational heat source model, refer to Section 2.3 and Section 3.4.
- Develop and verify an empirical model for uranium leaching analysis, refer to Section 2.4 and Section 3.5.
- Integrate the verified models, refer to Section 2.5 and Section 3.6.
- Conduct a feasibility study, refer to Section 2.6 and Section 3.7.

The study methodically described the development of a process to investigate and verify a heat recovery system. It was used and applied to a case study, starting with investigating and verifying a current working heat recovery system. It was further used to investigate a heat source system that could be form part of a heat recovery system.

Furthermore, an empirical model was developed to analyse the uranium dissolution data and verify the data obtained from the uranium plant. Lastly, a potential heat recovery system was identified that could use the heat source to form part of a heat recovery system to improve the efficiency of the process. Once the solution model had been verified, the results were used to evaluate the improved efficiency of the plant.

The heat recovery model and the heat source model were verified successfully. Both models simulated to an accuracy higher than 95% by comparing the simulation results with the actual data obtained from the systems. The systems can be used to predict system behaviour with an error of approximately 5%, which is a good guideline to adhere to. The results presented revealed that the dissolution rates at the uranium plant could be improved. In the past, boilers had been used for heating purposes; however, as concluded in this study, it is not a feasible method. A model that recovers the heat at the compressors of Mine B was simulated and assessed.

The simulation included all the necessary components required for the simulation, the correct dimensions and design specifications using current heat produced instead of the heat being wasted. Once the simulation model had been verified, an empirical model was developed to analyse the data obtained from the uranium plant, which was verified during this study.

After model verification, the models were integrated to form a solution model to simulate the benefits illustrated by such a system. Clear benefits were obtained from the solution model simulation and it was used to conduct the feasibility study, which included all the benefits obtained and the expenditures relating to the study such as capital and operating expenditure.

The study was conducted over the entire life of the uranium plant, and included summer and winter temperatures, separately. Yearly benefits were obtained and the overall benefit of the entire system was quantified. The feasibility study determined a payback period of 2.6 years, resulting in a R16m benefit for a six-year life of mine.

In conclusion, the study proved to be successful in achieving all the objectives. The methodology derived can be used to identify and simulate heat recovery systems and integrate them with other plants, such as uranium plants. The developed models can be used to predict the performance of the systems before implementation. The models can further be used to aid with the preplanning and predesigning processes.

4.2 Future recommendations

This section’s objective is to provide recommendations for future possibilities by which the study could be of assistance. Typical problems during the case study included acquiring trusted and detailed information about the mining systems and uranium plant. This was due to the old infrastructure being used, which entailed that the information always had to be checked and verified to ensure the equipment used was correct. It is therefore recommended to update the equipment and infrastructure to enhance the reliability of the results.

The following recommendations are made and will be discussed:

- Implementing the project and verifying the improved uranium plant's performance with actual data.
- Investigating the effect of acid concentration since it also has a great effect on uranium leaching.
- Testing the methodology on other industrial plants.

Referring to Section 3.7, the results of the solution heat recovery model were used to calculate the yield provided by the heat recovery model. Implementing and testing the methodology developed with increased uranium dissolution rates could lead to more accurate results and alterations could be made to the system. The data obtained during this study for the uranium plant was verified against literature that conducted similar work and used to analyse the benefit. However, if the results could be compared with actual physical measurements, it should ensure a higher degree of accuracy.

As mentioned in Section 1.3.6, various parameters affect the uranium leaching process. Since the influence of heat was used for the study, other aspects could also be investigated. The model could be used to test the behaviour of uranium leaching at different acid concentrations, which could be done by keeping the temperature within a certain range and testing three to five different concentrations. This test could further be repeated by using different temperature ranges. Thus, an ideal mix between the slurry temperature and acid concentration could be achieved, which would further increase the efficiency of the uranium processing plant.

Recalling from Section 3.5, the chosen industrial plant was a uranium processing plant. Since the methodology developed was a generic procedure for obtaining information and simulating the chosen systems, it could be used to test other industrial plants. Other plants, such as gold leaching, copper leaching and platinum plants, could be used to test the process as described in this study.

Other to be considered:

- What would the impact be if all the heat sources (intercooler, motor and oil cooler) were considered.
- Effect of insulated versus non-insulated pipes.

REFERENCE LIST

[1] Chamber of Mines of South Africa, “Facts and figures 2016,” Johannesburg. https://www.mineralscouncil.org.za/industry-news/publications/facts-and-figures.

[2] V. Madakkaruppan, A. Pius, T. Sreenivas, and K. Shiv Kumar, “Leaching kinetics of uranium from a quartz–chlorite–biotite rich low-grade Indian ore,” *Journal of Radioanalytical and Nuclear Chemistry*, 2014, doi: 10.1007/s10967-014-3760-3.

[3] K. Nalivaiko, S. Skripchenko, S. Titova, and V. Rychkov, “Characterization and processing of radioactive uranium containing waste sludge by sulfuric acid leaching,” *Journal of Environmental Chemical Engineering*, vol. 10, no. 1, 2022, doi: 10.1016/j.jece.2021.106972.

[4] R. Gilligan and A. N. Nikoloski, “The extraction of uranium from brannerite,” *Minerals Engineering,* p. 11.

[5] Y. Khawassek, M. Taha, and A. Eliwa, “Kinetics of leaching process using sulfuric acid for Sella uranium ore material, South Eastern Desert, Egypt,” *International Journal of Nuclear Energy Science and Engineering*, vol. 6, 2016, doi: 10.14355/ijnese.2016.06.006.

[6] M. J. Lottering, L. Lorenzen, N. S. Phala, J. T. Smit, and G. A. C. Schalkwyk, “Mineralogy and uranium leaching response of low grade South African ores,” *Minerals Engineering*, vol. 21, no. 1, pp. 16–22, 2008, doi: 10.1016/j.mineng.2007.06.006.

[7] R. Gilligan and A. N. Nikoloski, “The extraction of uranium from brannerite: A literature review,” *Minerals Engineering*, vol. 71, pp. 34–48, 2015, doi: 10.1016/j.mineng.2014.10.007.

[8] Y. Men, X. Liu, and T. Zhang, “A review of boiler waste heat recovery technologies in the medium-low temperature range,” *Energy*, vol. 237, 2021, doi: 10.1016/j.energy.2021.121560.

[9] E. Vyhmeister et al., “A combined photovoltaic and novel renewable energy system: An optimized techno-economic analysis for mining industry applications,” *Journal of Cleaner Production*, vol. 149, pp. 999–1010, 2017, doi: 10.1016/j.jclepro.2017.02.136.

[10] H. Jouhara, N. Khordehgah, S. Almahmoud, B. Delpech, A. Chauhan, and S. A. Tassou, “Waste heat recovery technologies and applications,” *Thermal Science and Engineering Progress*, vol. 6, pp. 268–289, 2018, doi: 10.1016/j.tsep.2018.04.017.

[11] C. P. Kiang, “Commercial and industrial spaces: Warming up to heat pumps,” Johnson Controls. [Online]. Available: https://www.johnsoncontrols.com/en_sg/insights/2021/in-the-news/warming-up-to-heat-pumps

[12] P. A. De Villiers and L. J. Grobler, “Measurement and verification methodology for an industrial waste heat recovery project in the mining industry,” in *Proceedings of the 10th Industrial and Commercial Use of Energy Conference*, p. 6, 2013.

[13] F. Winde, D. Brugge, A. Nidecker, and U. Ruegg, “Uranium from Africa – An overview on past and current mining activities: Re-appraising associated risks and chances in a global context,” *Journal of African Earth Sciences*, vol. 129, pp. 759–778, 2017, doi: 10.1016/j.jafrearsci.2016.12.004.

[14] N. Lioudis. “What Is the gold standard? Advantages, alternatives, and history,” *Investopedia*, 4 March 2022. [Online]. Available: https://www.investopedia.com/ask/answers/09/gold-standard.asp

[15] P. N. Neingo and T. Tholana, “Trends in productivity in the South African gold mining industry,” *Journal of the Southern African Institute of Mining and Metallurgy*, vol. 116, no. 2, 2016, doi: 10.17159/2411-9717/2016/v116n3a10.

[16] P. N Neingo and F. T. Cawood, “Correlation of productivity trends with market factors at three selected platinum mines,” *The 6th International Platinum Conference, ‘Platinum – Metal for the Future’*, The Southern African Institute of Mining and Metallurgy, p. 8, 2014.

[17] Chamber of Mines of South Africa, “Facts and figures 2020,” Johannesburg, 2020. https://www.mineralscouncil.org.za/industry-news/publications/facts-and-figures

[18] C. Msingwini, “Introduction of specialization in mine planning and optimisation within the master’s degree (MSc) programme at the University of Witwatersrand,” *The 6th International Platinum Conference, ‘Platinum – Metal for the Future*’, The Southern African Institute of Mining and Metallurgy, 2014.

[19] J. McKane. “These graphs show why Eskom is hiking electricity prices,” *MyBroadband*, 11 Aug. 2020. [Online]. Available: https://mybroadband.co.za/news/energy/362976-these-graphs-show-why-eskom-is-hiking-electricity-prices.html

[20] H. J. Brynard, L. C. Ainslie, and P. J. Van der Merwe, “Uranium in South Africa,” The Atomic Energy Corporation of South Africa, Pretoria, 1988.

[21] A. Kenan and E. Chirenje, “Uranium in South Africa: Exploration, mining and production,” Council for Geoscience, Pretoria [no date].

[22] D. C. Siedel, “Extracting uranium from its ores,” *IEAA Bulletin*, vol. 23, no. 2, p. 5, 1981.

[23] World Nuclear Association, “Uranium production figures, 2013–2022,” May 2023. [Online]. Available: https://world-nuclear.org/information-library/facts-and-figures/uranium-production-figures.aspx

[24] D. Lunt, P. Boshoff, M. Boylett, and Z. El-Ansary, “Uranium extraction: The key process drivers,” *Southern African Institute of Mining and Metallurgy*, p. 9, 2007.

[25] S. Vukcevic, “Comparison of alkali and acid methods for the extraction of Gold from low grade ores,” *Minerals Engineering*, vol. 9, p. 10, 1996.

[26] B. J. Youlton and J. A. Kinnaird, “Gangue–reagent interactions during acid leaching of uranium,” *Minerals Engineering*, vol. 52, pp. 62–73, 2013, doi: 10.1016/j.mineng.2013.03.030.

[27] A. H. Kraiz, W. M. Fathy, H. A. Abu Khoziem, A. M. Ramadan, D. M. El-Kholy, I. E. El-Aaasy, and M. R. Moharam, “Leachability of uranium from low grade uraniferous granites, Eastern Desert, Egypt,” *International Journal of Engineering Research and Advanced Technology (IJERAT)*, vol. 02, no. 02, 2016.

[28] Y. S. Ladola, S. V. Kadam, K. N. Hareendran, and S. B. S. Chowdhury, S. B. Roy, and A. B. Pandit, “Analysis of Uranium leaching process and effect of cake washing on uranium recovery,” *Journal of Materials Science and Engineering with Advanced Technology*, vol. 10, p. 14, 2014.

[29] A. Costine, A. N. Nikoloski, M. D. Costa, K. F. Chong, and R. Hackl, “Uranium extraction from a pure natural brannerite mineral by acidic ferric sulphate leaching,” *Minerals Engineering*, vol. 53, pp. 84–90, 2013, doi: 10.1016/j.mineng.2013.07.010.

[30] S. A. Zakia, M. M. Rashad, S. A. Mohamed, E.M. El Sheikh, H. E. Mira, G. M. Abd El Wahab, “Kinetics of uranium leaching process using sulfuric acid for Wadi Nasib ore, south western Sinai, Egypt,” *Aswan University Journal of Environmental Studies*, vol. 1, no. 2, pp. 171–182, 2020, doi: 10.21608/aujes.2020.127584.

[31] R. Gilligan and A. N. Nikoloski, “The process chemistry and mineralogy of brannerite leaching,” *Journal of the Southern African Institute of Mining and Metallurgy*, vol. 117, no. 8, pp. 765–770, 2017, doi: 10.17159/2411-9717/2017/v117n8a6.

[32] P. A. Laxen, “The dissolution of uranium minerals from South African ores in acid solutions,” 1967. [Online]. Available: https://www.osti.gov/biblio/4435046

[33] R. Gilligan, A. P. Deditius, and A. N. Nikoloski, “Leaching of brannerite in the ferric sulphate system. Part 2: Mineralogical transformations during leaching,” *Hydrometallurgy*, vol. 159, pp. 95–106, 2016, doi: 10.1016/j.hydromet.2015.11.006.

[34] H. S. Reynolds et al., “Kinetics of uranium extraction from coffinite: A comparison with other common uranium minerals,” *Transactions of Nonferrous Metals Society of China*, vol. 28, no. 10, pp. 2135–2142, 2018, doi: 10.1016/s1003-6326(18)64858-7.

[35] R. Gilligan and A. N. Nikoloski, “Leaching of brannerite in the ferric sulphate system – Part 1: Kinetics and reaction mechanisms,” *Hydrometallurgy*, vol. 156, pp. 71–80, 2017, doi: 10.1016/j.hydromet.2015.05.016.

[36] J. Vergara-Zambrano, W. Kracht, and F. A. Díaz-Alvarado, “Integration of renewable energy into the copper mining industry: A multi-objective approach,” *Journal of Cleaner Production*, vol. 372, 2022, doi: 10.1016/j.jclepro.2022.133419.

[37] M. C. Barma, R. Saidur, S. M. A. Rahman, A. Allouhi, B. A. Akash, and S. M. Sait, “A review on boilers energy use, energy savings, and emissions reductions,” *Renewable and Sustainable Energy Reviews*, vol. 79, pp. 970–983, 2017, doi: 10.1016/j.rser.2017.05.187.

[38] V. Ganapathy, *Industrial Boilers and Heat Recovery Steam Generators*, CRC Press, Boca Raton, FL. 2002.

[39] D. W. Einstein, E. Worrell, and M. Khrushch, “Steam systems in industry: Energy use and energy efficiency improvement potentials,” in *Proceedings of the 2001 ACEEE Summer Study on Energy Efficiency in Industry*, American Council for an Energy Efficient Economy, Washington, DC, 2001.

[40] M. Manni, A. Nicolini, and F. Cotana, “Performance assessment of an electrode boiler for power-to-heat conversion in sustainable energy districts,” *Energy and Buildings*, vol. 277, 2022, doi: 10.1016/j.enbuild.2022.112569.

[41] I. Shabbir, M. Mirzaeian, and F. Sher, “Energy efficiency improvement potentials through ene*rgy benchmarking in pulp and paper industry,”* Cleaner Chemical Engineering, vol. 3, 2022, doi: 10.1016/j.clce.2022.100058.

[42] A. Udara and S. H. M. Sajath, “Industrial boiler operation,” *Journal of Research Technology and Engineering,* vol. 1, no. 3, p. 11, 2020.

[43] R. Saidur, J. U. Ahamed, and H. H. Masjuki, “Energy, exergy and economic analysis of industrial boilers,” *Energy Policy*, vol. 38, no. 5, pp. 2188–2197, 2010, doi: 10.1016/j.enpol.2009.11.087.

[44] S. Nasirov and C. A. Agostini, “Mining experts' perspectives on the determinants of solar technologies adoption in the Chilean mining industry,” *Renewable and Sustainable Energy Reviews*, vol. 95, pp. 194–202, 2018, doi: 10.1016/j.rser. 2018.07.038.

[45] P. Naicker and G. A. Thopil, “A framework for sustainable utility scale renewable energy selection in South Africa,” *Journal of Cleaner Production*, vol. 224, pp. 637–650, 2019, doi: 10.1016/j.jclepro.2019.03.257.

[46] S. Dabiri and M. F. Rahimi, “Basic introduction of solar collectors and energy and exergy analysis of a heliostat plant,” *The 3rd International Conference and Exhibition on Solar Energy*, Tehran, Iran 2016.

[47] Y. Choi and J. Song, “Review of photovoltaic and wind power systems utilized in the mining industry,” *Renewable and Sustainable Energy Reviews*, vol. 75, pp. 1386–1391, 2017, doi: 10.1016/j.rser.2016.11.127.

[48] T. Igogo, K. Awuah-Offei, A. Newman, T. Lowder, and J. Engel-Cox, “Integrating renewable energy into mining operations: Opportunities, challenges, and enabling approaches,” *Applied Energy*, vol. 300, 2021, doi: 10.1016/j.apenergy.2021. 117375.

[49] US Department of Energy Energy Efficiency and Renewable Energy, *Industrial Heat Pumps for Steam and Fuel Savings*, 2003.

[50] R. O'Hegarty, O. Kinnane, D. Lennon, and S. Colclough, “Air-to-water heat pumps: Review and analysis of the performance gap between in-use and product rated performance,” *Renewable and Sustainable Energy Reviews*, vol. 155, 2022, doi: 10.1016/j.rser.2021.111887.

[51] M-Tech Industrial, “Heat pump water heaters for energy efficient water heating at centralized sanitary water heating systems,” Potchefstroom, p. 11.

[52] J. A. Jacobs, “Failure prediction of critical mine machinery,” PhD thesis in Mechanical Engineering, Potchefstroom, North-West University, 2021.

[53] S. J. Fouché, “Improving efficiency of a mine compressed air system,” Master’s thesis, Mechanical Engineering, North-West University, Potchefstroom, 2017.

[54] US Department of Energy, “Heat recovery with compressed air systems,” in *Improving Compressed Air System Performance: A Sourcebook for Industry*, 3rd ed.

[55] Compressed Air and Gas Institute, “Heat recovery from industrial compressed air systems,” Cleveland, OH.

[56] A. A. Moretta, “Spiral plate heat exchangers: Sizing units for cooling non-Newtonian slurries,” Gooch Thermal Systems, p. 50, May 2010.

[57] Alfa Laval. “Spiral heat exchangers.” https://www.alfalaval.com/products/heat-transfer/plate-heat-exchangers/welded-spiral-heat-exchangers/welded-spiral-heat-exchangers/

[58] A. Ciminoa, M. G. Gnonia, F. Longob, G. Baroneb, M. Fedeleb, and D. Le Plane, “Modeling & simulation as Industry 4.0 enabling technology to support manufacturing process design: a real industrial application,” *Science Direct*, vol. 2017, pp. 1877–1866, 2023.

[59] B. M. Friedenstein, C. Cilliers, and J. van Rensburg, “Simulating operational improvements on mine compressed air systems,” *South African Journal of Industrial Engineering*, vol. 29, no. 3, 2017.

[60] S. McLean, J. Chenier, S. Muinonen, C. A. Laamanen, and J. A. Scott, “Recovery and repurposing of low-grade thermal resources in the mining and mineral processing industry,” *Journal of Sustainable Mining*, vol. 19, no. 2, 2020. doi: 10.46873/2300-3960.1010.

[61] M. Zubair, R. R. Al Suwaidi, and A. A. Al Souqi, “Behavior of emergency core cooling system (ECCS) during the early stage of loss of coolant accident (LOCA) for APR 1400 with Flownex software,” *Progress in Nuclear Energy*, vol. 141, 2021, doi: 10.1016/j.pnucene.2021.103949.

[62] L. Räty, “Modelling thermodynamic properties of substances with neural networks in nuclear power plant simulation,” Master of Science in Technology, Department of Automation and Systems Technology, Helsinki University of Technology, 2005.

[63] B. Xia and D.-W. Sun, “Applications of computational fluid dynamics (CFD) in the food industry: A review,” *Computers and Electronics in Agriculture*, vol. 34, no. 1–3, pp. 5–24, 2002.

[64] H. Mikulčić et al., “The application of CFD modelling to support the reduction of CO_2 emissions in cement industry,” *Energy*, vol. 45, no. 1, pp. 464–473, 2012, doi: 10.1016/j.energy.2012.04.030.

[65] A. Nell, “Development of a dewatering control strategy to prevent flooding within deep-level mines,” Master’s thesis, Mechanical Engineering, North-West University, Potchefstroom, 2021.

[66] D. Nell, “Optimising production through improving the efficiency of mine compressed air networks with limited infrastructure,” Master’s thesis, Mechanical Engineering, North-West University, Potchefstroom, 2017.

[67] A. Firth, B. Zhang, and A. Yang, “Quantification of global waste heat and its environmental effects,” *Applied Energy*, vol. 235, pp. 1314–1334, 2019, doi: 10.1016/j.apenergy.2018.10.102.

[68] K. S. More, C. Wolkersdorfer, N. Kang, and A. S. Elmaghraby, “Automated measurement systems in mine water management and mine workings: A review of potential methods,” *Water Resources and Industry*, vol. 24, 2020, doi: 10.1016/j.wri.2020.100136.

[69] S. Taljaard, “Comparative study of mine dewatering control systems,” Master’s thesis, Mechanical Engineering, North-West University, Potchefstroom, 2018.

[70] P. Maré, J. H. Marais, and J. F. Van Rensburg, “Improved implementation strategies to sustain energy saving measures on mine cooling systems,” *13th International Conference on the Industrial and Commercial Use of Energy (ICUE)*, pp. 102–109, 2015, doi: 10.1109/ICUE.2015.7280254.

[71] R. F. Rahmat, I. S. Satria, B. Siregar, and R. Budiarto, “Water pipeline monitoring and leak detection using flow liquid meter sensor,” *IAES International Conference on Electrical Engineering, Computer Science and Informatics*, 2017.

[72] K. Rivera. “Checking water temperature with an infrared laser thermometer,” *DoItYourself*, 4 Jun. 2010. [Online]. Available: https://www.doityourself.com/stry/checking-water-temperature-with-an-infrared-laser-thermometer

[73] W. van der Wateren, “Optimising energy recovery on mine dewatering systems,” Master’s thesis, Mechanical Engineering, North-West University, Potchefstroom, 2018.

[74] Alfa Laval, *Waste Heat Recovery: Optimizing your Energy System*, Isando.

[75] P. A. Hohne, K. Kusakana, and B. P. Numbi, “Optimal energy management and economic analysis of a grid-connected hybrid solar water heating system: A case of Bloemfontein, South Africa,” *Sustainable Energy Technologies and Assessments*, vol. 31, pp. 273–291, 2019, doi: 10.1016/j.seta.2018.12.027.

[76] D. Jacobs, “Developing a digital twin for addressing complex mine ventilation problems,” Master’s thesis, Mechanical Engineering, North-West University, Potchefstroom, 2021.

[77] M. Picón-Núñez, L. Canizalez-Dávalos, and J. M. Medina-Flores, “Alternative sizing methodology for compact heat exchangers of the spiral type,” *Heat Transfer Engineering*, vol. 30, no. 9, pp. 744–750, 2009, doi: 10.1080/01457630802678508.

[78] AVK Southern Africa, *AVK Southern Africa Product Offering and Gross Price List 2021*, Alberton, 2021.

[79] J. Siecker, K. Kusakana, and B. P. Numbi, “A review of solar photovoltaic systems cooling technologies,” *Renewable and Sustainable Energy Reviews*, vol. 79, pp. 192-203, 2017, doi: 10.1016/j.rser.2017.05.053.

[80] Markets Insider. “Uranium commodity,” https://markets.businessinsider.com/commodities/uranium-price

APPENDIX A: SPIRAL HEAT EXCHANGER

This appendix serves to view the design purpose of the spiral heat exchanger chosen for the study.

Referring to Figure 13, the hot fluid enters at the centre of the heat exchanger and flows in a circular motion inside outwards, leaving the heat exchanger. The cold fluid enters from the outside of the heat exchanger and also flows in circular motion outside inwards, creating a countercurrent flow in the heat exchanger.

Figure 52 shows the self-cleaning effect of the spiral heat exchanger. As the fluid flows in the inner or outer direction (Figure 13), there is a constant change in direction. High shear stresses are generated that remove the solids in the stagnant zones that cause fouling or sedimentation [77]. This further leads to greater heat transfer coefficients since there is closer contact between the two fluids. Another advantage is the single channel flow, which ensures that the two mediums do not mix and only transfer heat.

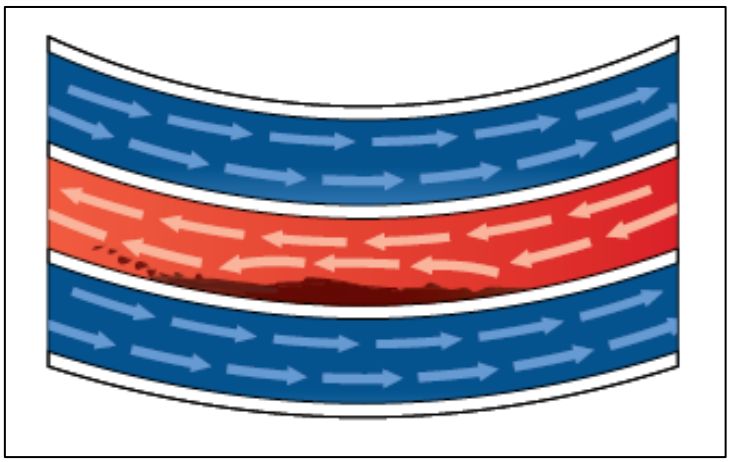

Figure 52: Spiral heat exchanger self-cleaning channel [57]

Cold water flows through the coils, which absorbs the heat from the hot air and cools the air. In this process, the water receives the heat and it is pumped away. There is an opportunity to use the heat to preheat the uranium-carrying slurry. The impact that an increase in the temperature of the slurry has on its uranium extraction was investigated during the literature review along with other factors that could lead to a better leaching.

Figure 53 shows an actual representation of a spiral heat exchanger.

Figure 53: Spiral heat exchanger as in the industry[4]

The process flow that happens in the shell of the spiral heat exchanger cannot be observed in Figure 53. The process flow is depicted in Figure 54.

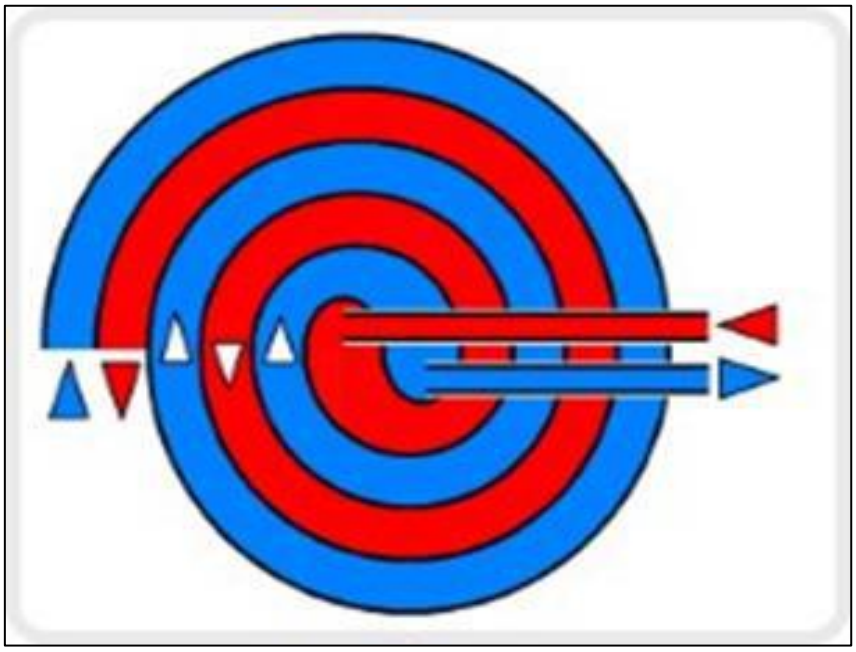

Figure 54: Flow process of spiral heat exchanger [57]

The technical design specifications were used to calculate the duty and flow used in the simulations done in Section 3.5. These design specifications are shown in Figure 55.

[4] Cost estimate with technical notes issued by Zonke Engineering on 19 May 2021.

Spiral Plate Heat Exchanger	TECHNICAL SPECIFICATION		
CUSTOMER			
ITEM			
Date	13.05.2021		
Rev	0		
	HOT SIDE		**COLD SIDE**
Fluid	WATER		LIME SLURRY
Total Flow rate (Kg/s)	100		67
Inlet temperature (oC)	40		12
Outlet temperature (oC)	30.3		31
Vapor in (Tot Flow)			
Vap/Liqui (OUT)			
Inlet Pressure (Bar g)	-		-
Water-Steam (Tot Flow)	-	-	-
Vap/Liqui (OUT)	-	-	-
Physical properties	**Vapor**	**Liquid**	**Liquid**
Density In/out (kg/m³)	-	993	1500
Spec heat capacit kJ/(kg·K)	-	4.180	3.200
Thermal cond W/(m·K)°	-	0.625	0.600
Viscosity In/Out (cP)	-	0.650 / 0.800	3 / 1.95
Heat exchanged (KW)			4 075
Plate area (m2)			273
Type of heat exchanger			Spiral Plate Heat Exchanger TYPE 1H-1
Number of heat exchangers			1
Pressure drop (kPa)	00		100
Width [mm] Thickness (mm)			2000
Outer diameter [mm]			1900
Direction of fluids	Spiral Flow		Spiral Flow
Code	Section VIII Div 1 without U stamp		
Design pressure [barg]	10		10
Test pressure [barg]	PER CODE		PER CODE
Design temp [°c] max/min	60		60
M D M T [°c]	/		
Connections (Vap.Con.In)	DN 250 - 2 x DN 200		2 x DN 150 – DN 200
Material			316/316 L
Plate thickness [mm]			3

Figure 55: Design specification of the spiral heat exchanger [57]

APPENDIX B: HEAT RECOVERY SYSTEM

This section serves as the information gathered and used for the heat recovery system of Mine A. Referring to Section 3.3, the remaining data and results are presented in this section. The aftercooler process as displayed on the SCADA system and discussed in Section 3.3, is shown in Figure 56.

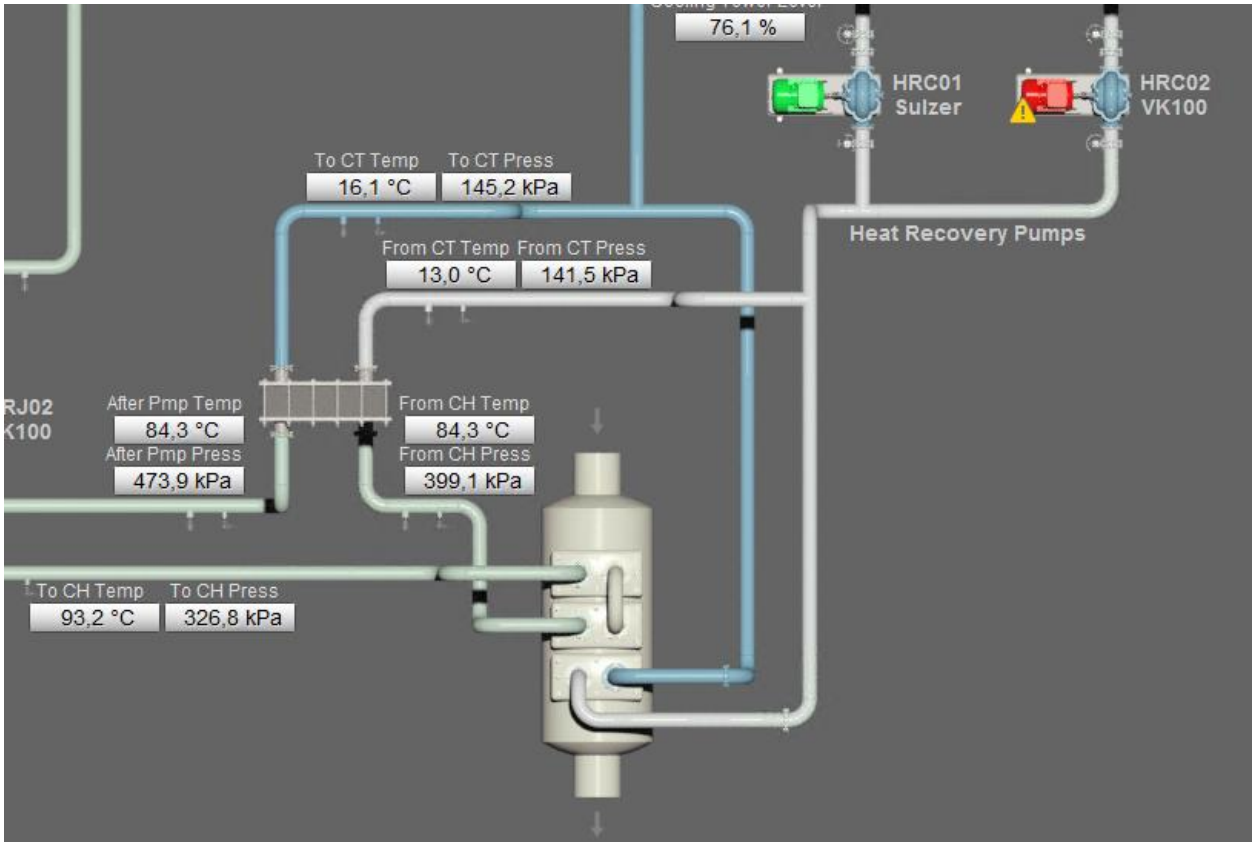

Figure 56: SCADA view of the two-stage aftercooler used at Mine A

Figure 57 depicts the simulation used to calculate the airflow used for the aftercooler system. The pressures and temperatures were obtained and inserted into the simulation, from where the airflow was calculated to satisfy the temperature drop. This value was used in numerous tables throughout the study.

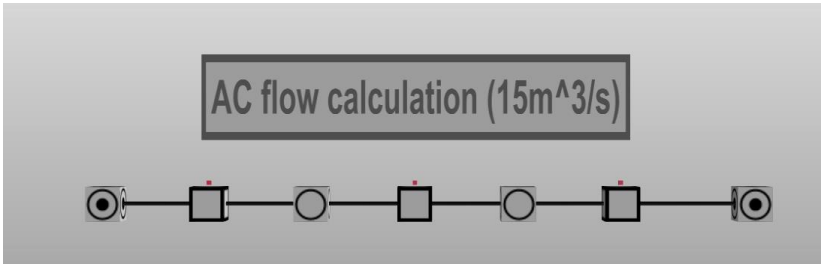

Figure 57: Simulation used to calculate the airflow needed in the aftercooler

APPENDIX C: HEAT SOURCE SYSTEM

This section serves as the information gathered and used for the heat source system used in Mine B. Referring to Section 3.4, the remaining data and results of the heat source system at Mine B are presented in this section. Figure 58 and Figure 59 show the results of the comparison between the simulated and acquired data of Compressor 1 and Compressor 2, respectively, during winter conditions. Figure 60 and Figure 61 display the same results for summer conditions.

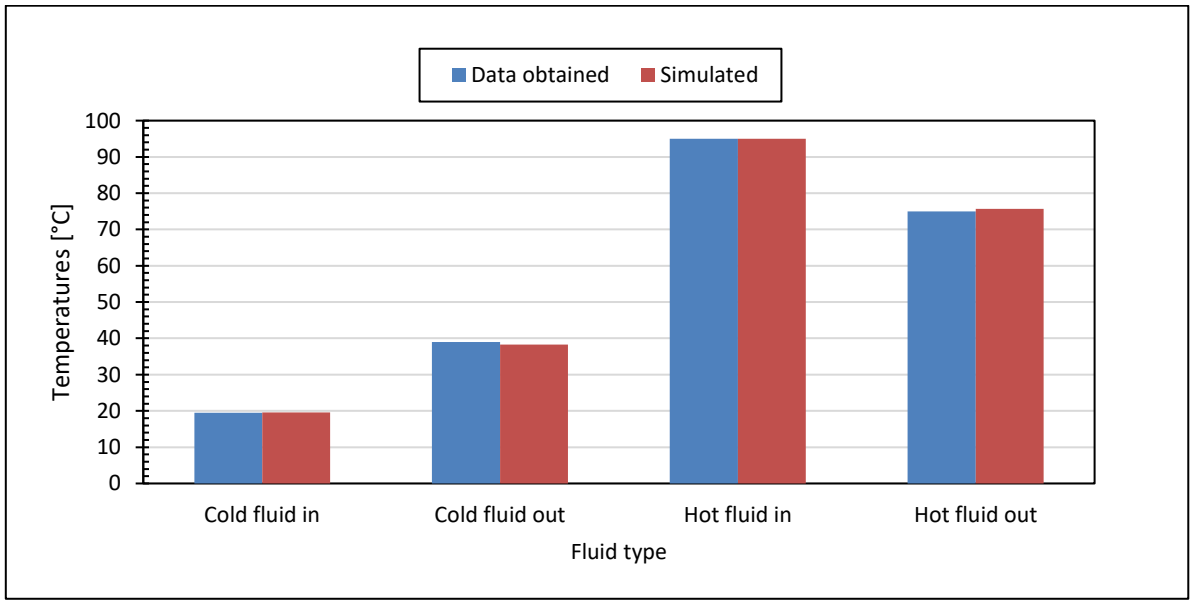

Figure 58: Compressor 1 aftercooler winter temperatures comparison

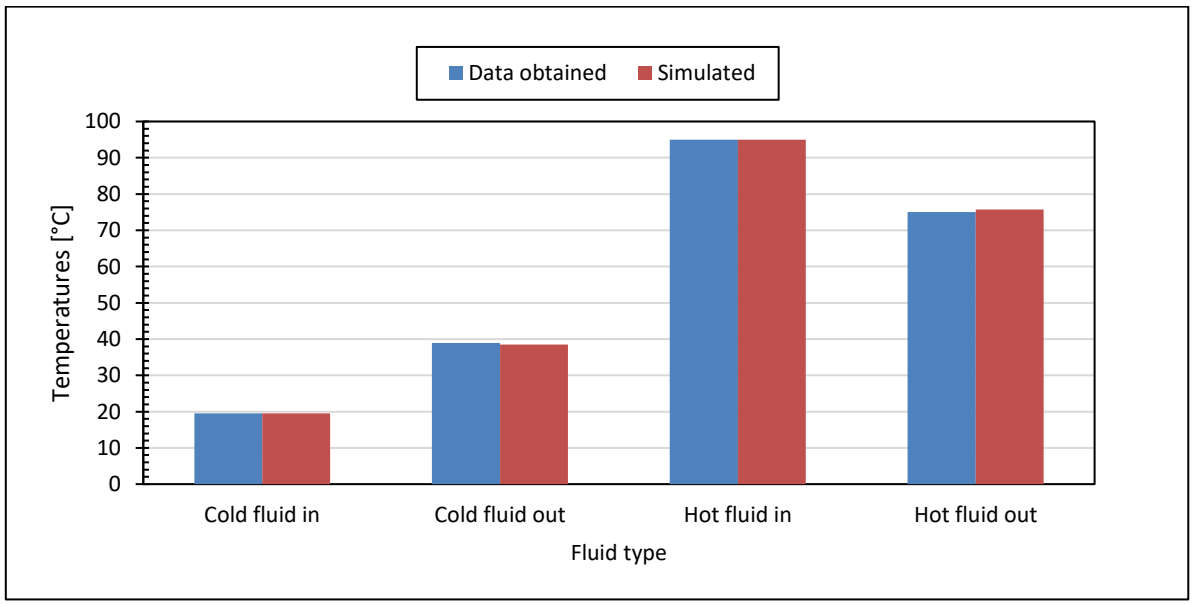

Figure 59: Compressor 2 aftercooler winter temperatures comparison

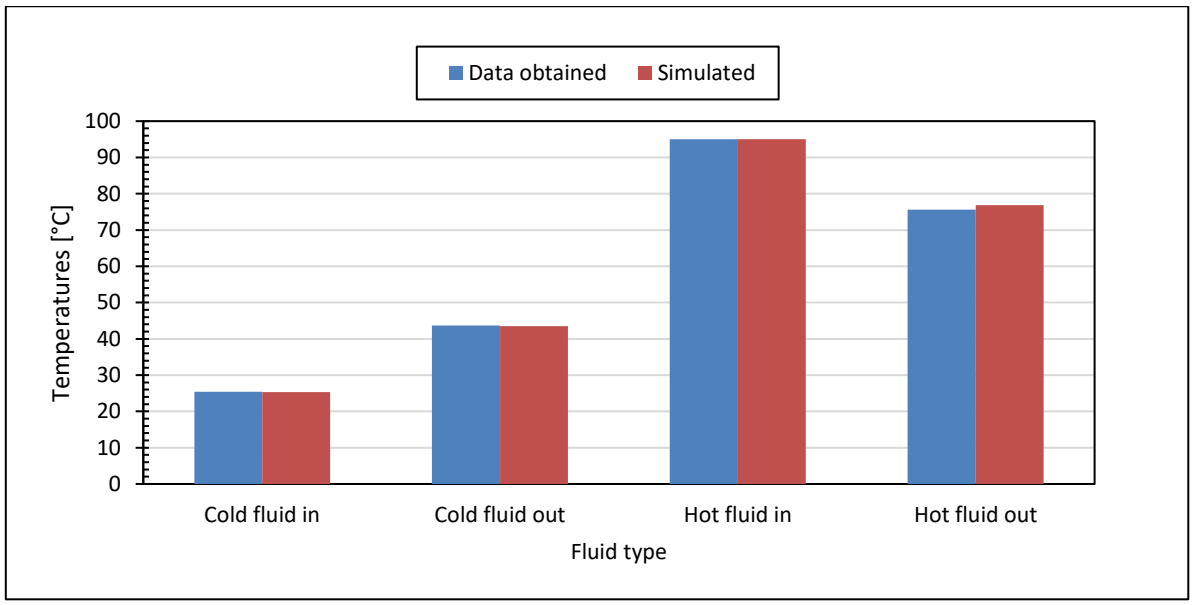

Figure 60: Compressor 1 aftercooler summer temperatures comparison

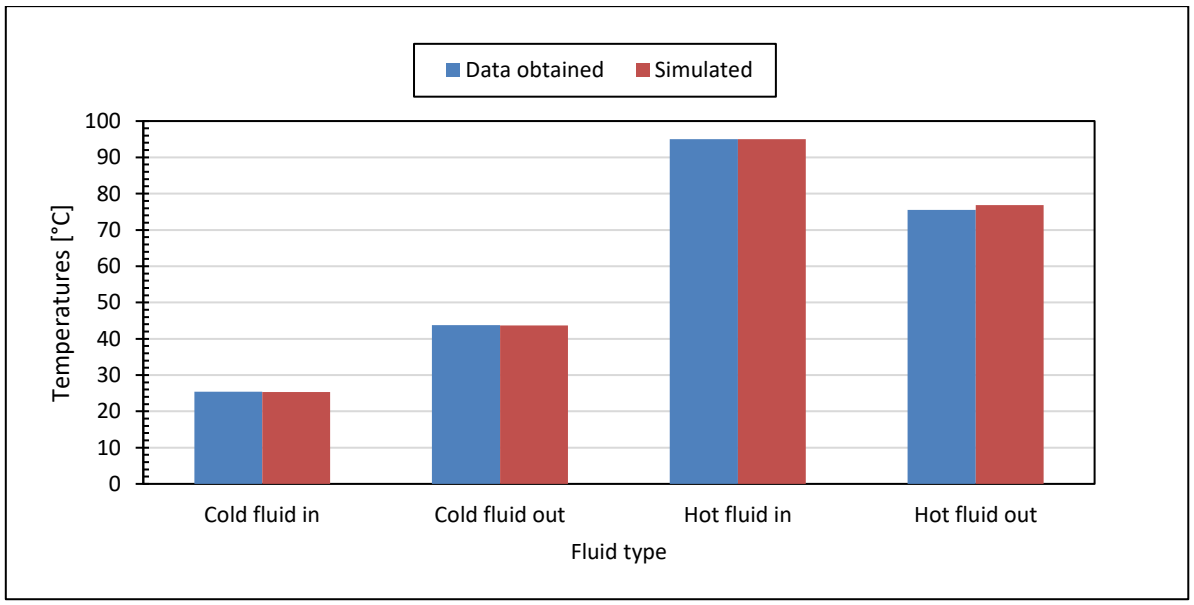

Figure 61: Compressor 2 aftercooler summer temperatures comparison

APPENDIX D: HEAT RECOVERY ANALYSIS

This section serves as the information gathered and used for the heat recovery analysis of the uranium plant, which is also the solution model. Referring to Section 3.7, the remaining data and results of the heat recovery system for the solution model are presented in this section.

The results of Year 1 and Year 2 of the benefit were calculated in Section 3.7. The remaining years are presented in Figure 62, Figure 63, Figure 64 and Figure 65, respectively. The total benefit increased as mentioned throughout the study.

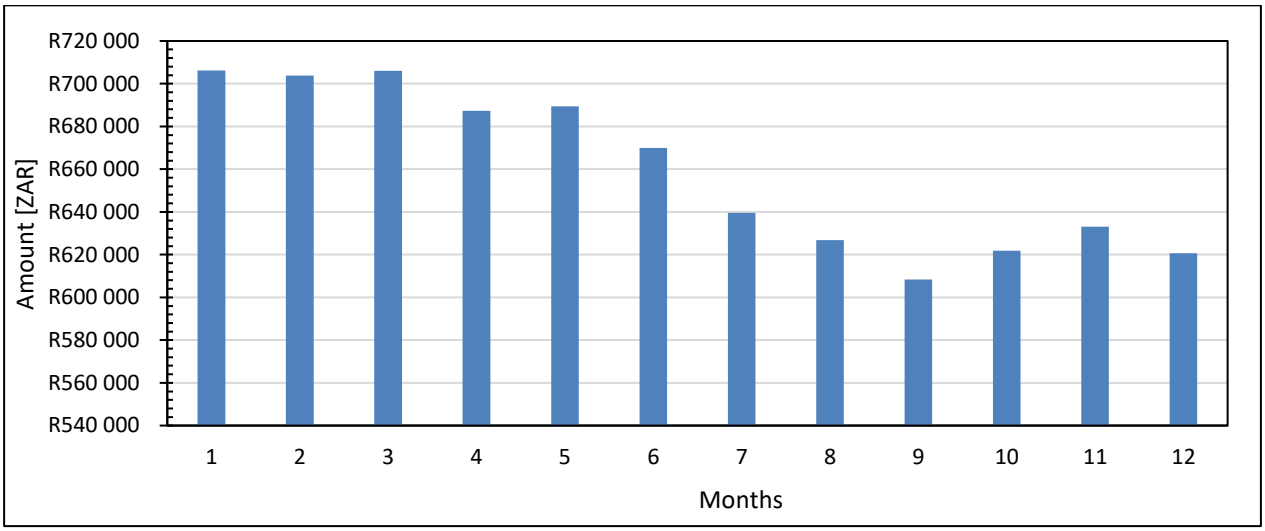

Figure 62: Monthly cost versus benefit for Year 3 of heat recovery model

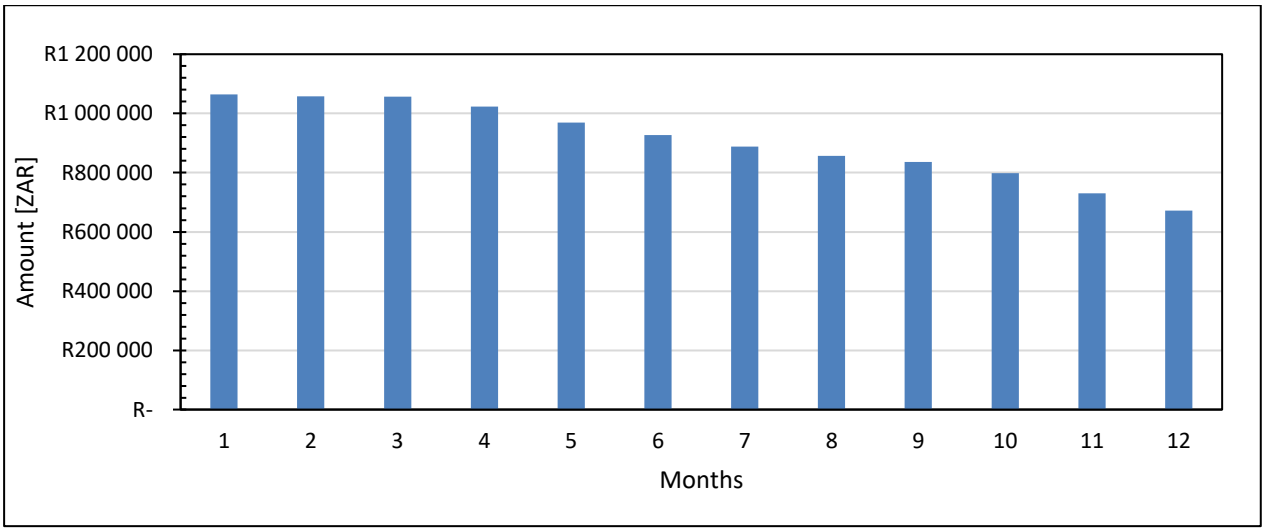

Figure 63: Monthly cost versus benefit for Year 4 of heat recovery model

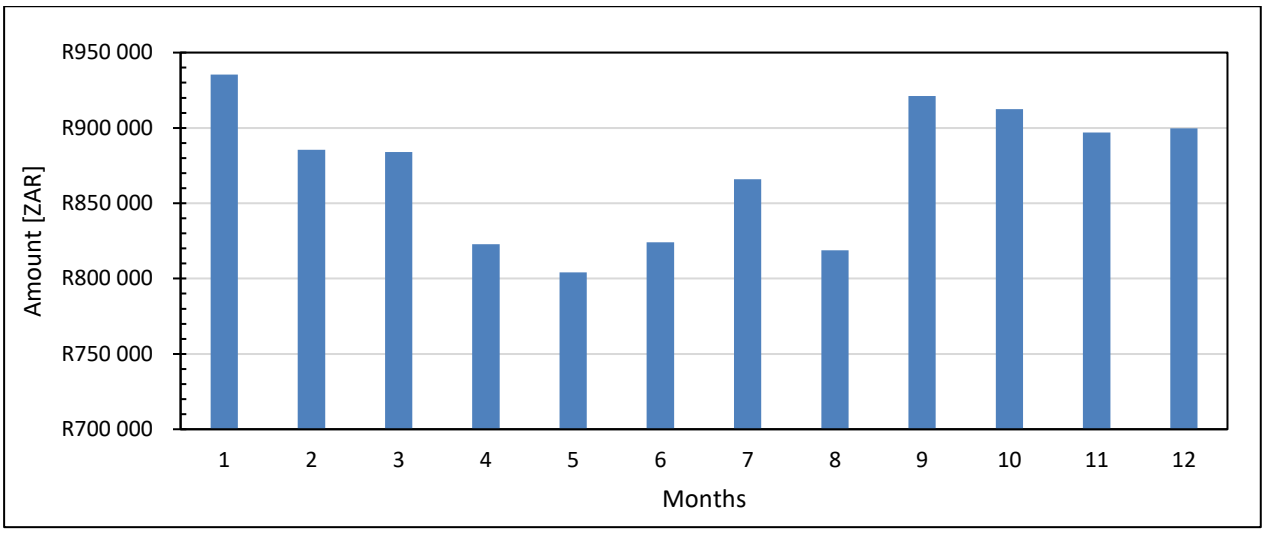

Figure 64: Monthly cost versus benefit for Year 5 of heat recovery model

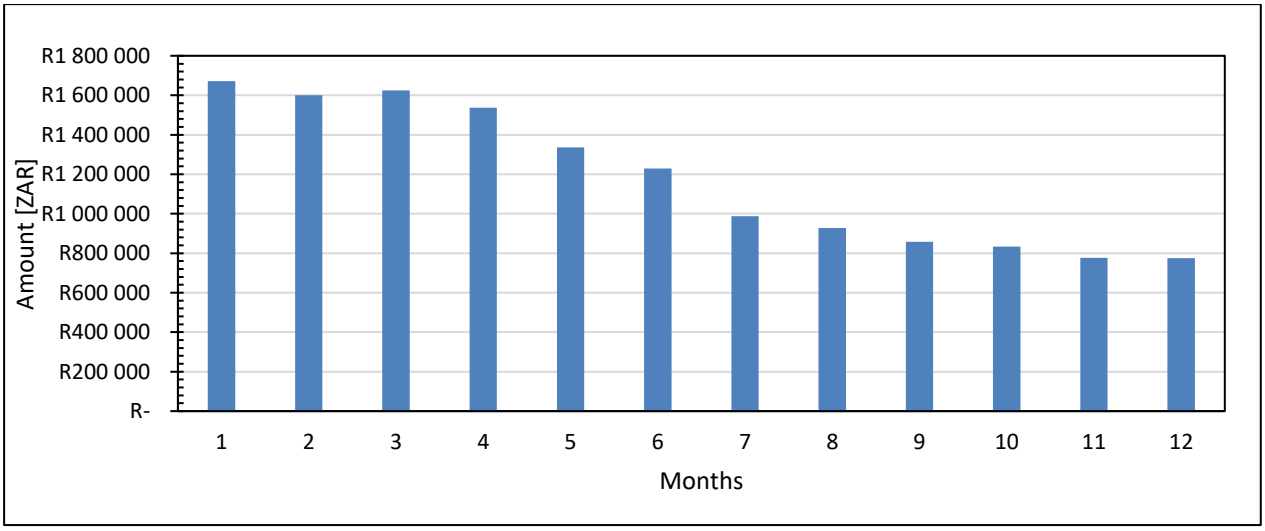

Figure 65: Monthly cost versus benefit for Year 6 of heat recovery model